ISSN 1007-9327 (print)
ISSN 2219-2840 (online)

World Journal of *Gastroenterology*

World J Gastroenterol 2021 January 21; 27(3): 233-304

Published by Baishideng Publishing Group Inc

World Journal of Gastroenterology

Contents

Weekly Volume 27 Number 3 January 21, 2021

EDITORIAL

ORIGINAL ARTICLE

Basic Study

Retrospective Study

Observational Study

CASE REPORT

World Journal of Gastroenterology

Weekly Volume 27 Number 3 January 21, 2021

Contents

ABOUT COVER

Michael Linnebacher, PhD, Academic Fellow, Research Fellow, Research Scientist, Senior Researcher, Senior Scientist, Molecular Oncology and Immunotherapy, Department of General, Visceral, Vascular and Transplantation Surgery, University Medical Center Rostock, Schillingallee 69, Rostock 18057, Germany. michael.linnebacher@med.uni-rostock.de

AIMS AND SCOPE

The primary aim of *World Journal of Gastroenterology* (*WJG*, *World J Gastroenterol*) is to provide scholars and readers from various fields of gastroenterology and hepatology with a platform to publish high-quality basic and clinical research articles and communicate their research findings online. *WJG* mainly publishes articles reporting research results and findings obtained in the field of gastroenterology and hepatology and covering a wide range of topics including gastroenterology, hepatology, gastrointestinal endoscopy, gastrointestinal surgery, gastrointestinal oncology, and pediatric gastroenterology.

INDEXING/ABSTRACTING

The *WJG* is now indexed in Current Contents®/Clinical Medicine, Science Citation Index Expanded (also known as SciSearch®), Journal Citation Reports®, Index Medicus, MEDLINE, PubMed, PubMed Central, and Scopus. The 2020 edition of Journal Citation Report® cites the 2019 impact factor (IF) for *WJG* as 3.665; IF without journal self cites: 3.534; 5-year IF: 4.048; Ranking: 35 among 88 journals in gastroenterology and hepatology; and Quartile category: Q2. The *WJG*'s CiteScore for 2019 is 7.1 and Scopus CiteScore rank 2019: Gastroenterology is 17/137.

RESPONSIBLE EDITORS FOR THIS ISSUE

Production Editor: *Yu-Jie Ma*; **Production Department Director:** *Xiang Li*; **Editorial Office Director:** *Ze-Mao Gong*.

NAME OF JOURNAL
World Journal of Gastroenterology

ISSN
ISSN 1007-9327 (print) ISSN 2219-2840 (online)

LAUNCH DATE
October 1, 1995

FREQUENCY
Weekly

EDITORS-IN-CHIEF
Andrzej S Tarnawski, Subrata Ghosh

EDITORIAL BOARD MEMBERS
http://www.wjgnet.com/1007-9327/editorialboard.htm

PUBLICATION DATE
January 21, 2021

INSTRUCTIONS TO AUTHORS
https://www.wjgnet.com/bpg/gerinfo/204

GUIDELINES FOR ETHICS DOCUMENTS
https://www.wjgnet.com/bpg/GerInfo/287

GUIDELINES FOR NON-NATIVE SPEAKERS OF ENGLISH
https://www.wjgnet.com/bpg/gerinfo/240

PUBLICATION ETHICS
https://www.wjgnet.com/bpg/GerInfo/288

PUBLICATION MISCONDUCT
https://www.wjgnet.com/bpg/gerinfo/208

ARTICLE PROCESSING CHARGE
https://www.wjgnet.com/bpg/gerinfo/242

STEPS FOR SUBMITTING MANUSCRIPTS
https://www.wjgnet.com/bpg/GerInfo/239

ONLINE SUBMISSION
https://www.f6publishing.com

World Journal of Gastroenterology

Submit a Manuscript: https://www.f6publishing.com

World J Gastroenterol 2021 January 21; 27(3): 233-239

DOI: 10.3748/wjg.v27.i3.233

ISSN 1007-9327 (print) ISSN 2219-2840 (online)

EDITORIAL

Screening colonoscopy: The present and the future

Chelsea V Hayman, Dinesh Vyas

ORCID number: Chelsea V Hayman 0000-0002-5555-6861; Dinesh Vyas 0000-0002-5330-9429.

Author contributions: Hayman CV and Vyas D contributed to this paper; Vyas D designed the overall concept and outline of this manuscript; Hayman CV and Vyas D contributed to the discussion and design of the manuscript; Hayman CV contributed to the writing, and editing of the manuscript, illustrations, and review of the literature

Conflict-of-interest statement: Chelsea V Hayman and Dinesh Vyas have nothing to disclose.

Manuscript source: Unsolicited manuscript

Specialty type: Gastroenterology

Chelsea V Hayman, Dinesh Vyas, College of Medicine, California Northstate University, Elk Grove, CA 95757, United States

Dinesh Vyas, Department of Surgery, San Joaquin General Hospital, French Camp, CA 95231, United States

Corresponding author: Dinesh Vyas, MD, MSc, Associate Professor, Director, Surgeon, Department of Surgery, San Joaquin General Hospital, 500 West Hospital Road, French Camp, CA 95231, United States. dineshvyas@yahoo.com

Abstract

In the United States, colorectal cancer (CRC) is the second leading cause of mortality in men and women. We are now seeing an increasing number of patients with advanced-stage diagnosis and mortality from colorectal cancer before 50 years of age, which requires earlier screening. With the increasing need for CRC screening through colonoscopy, and thus endoscopists, easier and simpler techniques are needed to train proficient endoscopists. The most widely used approach by endoscopists is air insufflation colonoscopy, where air distends the colon to allow visualization of the colonic mucosa. This technique is uncomfortable for patients and requires an anesthetist to administer sedation. In addition, patients commonly complain about discomfort post-op as air escapes into the small bowel and cannot be adequately removed. Current research into the use of water insufflation colonoscopies has proved promising in reducing the need for sedation, decreasing discomfort, and increasing the visibility of the colonic mucosa. Future direction into water insufflation colonoscopies which have shown to be simpler and easier to teach may increase the number of proficient endoscopists in training to serve our aging population.

Key Words: Colorectal cancer; Water-insufflation colonoscopy; Air-insufflation colonoscopy; Adenomatous polyps; Adenoma detection rate

Core Tip: Training residents in water-insufflation colonoscopy techniques are simpler and easier to teach and lead to a reduction in patient pain, need for sedation, and increased visibility of the colonic mucosa. As more endoscopists are comfortable with this technique, more people in our growing population will be able to obtain the

and hepatology

Country/Territory of origin: United States

Peer-review report's scientific quality classification
Grade A (Excellent): 0
Grade B (Very good): B
Grade C (Good): 0
Grade D (Fair): 0
Grade E (Poor): 0

Received: October 16, 2020
Peer-review started: October 16, 2020
First decision: October 27, 2020
Revised: November 10, 2020
Accepted: December 11, 2020
Article in press: December 11, 2020
Published online: January 21, 2021

P-Reviewer: Mizukami T
S-Editor: Liu M
L-Editor: A
P-Editor: Ma YJ

necessary screening colonoscopies.

Citation: Hayman CV, Vyas D. Screening colonoscopy: The present and the future. *World J Gastroenterol* 2021; 27(3): 233-239
URL: https://www.wjgnet.com/1007-9327/full/v27/i3/233.htm
DOI: https://dx.doi.org/10.3748/wjg.v27.i3.233

INTRODUCTION

In the United States, colorectal cancer (CRC) is the second leading cause of mortality in men and women. The most effective tool for reducing the morbidity and mortality associated with CRC is the use of colonoscopy. With nearly 14.2 million procedures performed in the United States alone[1], the colonoscopy is one of the most common procedures performed. However, colonoscopies can only benefit the population with endoscopists who have proficiency in both technical and cognitive skills. The guidelines for training in colonoscopy techniques and grading proficiency continue to evolve as new advances in the tools used by endoscopists are discovered. In the 1960s, retrograde colonoscopy and endoscopic excision of polyps were developed in Japan to advance the visualization and removal of polyps from the entire large intestine[2]. Previous techniques such as the barium enema were challenging without considerable training and practice, and the presence of polypoid tumors could not be reliably excluded. As it was demonstrated that CRC did not occur *de-novo* but arose from a premalignant polyp, the use of the colonoscopy as a screening technique increased. Research into the use of the colonoscopy and the colonoscopy polypectomy proved that the detection of cancer at an earlier, pre-symptomatic stage was associated with better survival[3].

For a successful screening colonoscopy, partial distention of the lumen is needed to allow proper visualization and inspection of the colonic mucosa. The current standard technique for colonic distention is the use of air insufflation (AI) using an integrated air pump[4,5]. However, one of the major sources of pain and discomfort for patients undergoing a colonoscopy is the volume of air insufflated which causes significant abdominal distention and looping of the instrument. Potential risks for this procedure include perforation, bleeding, and infection. To minimize discomfort and pain during the procedure, patients undergoing colonoscopy with AI often require sedation which adds additional risks including medication side effects, higher medical costs, and longer recovery time when compared with unsedated colonoscopy[6]. At the end of the procedure, the air can only be partially removed, as some of it escapes into the small bowel. This leads to post-procedure cramping, gas, and bloating which can only be relieved by passing gas.

Recent clinical trials have proposed that using water infusion to distend the colon may reduce patient pain and discomfort and improve colonic visualization through difficult segments of the colon. This was first described by Falchuk and Griffin in 1984 in patients who could not undergo AI due to severe diverticular disease[7]. For water infusion colonoscopy, instead of expanding the colon, the water weighs it down utilizing gravity. It was Japanese endoscopists who evolved this technique by using syringes for water infusion and complete air suction to "collapse" the colonic lumen and continuously infusing water to advance the colonoscope[8]. This method straightens the colon and allows for better navigation of the scope through less extreme angles. As no air is left behind, this technique reduces post-procedure pain and allows for faster recovery. The first randomized control trial in 2010 showed that using the water immersion technique compared to standard AI increases the success rate of minimal sedation colonoscopy[9]. This along with other studies has shown the use of water improves the rate and time of cecal intubation, alleviates abdominal pain, and increases patients' willingness to undergo a repeat procedure[7]. This technique is shown in Figure 1.

The overall effectiveness of colonoscopy is the achievement of various quality measurements. The most important quality measurement is the adenoma detection rate (ADR) which is the frequency with which adenomas are detected in asymptomatic, average-risk individuals in a screening colonoscopy[10]. Another quality measurement is cecal intubation or the ability to pass the colonoscope through the tip

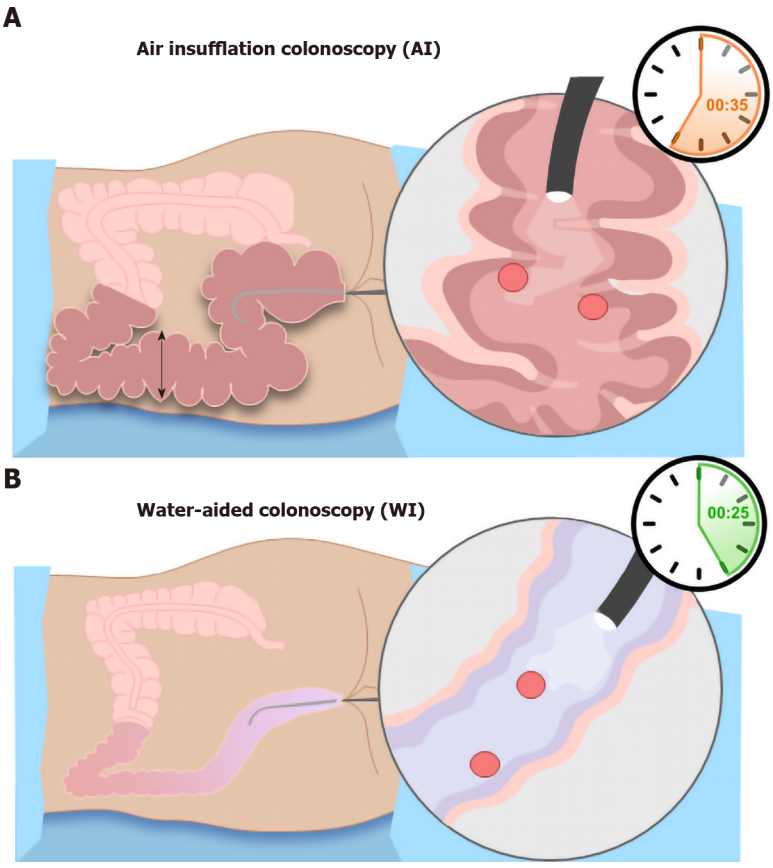

Figure 1 Image of colonic distension and bowel looping in air insufflation colonoscopy *vs* water-aided colonoscopy. A: Air insufflation colonoscopy causes significant distention of the colon in both length and width. The air promotes looping of the bowl at the flexure points leading to difficult navigation of the colonoscope; B: Water insufflation utilizes gravity to pull the colon down while providing minimal distention and looping. AI: Air insufflation; WI: Water insufflation.

of the ileocecal valve. This ensures adequate visualization of the entire colonic mucosa. Bowel preparation is an important measure as its effectiveness rests in the hands of the patient. Without adequate bowel preparation, clear visualization of the colon is difficult and may require repeat procedures. Sedation and the use of an anesthetist decrease intra-op and post-op pain, yet it is associated with increased cost.

New advances in colonoscopy have led to the development of virtual colonoscopy and robotic colonoscopy. Virtual colonoscopies, or computed tomography colonography (CTC), use helical CT scanners and AI to take 3D images of the colon. This technique is non-invasive, requires no sedation, can be completed in 10-15 min, and is overall much safer[11]. However, there are some limitations to this approach. Incomplete distention of colonic segments and flat lesions can lead to false-negative diagnoses. In addition, CTC does not allow for removal or biopsy of lesions. Robotic colonoscopy has benefits over the traditional endoscope approach including better viewing of the gastrointestinal tract, decreased pain, and the ability to navigate tortuous colons successfully. Multiple models of robotic instruments are currently being studied including robotic capsules and robotically controlled advanced colonoscopies. These new advances and the ease with which they can be used may aid in the training of future endoscopists. New research shows that training residents in water insufflation colonoscopic technique leads to increased patient comfort and decreased complications with comparable success rates[12]. As the number of people needing screening colonoscopies continues to grow, so will the need for competent endoscopists and successful endoscopic techniques.

ADR

ADR is the proportion of screening colonoscopies that detect at least one adenoma[13]. The goal of endoscopic screening is checking for CRC, so detection of adenoma in the large bowel can limit the advancement to larger adenomas. The recommended ADR is

20%, based on studies that showed adenoma prevalence in asymptomatic adults to be between 25% to 40%[14,15]. In a study with over 10000 patients, the overall ADR (95% confidence interval) for water insufflation was 34.4% and 30.2% for AI[16]. ADRs are inversely correlated with interval cancers which makes them an important measure in colonoscopies. Interval cancers, or post-colonoscopy CRCs, are cancers detected within the surveillance interval, or 6-36 mo post-cleared colonoscopy. The incidence of interval cancers is 3.4%-9.2%, and improving ADR and colonoscopy techniques can decrease this number substantially[17].

CECAL INTUBATION

Cecal intubation is successfully achieved when the tip of the colonoscope is passed through the ileocecal valve into the caput. This allows for a complete examination of the colonic mucosa at the medial wall of the cecum. AI distends the length of the colon, often farther than the length of the colonoscope. This attributes to the difficulty of adequate cecal intubation with AIC. Gravity allows water infusion into the sigmoid colon to open a passage through the loops and bends of the colon. In addition, abdominal compression and proper positioning of the patient facilitates the passage of the colonoscope and enhances cecal intubation. Some studies have reported that warm water insulation reduces colonic spasms which may also contribute to a higher cecal intubation rate. Some studies have shown that WIC improved cecal intubation time compared with AIC[7,18]. Increasing cecal intubation time can decrease the total OR time and thus, decrease the overall cost.

BOWEL PREP QUALITY

In order to optimize the effectiveness of colonoscopy as a screening tool, patients need to accept the procedure and the necessity of adequate bowel preparation[19]. Preparation quality affects the mucosal visualization, the ability to complete the exam, and the procedure duration. Only three-quarters of colonoscopies have adequate colon preparation[20]. Poor bowel prep can lead to lower ADRs and may force patients to undergo follow-up colonoscopies sooner. In water insufflation (WI), the suction of dirty water and infusion of clean water in the colonic lumen provides serendipitously salvage bowel cleaning in patients with suboptimal bowel preparation[21]. Ineffective bowel preparation may lead to cancelations or rescheduling procedures, which is a major contributor to costs[22].

SEDATION

Sedation for colonoscopy procedure increases the cost and post-procedure recovery time for patients. Patients who have more challenging anatomy often require more sedation as they experience more pain. Studies have shown that water exchange has minimized the requirement for sedation compared with AI. In one study, only 11.5% of patients required on-demand sedation with water exchange compared with 26% in the AI group[23]. Another benefit of limiting sedation is to decrease the risk of cardiopulmonary complications associated with anesthesia. In a study that used the Clinical Outcomes Research Initiative database, cardiopulmonary complications occurred in 0.9% of procedures and made up 67% of unplanned events in endoscopic procedures with sedation[24]. Patients with increased risk of CVP complications include those with advanced age and presence of comorbidities. These patients could benefit greatly from water insufflation colonoscopy, which requires little if any, pain management.

LIMITING PRE AND POST-PROCEDURE PAIN

Intraoperatively, AI causes more pain during colonoscopy as it elongates and distends the colon. Post-operatively, patients experience discomfort as the gas escapes the colon into the small bowel and leads to abdominal distention. Water insufflation reduces intraoperative pain by weighing down and straightening the sigmoid and decreasing

colonic spasm[25]. Fewer patients require sedation with water insufflation compared with AI[26]. Several studies revealed that WIC significantly increased the number of patients who were willing to undergo another colonoscopy due to limited pain during the procedure; this was found to be significantly higher in WIC than in AIC[18,27,28]. With AI, undesired outcomes including perforation and bleeding are partly due to increased colonic distention, angulations exaggeration at flexures, and the increased looping of the instrument. The current rate of perforation is low, ranging from 0.08% to 0.3% in various studies[29]. Pain during colonoscopy indicates the risk of perforation, but sedation can mask this important warning[30]. WI colonoscopy minimizes colonic distention, improves visibility, and reduces the need for sedation, thus reducing the risk of perforation.

TEACHING ENDOSCOPY TECHNIQUES IN TRAINING PROGRAMS

There are multiple different methods currently used for colonoscopy training, including mechanical simulators, virtual reality simulators, computer-simulating endoscopy, magnetic endoscopic imaging, and composite and explanted animal organ simulators. One of the main factors that leads to a lack of polyp discovery is the inexperience of the endoscopist[30,31]. However, there have been some limitations to colonoscopy instruction, including time management and potential trauma to patients involved. Endoscopists in training may benefit from learning the water insufflation technique, as the scope becomes easier to navigate through a minimally looped colon. In addition, detorsion becomes easier for trainees with water insufflation as there is a decreased risk of perforation from AI. Studies have shown that WIC has significantly shorter cecal intubation time for endoscopists in training compared with AIC[7]. The increasing need for colonoscopy screening has increased the demand for high-quality training. Stimulation models are a key tool that many programs use to ease the learning curve of colonoscopy techniques. Another tool that should be introduced into training programs is the use of water insufflation colonoscopy. Trainees may benefit from training with the water insufflation technique as there is the ease of insertion, reduced cecal intubation time, more comfort for the patient, and less looping of the bowel[12]. The strengths and weaknesses of these two techniques are shown in Table 1.

CONCLUSION

Colorectal cancer is the second leading cause of mortality in men and women in the United States. Since the onset of screening colonoscopies, the conventional colonoscope has not changed much since its development. Many colonoscopy practices use deep sedation to provide comfort for the patients, which adds to the overall cost of the procedure. There is still a lack of widespread acceptance of the use of colonoscopies (*vs* other non-invasive screening techniques), as up to 75% of patients diagnosed with colon cancer present with locally advanced disease[32]. In addition, 1 in 10 patients has developed interval cancers after clear colonoscopies. Beyond the water insufflation technique, there have been new advances in the use of robotic endoscopic techniques for screening colonoscopies. These devices can give a more in-depth view of the gastrointestinal tract, decrease pain associated with endoscopy, and perform well in more challenging colons[33]. Future directions should aim at getting a true 360-degree view of the colon with minimal pain, sedation, and total procedure time. In addition, colonoscopy practices should be geared toward practices that can be safely done during the COVID pandemic without the risk of aerosolizing viral particles.

Table 1 Strengths and weaknesses of air insufflation *vs* water insufflation

AI: Strengths	AI: Weaknesses	WI: Strengths	WI: Weaknesses
Distended bowel allows for better visualization	Increased pain on insertion	Increased ADR	Decreased visualization through fluid
More widely accepted	Increased postoperative pain	Decreased looping of bowel	Longer insertion time
Current teaching method	Increased sedation requirement	Decreased sedation requirement	Not widely accepted or utilized
Current patient preference	Increased risk of perforation	Increased cecal intubation rate	

AI: Air insufflation; WI: Water insufflation; ADR: Adenoma detection rate.

REFERENCES

1 **Seeff LC**, Richards TB, Shapiro JA, Nadel MR, Manninen DL, Given LS, Dong FB, Winges LD, McKenna MT. How many endoscopies are performed for colorectal cancer screening? *Gastroenterology* 2004; **127**: 1670-1677 [PMID: 15578503 DOI: 10.1053/j.gastro.2004.09.051]

2 **Wolff WI**. Colonoscopy: history and development. *Am J Gastroenterol* 1989; **84**: 1017-1025 [PMID: 2672788]

3 **Muto T**, Bussey HJ, Morson BC. The evolution of cancer of the colon and rectum. *Cancer* 1975; **36**: 2251-2270 [PMID: 1203876 DOI: 10.1002/cncr.2820360944]

4 **Phaosawasdi K**, Cooley W, Wheeler J, Rice P. Carbon dioxide-insufflated colonoscopy: an ignored superior technique. *Gastrointest Endosc* 1986; **32**: 330-333 [PMID: 3095169 DOI: 10.1016/s0016-5107(86)71877-4]

5 **Janssens F**, Deviere J, Eisendrath P, Dumonceau JM. Carbon dioxide for gut distension during digestive endoscopy: technique and practice survey. *World J Gastroenterol* 2009; **15**: 1475-1479 [PMID: 19322921 DOI: 10.3748/wjg.15.1475]

6 **Stock C**, Ihle P, Sieg A, Schubert I, Hoffmeister M, Brenner H. Adverse events requiring hospitalization within 30 days after outpatient screening and nonscreening colonoscopies. *Gastrointest Endosc* 2013; **77**: 419-429 [PMID: 23410698 DOI: 10.1016/j.gie.2012.10.028]

7 **Hafner S**, Zolk K, Radaelli F, Otte J, Rabenstein T, Zolk O. Water infusion *vs* air insufflation for colonoscopy. *Cochrane Database Syst Rev* 2015; **26**: CD009863 [PMID: 26011829 DOI: 10.1002/14651858.CD009863.pub2]

8 **Mizukami T**, Yokoyama A, Imaeda H, Kumai K. Collapse-submergence method: simple colonoscopic technique combining water infusion with complete air removal from the rectosigmoid colon. *Digest Endosc* 2007; **19**: 43-48 [DOI: 10.1111/j.1443-1661.2007.00670.x]

9 **Leung CW**, Kaltenbach T, Soetikno R, Wu KK, Leung FW, Friedland S. Water immersion *vs* standard colonoscopy insertion technique: randomized trial shows promise for minimal sedation. *Endoscopy* 2010; **42**: 557-563 [PMID: 20593332 DOI: 10.1055/s-0029-1244231]

10 **Rex DK**, Schoenfeld PS, Cohen J, Pike IM, Adler DG, Fennerty MB, Lieb JG 2nd, Park WG, Rizk MK, Sawhney MS, Shaheen NJ, Wani S, Weinberg DS. Quality indicators for colonoscopy. *Gastrointest Endosc* 2015; **81**: 31-53 [PMID: 25480100 DOI: 10.1016/j.gie.2014.07.058]

11 **Heiken JP**, Peterson CM, Menias CO. Virtual colonoscopy for colorectal cancer screening: current status. *Cancer Imaging* 2005; **5** Spec No A: S133-S139 [PMID: 16361129 DOI: 10.1102/1470-7330.2005.0108]

12 **Vyas D**, Chang J, Goyal M, Obad N, Ramdass P, Sodavarapu S. Training surgery residents in underwater colonoscopies is more effective than training them in air-insufflation colonoscopies. *medRxiv* 2020; Epub ahead of print [DOI: 10.1101/2020.06.06.20124339]

13 **Rex DK**, Bond JH, Winawer S, Levin TR, Burt RW, Johnson DA, Kirk LM, Litlin S, Lieberman DA, Waye JD, Church J, Marshall JB, Riddell RH; U. S. Multi-Society Task Force on Colorectal Cancer. Quality in the technical performance of colonoscopy and the continuous quality improvement process for colonoscopy: recommendations of the U.S. Multi-Society Task Force on Colorectal Cancer. *Am J Gastroenterol* 2002; **97**: 1296-1308 [PMID: 12094842 DOI: 10.1111/j.1572-0241.2002.05812.x]

14 **Lieberman DA**, Weiss DG, Bond JH, Ahnen DJ, Garewal H, Chejfec G. Use of colonoscopy to screen asymptomatic adults for colorectal cancer. Veterans Affairs Cooperative Study Group 380. *N Engl J Med* 2000; **343**: 162-168 [PMID: 10900274 DOI: 10.1056/NEJM200007203430301]

15 **Imperiale TF**, Wagner DR, Lin CY, Larkin GN, Rogge JD, Ransohoff DF. Risk of advanced proximal neoplasms in asymptomatic adults according to the distal colorectal findings. *N Engl J Med* 2000; **343**: 169-174 [PMID: 10900275 DOI: 10.1056/NEJM200007203430302]

16 **Faccio L**, Frazzoni L, Hassan C, La Marca M, Paci V, Smania V, De Bortoli N, Bazzoli F, Repici A, Rex D, Cadoni S. Water exchange colonoscopy increases adenoma detection rate: a systematic review with network meta-analysis of randomized controlled studies. *Gastrointest Endosc* 2018; **88**: 589-597.e11 [PMID: 29981753 DOI: 10.1016/j.gie.2018.06.028]

17 **Jang HJ**. Training in Endoscopy: Colonoscopy. *Clin Endosc* 2017; **50**: 322-327 [PMID: 28783920 DOI: 10.5946/ce.2017.077]

18 **Leung FW**, Harker JO, Jackson G, Okamoto KE, Behbahani OM, Jamgotchian NJ, Aharonian HS, Guth PH, Mann SK, Leung JW. A proof-of-principle, prospective, randomized, controlled trial demonstrating improved outcomes in scheduled unsedated colonoscopy by the water method. *Gastrointest Endosc* 2010; **72**: 693-700 [PMID: 20619405 DOI: 10.1016/j.gie.2010.05.020]

19 **McLachlan SA**, Clements A, Austoker J. Patients' experiences and reported barriers to colonoscopy in the screening context--a systematic review of the literature. *Patient Educ Couns* 2012; **86**: 137-146 [PMID: 21640543 DOI: 10.1016/j.pec.2011.04.010]

20 **Harewood GC**, Sharma VK, de Garmo P. Impact of colonoscopy preparation quality on detection of suspected colonic neoplasia. *Gastrointest Endosc* 2003; **58**: 76-79 [PMID: 12838225 DOI: 10.1067/mge.2003.294]

21 **Ramirez FC**, Leung FW. A head-to-head comparison of the water vs. air method in patients undergoing screening colonoscopy. *J Interv Gastroenterol* 2011; **1**: 130-135 [PMID: 22163084 DOI: 10.4161/jig.1.3.18512]

22 **Rex DK**, Imperiale TF, Latinovich DR, Bratcher LL. Impact of bowel preparation on efficiency and cost of colonoscopy. *Am J Gastroenterol* 2002; **97**: 1696-1700 [PMID: 12135020 DOI: 10.1111/j.1572-0241.2002.05827.x]

23 **Cadoni S**, Gallittu P, Sanna S, Fanari V, Porcedda ML, Erriu M, Leung FW. A two-center randomized controlled trial of water-aided colonoscopy *vs* air insufflation colonoscopy. *Endoscopy* 2014; **46**: 212-218 [PMID: 24218307 DOI: 10.1055/s-0033-1353604]

24 **Sharma VK**, Nguyen CC, Crowell MD, Lieberman DA, de Garmo P, Fleischer DE. A national study of cardiopulmonary unplanned events after GI endoscopy. *Gastrointest Endosc* 2007; **66**: 27-34 [PMID: 17591470 DOI: 10.1016/j.gie.2006.12.040]

25 **Rapelli S**, Montorfano G, Gornati R, Berra B. Tissue and serum gangliosides determination in patients with meningiomas. *Ital J Biochem* 1989; **38**: 289A-291A [PMID: 2583983 DOI: 10.1016/j.giec.2014.11.002]

26 **Chaubal A**, Pandey V, Patel R, Poddar P, Phadke A, Ingle M, Sawant P. Difficult colonoscopy: air, carbon dioxide, or water insufflation? *Intest Res* 2018; **16**: 299-305 [PMID: 29743844 DOI: 10.5217/ir.2018.16.2.299]

27 **Ransibrahmanakul K**, Leung J, Mann S; Siao-Salera R; Lim B; Hasyagar C; Yen D; Nastaskin I; Leung F. Water Infusion in Lieu of Air Insufflation (Water Method) Diminished Discomfort in Patients Undergoing Minimal Sedation Colonoscopy in the Hands of Supervised Trainees. *Am J Gastroenterol* 2009; **104**: S509-S510

28 **Hsieh YH**, Lin HJ, Tseng KC. Limited water infusion decreases pain during minimally sedated colonoscopy. *World J Gastroenterol* 2011; **17**: 2236-2240 [PMID: 21633535 DOI: 10.3748/wjg.v17.i17.2236]

29 **ASGE Standards of Practice Committee**, Fisher DA, Maple JT, Ben-Menachem T, Cash BD, Decker GA, Early DS, Evans JA, Fanelli RD, Fukami N, Hwang JH, Jain R, Jue TL, Khan KM, Malpas PM, Sharaf RN, Shergill AK, Dominitz JA. Complications of colonoscopy. *Gastrointest Endosc* 2011; **74**: 745-752 [PMID: 21951473 DOI: 10.1016/j.gie.2011.07.025]

30 **Leung FW**, Aljebreen AM, Brocchi E, Chang EB, Liao WC, Mizukami T, Schapiro M, Triantafyllou K. Sedation-risk-free colonoscopy for minimizing the burden of colorectal cancer screening. *World J Gastrointest Endosc* 2010; **2**: 81-89 [PMID: 21160707 DOI: 10.4253/wjge.v2.i3.81]

31 **Papanikolaou IS**, Karatzas PS, Varytimiadis LT, Tsigaridas A, Galanopoulos M, Viazis N, Karamanolis DG. Effective colonoscopy training techniques: strategies to improve patient outcomes. *Adv Med Educ Pract* 2016; **7**: 201-210 [PMID: 27099542 DOI: 10.2147/AMEP.S99617]

32 **Johnston PG**. The Colorectal Cancer Coalition: reflections on the future. *Oncologist* 2006; **11**: 970-972 [PMID: 17030636 DOI: 10.1634/theoncologist.11-9-970]

33 **Cater D**, Vyas A, Vyas D. Robotics in Colonoscopy. *Am J Robot Surg* 2014; **1**: 48-54 [PMID: 26380845 DOI: 10.1166/ajrs.2014.1008]

World Journal of Gastroenterology

Submit a Manuscript: https://www.f6publishing.com

World J Gastroenterol 2021 January 21; 27(3): 240-254

DOI: 10.3748/wjg.v27.i3.240

ISSN 1007-9327 (print) ISSN 2219-2840 (online)

ORIGINAL ARTICLE

Basic Study

Circular RNA AKT3 governs malignant behaviors of esophageal cancer cells by sponging miR-17-5p

Hong-Liang Zang, Fu-Jian Ji, Hai-Ying Ju, Xiao-Feng Tian

ORCID number: Hong-Liang Zang 0000-0002-9837-0805; Fu-Jian Ji 0000-0002-6041-6089; Hai-Ying Ju 0000-0001-8243-5224; Xiao-Feng Tian 0000-0002-6544-0395.

Author contributions: Zang HL contributed to the study design and reviewed the manuscript; Ji FJ and Tian XF analyzed the data and wrote the manuscript; Ju HY and Zang HL contributed to the data collection, data interpretation, and manuscript writing; all authors read and approved the final manuscript.

Institutional review board statement: This research was reviewed and approved by the Ethics Committee of China-Japan Union Hospital of Jilin University and complied with the guidelines of Declaration of Helsinki.

Institutional animal care and use committee statement: The procedures were in accordance with guidelines of Animal Use and Care Committee of China-Japan Union Hospital of Jilin University.

Conflict-of-interest statement: All the authors have no conflict of interest related to the manuscript.

Data sharing statement: No additional data are available.

Hong-Liang Zang, Xiao-Feng Tian, Department of Hepatobiliary and Pancreatic Surgery, China-Japan Union Hospital of Jilin University, Changchun 130033, Jilin Province, China

Fu-Jian Ji, Department of Colorectal Surgery, China-Japan Union Hospital of Jilin University, Changchun 130033, Jilin Province, China

Hai-Ying Ju, Department of Hematology, Jilin Province Blood Center, Changchun 130000, Jilin Province, China

Corresponding author: Xiao-Feng Tian, MD, Chief Doctor, Department of Hepatobiliary and Pancreatic Surgery, China-Japan Union Hospital of Jilin University, No. 126 Xiantai Street, Erdao District, Changchun 130033, Jilin Province, China. fengwykctut4210@163.com

Abstract

BACKGROUND

Recent studies have demonstrated that circular RNA AKT3 (circAKT3) plays a crucial role in regulating the malignant phenotypes of tumor cells. However, the potential effects of circAKT3 on esophageal cancer have not been investigated.

AIM

To illuminate the role of circAKT3 in malignant behaviors of esophageal cancer cells and its underlying mechanism.

METHODS

Clinical samples were collected to detect the expression of *circAKT3*. The role of circAKT3 in proliferation, migration, invasion, and apoptosis of esophageal cancer cells was evaluated using Cell Counting Kit-8, wound healing assays, Transwell assays, and fluorescence analysis, respectively. The target of circAKT3 was screened and identified using an online database and luciferase reporter assay. A xenograft nude mouse model was established to investigate the role of circAKT3 *in vivo*.

RESULTS

In vitro assays showed that proliferative, migratory, and invasive capacities of esophageal cancer cells were significantly enhanced by *circAKT3* overexpression. Furthermore, miR-17-5p was screened as the target of circAKT3, and miR-17-5p antagonized the effects of circAKT3 on esophageal cancer cells. Moreover, we identified RHOC and STAT3 as the direct target molecules of miR-17-5p, and

ARRIVE guidelines statement: The authors have read the ARRIVE guidelines, and the manuscript was prepared and revised according to the ARRIVE guidelines.

Manuscript source: Unsolicited manuscript

Specialty type: Gastroenterology and hepatology

Country/Territory of origin: China

Peer-review report's scientific quality classification

Grade A (Excellent): A
Grade B (Very good): 0
Grade C (Good): 0
Grade D (Fair): 0
Grade E (Poor): 0

Received: October 30, 2020
Peer-review started: October 30, 2020
First decision: November 30, 2020
Revised: December 4, 2020
Accepted: December 16, 2020
Article in press: December 16, 2020
Published online: January 21, 2021

P-Reviewer: Kravtsov V
S-Editor: Chen XF
L-Editor: Filipodia
P-Editor: Ma YJ

circAKT3 facilitated expression of *RHOC* and *STAT3* by inhibiting miR-17-5p. *In vivo* assays showed *circAKT3* knockdown inhibited growth of esophageal cancer.

CONCLUSION

CircAKT3 contributed to the malignant behaviors of esophageal cancer *in vitro* and *in vivo* by sponging miR-17-5p thus providing a potential target for treatment of esophageal cancer.

Key Words: Esophageal cancer; Circular RNA AKT3; miR-17-5p; Proliferation; Migration; Invasion

Core Tip: Circular RNA AKT3 was overexpressed in esophageal cancer and enhanced proliferative, migratory, and invasive capacities of esophageal cancer cells by sponging miR-17-5p to exert protumor effects. Downregulation of circular RNA AKT3 inhibited xenograft tumor growth of esophageal cancer *in vivo*. This research provided a potential target for better understanding the underlying mechanism of esophageal cancer.

Citation: Zang HL, Ji FJ, Ju HY, Tian XF. Circular RNA AKT3 governs malignant behaviors of esophageal cancer cells by sponging miR-17-5p. *World J Gastroenterol* 2021; 27(3): 240-254
URL: https://www.wjgnet.com/1007-9327/full/v27/i3/240.htm
DOI: https://dx.doi.org/10.3748/wjg.v27.i3.240

INTRODUCTION

As one of the most malignant tumors, esophageal cancer ranks in the top ten in morbidity and mortality of the tumors worldwide[1]. However, the exact mechanism is still in discussion. Currently, surgery is the predominant approach for treatment of esophageal cancer in combination with some other alternatives[2,3]. Although great progress has been made in the diagnosis and treatment of esophageal cancer, the prognosis has not been improved satisfactorily with a 5-year survival rate of less than 30%[4]. Thus, investigating the underlying mechanism is conducive to deepening the pathogenesis of esophageal cancer and developing targeted therapies.

Circular RNAs (circRNAs) belong to endogenous noncoding RNAs, which could be expressed in eukaryotic cells[5]. Unlike other RNA molecules, circRNAs possess the structure of a closed loop and cannot be degraded by RNase R[6]. Accumulating evidence has demonstrated that circRNAs participate in the modulation of protein expression by sponging microRNAs (miRNAs) or interacting with RNA binding proteins[7,8]. In tumor tissues and cell lines, the aberrant expression of circRNAs is involved in the regulation of malignant phenotypes of tumor cells. Wang *et al*[9] reported that circLMTK2 is overexpressed in gastric cancer, which could also be a predictor for a poor prognosis in patients with gastric cancer. In colorectal cancer, *circFBXW7* is significantly downregulated, and *circFBXW1* overexpression suppresses proliferative, migratory, and invasive abilities of colorectal cancer cells[10]. Therefore, differential expression of circRNAs exerts the opposite effects on tumor cells. However, only a few studies have concentrated on the effects of circRNAs on esophageal cancer.

Circular RNA AKT3 (circAKT3) is a novel molecule, which is derived from the *AKT3* gene and identified in gastric cancer with cisplatin resistance[11]. The *in vitro* and *in vivo* assays have revealed that circAKT3 is overexpressed in cisplatin resistant-gastric cancer and leads to the increased expression of *PIK3R1* to mediate resistance of gastric cancer cells to cisplatin[11]. However, Xia *et al*[12] demonstrated that glioblastoma expressed a low level of *circAKT3*, and *circAKT3* overexpression suppressed proliferation and promoted sensitivity to radiation of glioblastoma cells. The contradictory findings remind us of the potential role of circAKT3 in esophageal cancer.

MATERIALS AND METHODS

Collection of clinical samples

The clinical tissue samples were acquired from patients with esophageal cancer (n = 82) who underwent surgery at China-Japan Union Hospital of Jilin University. The relative expression of *circAKT3* less than the mean value was classified into the circAKT3 low group (n = 43), and the relative expression of *circAKT3* more than the mean value was classified into the circAKT3 high group (n = 39).

In vivo assay

The nude mice (n = 12) were purchased from Experimental Animal Center of China-Japan Union Hospital of Jilin University, housed in cages under the condition of the 12-h shift of light-dark cycles, and randomly divided into two groups. Negative control short hairpin RNA and short hairpin RNA against circAKT3, purchased from Integrated Biotech Solutions Co. (China), were transfected into TE-1 cells in the presence of puromycin (3 mg/mL; Thermo Fisher Scientific, United States) to establish the *circAKT3* knockdown cell lines. The mice injected with the negative control short hairpin RNA-transfected TE-1 cells were designated as the negative control short hairpin RNA group, and mice injected with the short hairpin RNA against circAKT3-transfected TE-1 cells were designated as the short hairpin RNA against circAKT3 group. After feeding for 30 d, the mice were anesthetized with pentobarbital sodium (25 mg/kg; Sigma-Aldrich, United States) intraperitoneally and killed by decapitation. The xenografts were isolated carefully and weighed.

Cell culture

Human esophageal cancer cell lines (KYSE-150, TE-10, TE-1) and human embryonic kidney cell line (HEK-293T) were cultured in Dulbecco's Modified Eagle Medium containing 10% fetal bovine serum (Gibco, United States). Human normal esophageal epithelial cell line (HEEC) was cultured in Dulbecco's Modified Eagle Medium with high glucose containing 10% fetal bovine serum (Gibco, United States). All of the cells were cultured in a CO_2 incubator chamber (Thermo Fisher Scientific, United States).

Quantitative real time-polymerase chain reaction

TRIzol (Ambion, United States) was utilized to extract the total RNA. SuperScript III (Invitrogen, United States) was used to obtain cDNA. SYBR Premix Ex Taq II (Takara, Japan) was utilized to perform quantitative real time(qRT)-PCR. The primer sequences of circAKT3 and U6 were adopted as previously reported[11]. The primer sequences of miR-17-5p were obtained from recent research[13]. The primer sequences of AKT3, RHOC, STAT3, and GAPDH were obtained from the NCBI online database (https://www.ncbi.nlm.nih.gov/gene/). CircAKT3 (forward, 5′-TCCAAATAAACGCCTTGGTGG-3′; reverse, 5′-CCTCAGAGAACACCCGCTCT-3′); miR-17-5p (forward, 5′-CGGCGGCAAAGTGCTTACAG-3′; reverse, 5′-GTGCAGGGTCCGAGGT-3′); U6 (forward, 5′-CTCGCTTCGGCAGCACA-3′; reverse, 5′-AACGCTTCACGAATTTGCGT-3′); AKT3 (forward, 5′-CGGCTTTCTCACGGATCACA-3′; reverse, 5′-CGGGACACTTTCCTTCCTCC-3′); RHOC (forward, 5′-AAGTTCCCTTTGCCCGTCTG-3′; reverse, 5′-ACAGTGGCAACTCAAGGGTC-3′); STAT3 (forward, 5′-CCAGGTACCGTGTGTCAAGC-3′; reverse, 5′-CAGACCTGACACCTGTGTTG-3′); GAPDH (forward, 5′-TGAAATGTGCACGCACCAAG-3′; reverse, 5′-GGGAAGCAGCATTCAGGTCT-3′). All of the primers were synthesized by Sangon (China).

Cell transfection

The siRNAs against circAKT3, miR-17-5p mimics, miR-17-5p inhibitor, indicated negative control, and plasmids were synthesized and purchased from Sangon (China). Lipofectamine 3000 (Invitrogen, United States) was used to conduct the transfection. RNase R (Epicentre, United States) was used to digest linear RNAs (but not circRNAs) in line with the manufacturer's instruction.

Fluorescence analysis

The Hoechst Staining Kit (Beyotime, China) was used to evaluate apoptotic cells. In brief, TE-1 cells were seeded at a density of 2.0×10^5 cells per well. After cell transfection with indicated vectors, 4% paraformaldehyde was used to fix the cultured TE-1 cells, followed by using Hoechst 33258 to stain the cells. A fluorescence microscope (Olympus, Japan) was utilized to observe the cells.

Measurement of cell viability

The Cell Counting Kit-8 (CCK-8; Beyotime, China) was utilized to measure cell viability. After transfection, TE-1 cells were seeded at a density of 1×10^4 cells per well for the indicated time. CCK-8 solution was added into each well for 2 h, and the Microplate Reader (Bio-Rad, United States) was used to record the value at 450 nm.

Wound healing assay

The wound healing assay was used to measure the migratory ability. After transfection, TE-1 cells were seeded into a 6-well plate for 24 h. The cells were scratched by a 10 mL Finntip and cultured in serum-free medium. Images were captured at 0 h and 24 h and analyzed by ImageJ software.

Measurement of invasive ability

The Transwell assay was conducted to evaluate the invasive ability. TE-1 cells with indicated transfection were cultured in Millicell Standing Cell Culture 24 well (Millipore, United States). After incubation for 24 h, glutaraldehyde solution was used to fix the cells, and crystal violet was used to stain the cells.

Luciferase reporter assay

ENCORI database was used to acquire the predicted binding sites between circAKT3 and miR-17-5p. TargetScanHuman database was utilized to acquire the potential binding sites of miR-17-5p with RHOC or STAT3. The procedures of the luciferase reporter assay were conducted in line with the previous study[11]. In our research, HEK-293T cells were utilized to detect the binding ability by cotransfecting the indicated vectors (Sangon, China) with Lipofectamine 3000 (Invitrogen, United States). The luciferase activity was evaluated by Bio-Glo™ Luciferase Assay System (Promega, United States).

Western blot

Western blot was carried out in line with the previous report[14]. In brief, the total protein was lysed by RIPA lysis buffer (Beyotime, China), and the BCA Kit (Thermal Fisher Scientific, United States) was used to detect the precise concentration. The total protein was added into SDS-PAGE gel (Beyotime, China). Primary antibodies [STAT3 rabbit monoclonal antibody (Cell Signaling Technology, United States); RHOC rabbit monoclonal antibody (Cell Signaling Technology, United States); GAPDH mouse monoclonal antibody (Cell Signaling Technology, United States)] were used overnight at 4 °C. Secondary antibodies with horseradish peroxidase (Beyotime, China) were applied for 2 h, and the indicated proteins were monitored by ChemDoc™ XRS+ System (Bio-Rad, United States).

Statistical analysis

The data in our research were displayed as mean ± standard deviation and analyzed by GraphPad Prism 8.0 Software (GraphPad, United States). The *t*-test, two-way ANOVA or Chi-squared test was used. Statistical significance was set as the *P* value less than 0.05.

RESULTS

CircAKT3 was overexpressed in esophageal cancer

First, we detected the expression of *circAKT3* in the esophageal cancer tissue samples and cell lines. The qRT-PCR results showed that circAKT3 was significantly upregulated in esophageal cancer tissue samples (Figure 1A). The characteristic analysis of the patients with esophageal cancer indicated that the tumor size, lymphatic metastasis, and clinical tumor node metastasis staging were positively related to the upregulation of circAKT3 in the tissue samples (Table 1). We also found that human esophageal cancer cell lines TE-1 cells, TE-10 cells, and KYSE-150 cells expressed a significantly higher level of circAKT3 compared to human normal esophageal epithelial cell line HEEC cells (Figure 1B).

CircAKT3 promoted malignant behaviors of TE-1 cells

Next, siRNAs against circAKT3 were transfected into TE-1 cells, and qRT-PCR analysis revealed a marked efficiency of *circAKT3* knockdown (Figure 1C). As the differential structure between circAKT3 and AKT3 mRNA, circAKT3 was resistant to RNase R,

Table 1 Characteristics of patients with esophageal cancer

Characteristic	CircAKT3 low	CircAKT3 high	*P* value
Age in yr			0.824
< 50	19	19	
≥ 50	24	20	
Tumor diameter in cm			0.026
< 3	27	14	
≥ 3	16	25	
Lymphatic metastasis			0.027
No	24	12	
Yes	19	27	
TNM staging			0.016
I-II	26	13	
III-IV	17	26	

CircAKT3: Circular RNA AKT3; TNM: Tumor node metastasis.

while AKT3 mRNA was sensitive to RNase R (Figure 1C and 1D), which confirmed the circular structure of circAKT3. Moreover, the *circAKT3* overexpression plasmids were transfected into TE-1 cells and could significantly increase the expression of *circAKT3* (Figure 1E). CCK-8 assay showed that circAKT3 siRNAs inhibited proliferation of TE-1 cells, while *circAKT3* overexpression plasmids facilitated proliferation of TE-1 cells (Figure 1F). We also found that *circAKT3* knockdown suppressed migration and invasion of TE-1 cells, while *circAKT3* overexpression exerted the opposite role by conducting the wound healing assay and Transwell assay, respectively (Figure 1G and 1H). We also measured the effect of circAKT3 on apoptosis. The fluorescence analysis indicated that circAKT3 siRNAs increased the number of condensed nuclei in TE-1 cells; however, *circAKT3* overexpression had no effect on the apoptotic rate of TE-1 cells (Figure 1I). These findings suggested that circAKT3 facilitated proliferative, migratory, and invasive capacities of esophageal cancer cells.

miR-17-5p acted as the downstream molecule of circAKT3 to antagonize the effects of circAKT3 on TE-1 cells

Accumulating evidence has reported that circRNAs regulate cell functions by sponging miRNAs[7]. The ENCORI database (http://starbase.sysu.edu.cn/index.php) was utilized to predict the potential target of circAKT3, and we identified miR-17-5p as the target of circAKT3. We carried out a luciferase reporter assay and found that TE-1 cells with wild-type circAKT3 and miR-17-5p mimics cotransfection presented a remarkably decreased luciferase activity (Figure 2A). Next, we detected the expression of *miR-17-5p* and found a lower level of miR-17-5p in esophageal cancer tissue samples (Figure 2B). Moreover, *miR-17-5p* expression was inversely associated with the expression of *circAKT3* in clinical tissue samples (Figure 2C). Meanwhile, esophageal cancer cell lines showed decreased expression of *miR-17-5p* (Figure 2D). These results indicated that miR-17-5p was inhibited by circAKT3. We then explored the role of miR-17-5p functioning as a downstream molecule of circAKT3 in TE-1 cells. CCK-8 assay showed that cell viability of TE-1 cells with cotransfection of *circAKT3* overexpression plasmids and miR-17-5p mimics was decreased compared to that with *circAKT3* overexpression plasmids transfection (Figure 2E). Moreover, miR-17-5p mimics suppressed migratory and invasive abilities of *circAKT3* overexpression plasmids-transfected TE-1 cells by the wound healing assay and Transwell assay, respectively (Figure 2F and 2G). In parallel, miR-17-5p mimics increased the apoptotic rate of *circAKT3* overexpression plasmids-transfected TE-1 cells (Figure 2H).

RHOC and STAT3 were modulated by the circAKT3/miR-17-5p axis

We then identified RHOC and STAT3 as the potential targets of miR-17-5p by using TargetScanHuman database (http://www.targetscan.org/vert_72/). The luciferase

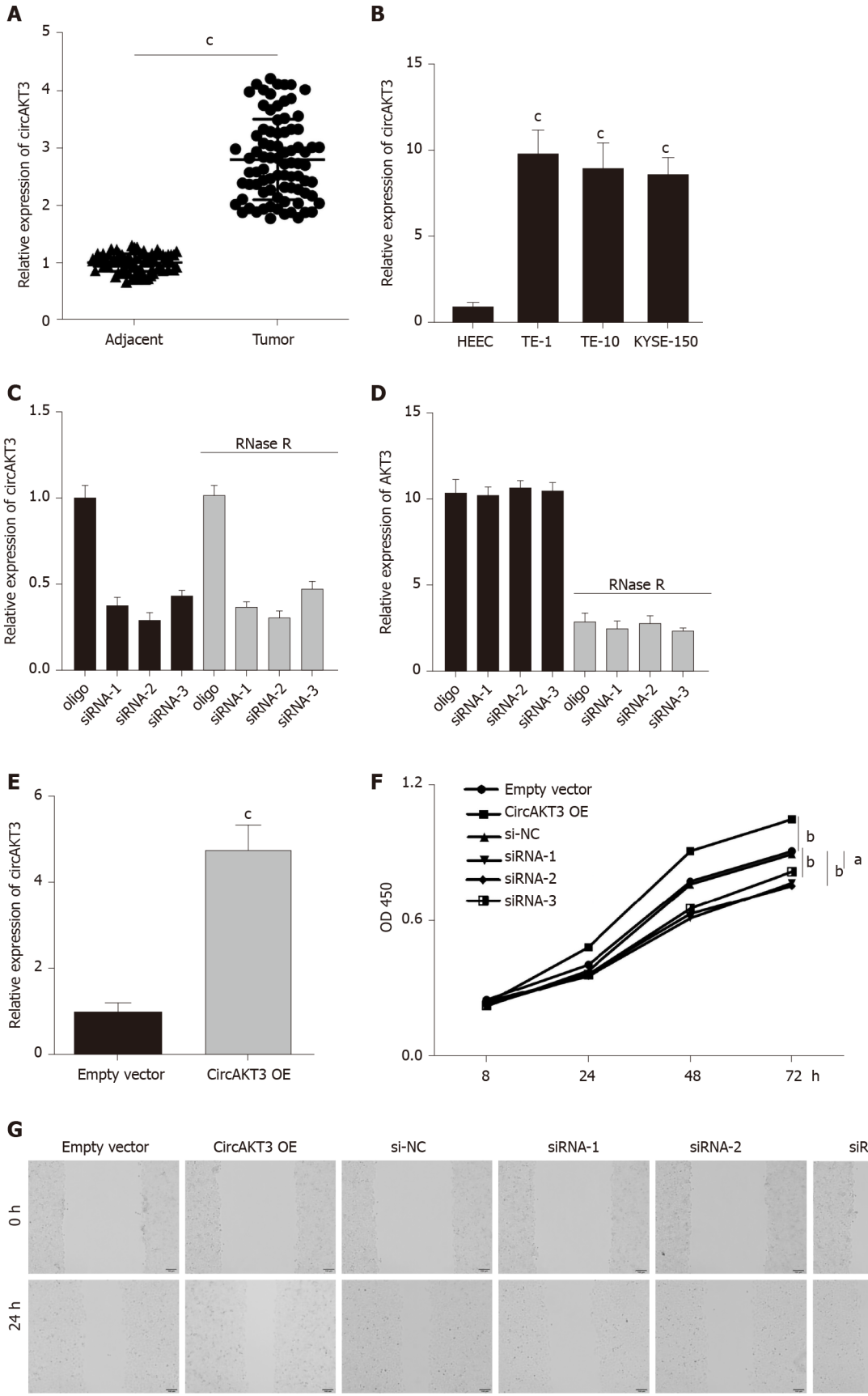
A
Relative expression of circAKT3
c
Adjacent
Tumor
B
Relative expression of circAKT3
c
c
c
HEEC
TE-1
TE-10
KYSE-150
C
Relative expression of circAKT3
RNase R
oligo
siRNA-1
siRNA-2
siRNA-3
D
Relative expression of AKT3
RNase R
E
Relative expression of circAKT3
c
Empty vector
CircAKT3 OE
F
OD 450
Empty vector
CircAKT3 OE
si-NC
siRNA-1
siRNA-2
siRNA-3
b
b
b
a
8
24
48
72 h
G
Empty vector
CircAKT3 OE
si-NC
siRNA-1
siRNA-2
siRNA-3
0 h
24 h

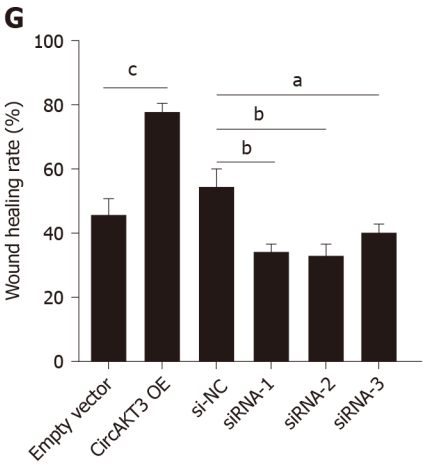
G
Wound healing rate (%)
100
80
60
40
20
0
c
a
b
b
Empty vector
CircAKT3 OE
si-NC
siRNA-1
siRNA-2
siRNA-3

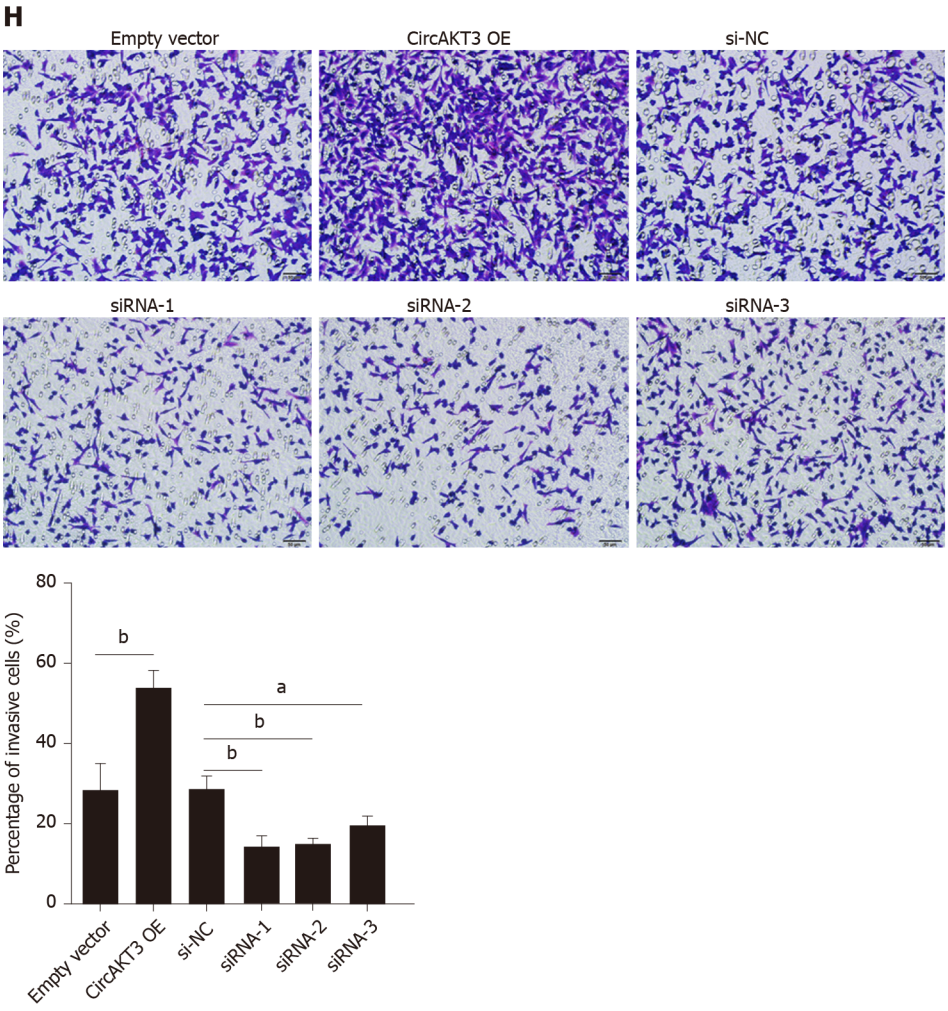
H
Empty vector
CircAKT3 OE
si-NC
siRNA-1
siRNA-2
siRNA-3
Percentage of invasive cells (%)
80
60
40
20
0
b
a
b
b
Empty vector
CircAKT3 OE
si-NC
siRNA-1
siRNA-2
siRNA-3

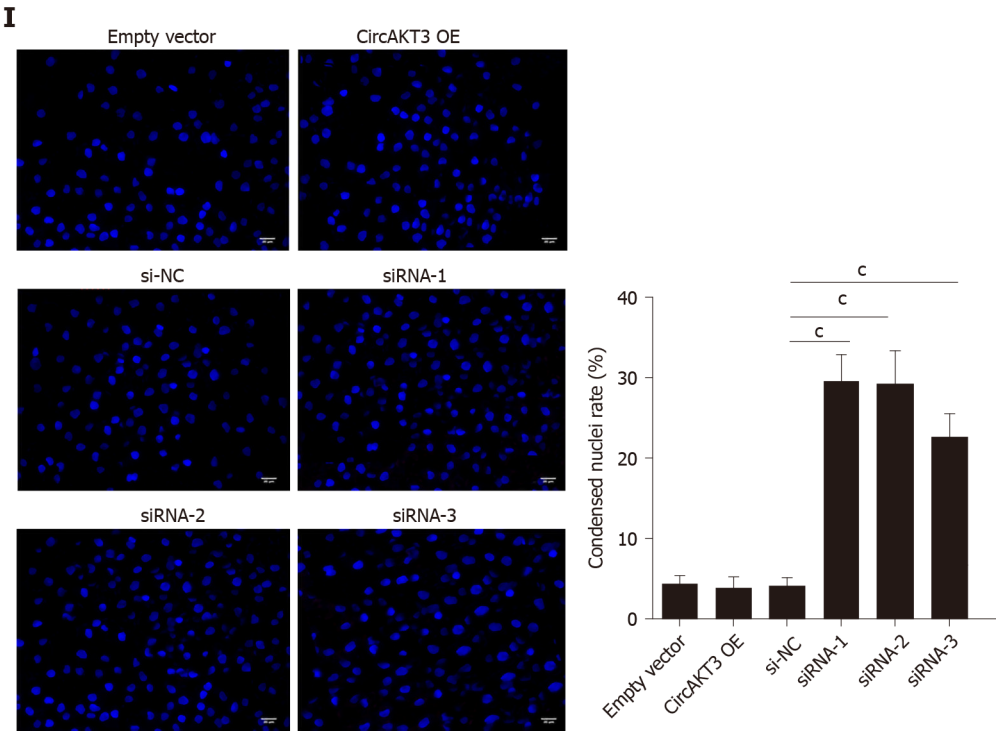

Figure 1 Circular RNA AKT3 promoted malignant phenotypes of TE-1 cells. A: The expression of *circular RNA AKT3* (*circAKT3*) in tissue samples; B: The expression of *circAKT3* human normal esophageal epithelial cell line (HEEC) and human esophageal cancer cell lines; C and D: TE-1 cells were transfected with control oligo and circAKT3 siRNAs in the presence or absence of RNase R to detect the expression of *circAKT3* and *AKT3*; E: The expression of *circAKT3* in TE-1 cells with *circAKT3* overexpression (OE); F: Cell viability of TE-1 cells as detected by the Cell Counting Kit-8 assay was performed to detect cell viability of TE-1 cells with indicated transfection; G: Migratory capacity of TE-1 cells with *circAKT3* OE and knockdown; H: Invasive ability of TE-1 cells with *circAKT3* OE and knockdown; I: Apoptosis of TE-1 cells with *circAKT3* OE and knockdown by Hoechst staining. $^{a}P < 0.05$; $^{b}P < 0.01$; $^{c}P < 0.001$. NC: Negative control; OD: Optical density.

reporter assay showed that TE-1 cells with cotransfection of wild-type RHOC and miR-17-5p mimics presented a lower luciferase activity (Figure 3A). In addition, the decreased luciferase activity was also shown in TE-1 cells with cotransfection of wild-type STAT3 and miR-17-5p mimics (Figure 3B). Next, we detected the mRNA level of RHOC and STAT3 in clinical samples and found that both RHOC and STAT3 were upregulated in esophageal cancer tissue samples (Figure 3C and 3D). Moreover, the expression of *RHOC* and *STAT3* was increased in TE-1 cells, TE-10 cells, and KYSE-150 cells (Figure 3E and 3F). Western blot analysis showed that circAKT3 promoted the expression of RHOC and STAT3 in TE-1 cells, and miR-17-5p led to the reduced expression of RHOC and STAT3, which was reversed by circAKT3 overexpression plasmids cotransfection (Figure 3G). Conversely, circAKT3 siRNA inhibited the expression of RHOC and STAT3 in TE-1 cells, and a miR-17-5p inhibitor promoted the expression of RHOC and STAT3, which was reverted by circAKT3 siRNA cotransfection (Figure 3H). In consequence, circAKT3 facilitated the expression of RHOC and STAT3 by sponging miR-17-5p in esophageal cancer cells.

CircAKT3 knockdown suppressed growth of esophageal cancer in vivo

CircAKT3 shRNA was transfected into TE-1 cells to establish the stable *circAKT3* knockdown cell line (Figure 4A). The *in vivo* assay showed that the size and weight of the xenograft tumor injected with circAKT3 shRNA-transfected TE-1 cells were smaller and lighter (Figure 4B and 4C). The qRT-PCR analysis indicated that the xenograft tumor injected with circAKT3 shRNA-transfected TE-1 cells expressed a lower level of circAKT3, RHOC, and STAT3 and a higher level of miR-17-5p (Figure 4D-G). In parallel, the protein levels of RHOC and STAT3 were decreased in the xenograft tumor injected with circAKT3 shRNA-transfected TE-1 cells (Figure 4H).

DISCUSSION

Increased proliferative, migratory, and invasive abilities are hallmarks of tumor cells[15]. Thus, exploring the exact mechanism of malignant phenotypes of tumor cells

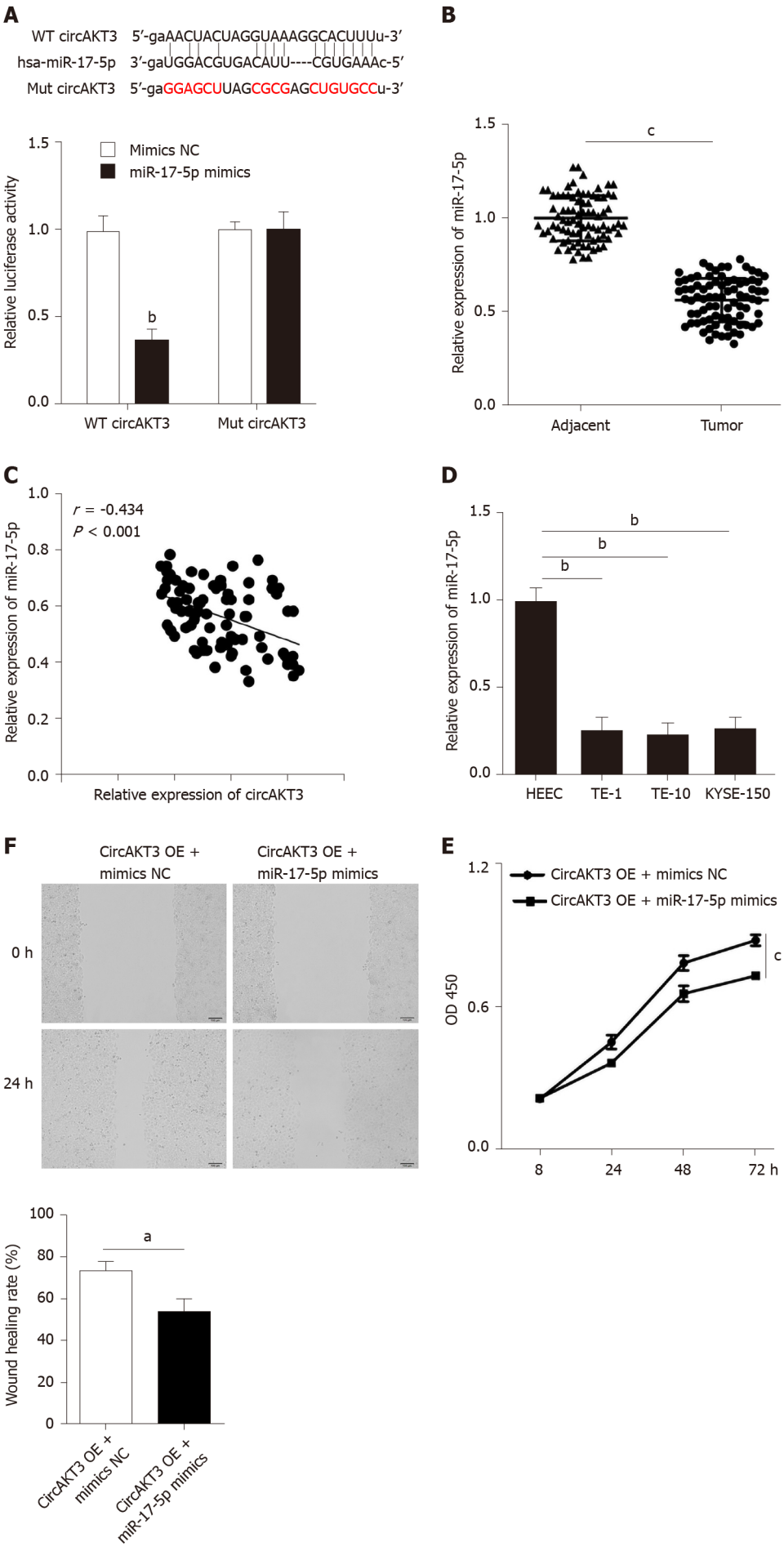
A
WT circAKT3 5′-gaAACUACUAGGUAAAGGCACUUUu-3′
hsa-miR-17-5p 3′-gaUGGACGUGACAUU----CGUGAAAc-5′
Mut circAKT3 5′-gaGGAGCUUAGCGCGAGCUGUGCCu-3′
B
C
D
E
F
Mimics NC
miR-17-5p mimics
Relative luciferase activity
WT circAKT3
Mut circAKT3
Relative expression of miR-17-5p
Adjacent
Tumor
r = -0.434
P < 0.001
Relative expression of circAKT3
HEEC
TE-1
TE-10
KYSE-150
CircAKT3 OE + mimics NC
CircAKT3 OE + miR-17-5p mimics
0 h
24 h
OD 450
Wound healing rate (%)

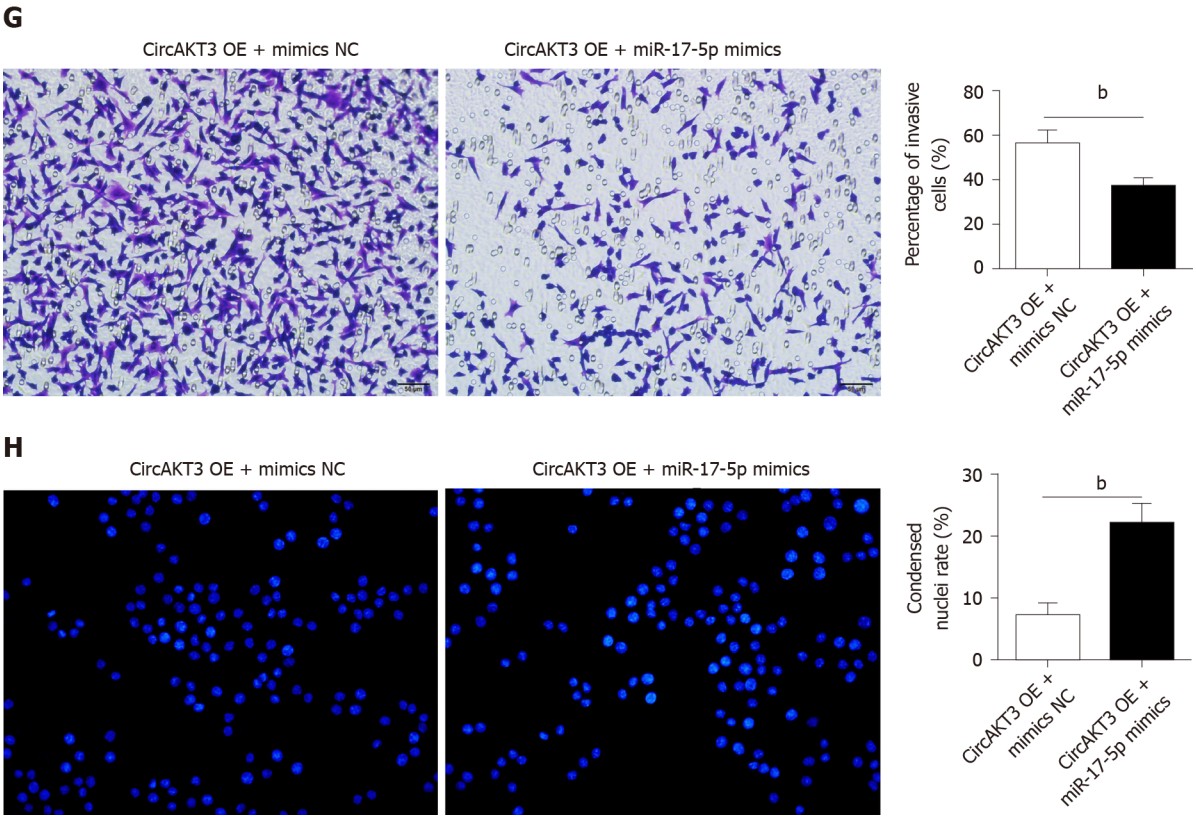

Figure 2 miR-17-5p acted as the downstream molecule of *circular RNA AKT3* to antagonize the effects of circular RNA AKT3 on TE-1 cells. A: Schematic of the miR-17-5p binding sites in wild-type (WT) *circular RNA AKT3* (*circAKT3*) and the mutant (Mut) *circAKT3* (up). Luciferase reporter assay was performed in HEK-293T cells to determine the binding ability between miR-17-5p and circAKT3 (down); B: The expression of *miR-17-5p* in tissue samples; C: CircAKT3 was negatively correlated with miR-17-5p in esophageal cancer tissue samples; D: *miR-17-5p* expression in indicated cell lines; E-H: Cell viability (E), migratory ability (F), invasive ability (G), and apoptosis (H) of *circAKT3* overexpression (OE)-transfected TE-1 cells in the presence or absence of miR-17-5p mimics. [a] $P < 0.05$; [b] $P < 0.01$; [c] $P < 0.001$. HEEC: Human normal esophageal epithelial cell line; NC: Negative control; OD: Optical density.

contributes to clarifying the pathogenesis of tumorigenesis. Herein, we reported the protumor role of circAKT3 in esophageal cancer cells by measuring the proliferative, migratory, and invasive abilities. In addition, miR-17-5p acted as a sponge molecule to inhibit the effects of circAKT3 on esophageal cancer cells. Furthermore, two protumor molecules, RHOC and STAT3, were the direct downstream targets of miR-17-5p, and circAKT3 upregulated RHOC and STAT3 by inhibiting miR-17-5p in esophageal cancer cells. Finally, we found *circAKT3* knockdown inhibited growth of esophageal cancer *in vivo*.

CircRNAs function among the complex molecular network and are implicated in the expression of functional proteins[5,7]. Mechanistically, the inhibitory effect of circRNAs on miRNAs is one of the predominant mechanisms involving regulation of proteins[7]. Increasing evidence has focused on the effects of circRNAs on the modulation of malignant phenotypes of tumor cells; however, only a few studies explore the relationship between circRNAs and esophageal cancer. A recent study reported that circZNF292 is upregulated in the esophageal cancer cell line Eca-109, and inhibition of circZNF292 enhanced the expression of *miR-206* to limit the proliferative, migratory, and invasive ability of Eca-109 cells[16]. In addition, Shi *et al*[17] demonstrated that overexpressed circPRKCI promoted the expression of *AKT3* by inhibiting miR-3680-3p to facilitate proliferation and migration of esophageal cancer cells. In addition, circSMAD7[18] and circFOXO3[19] could sponge different miRNAs to suppress malignant phenotypes of esophageal cancer cells. Therefore, it can be inferred that circRNAs exert the opposite roles in development and progression of esophageal cancer.

Our research identified circAKT3 as a motivator in development and progression of esophageal cancer cells. The gene symbol of circAKT3 is *AKT3*, which is a key member of the PI3K/AKT signaling pathway[11,20]. Previously, Huang *et al*[11] reported that *circAKT3* overexpression in gastric cancer participated in cisplatin resistance by restraining miR-198. However, the contradiction about the effects of circAKT3 on tumors is that circAKT3 could suppress development of glioblastoma[12] and

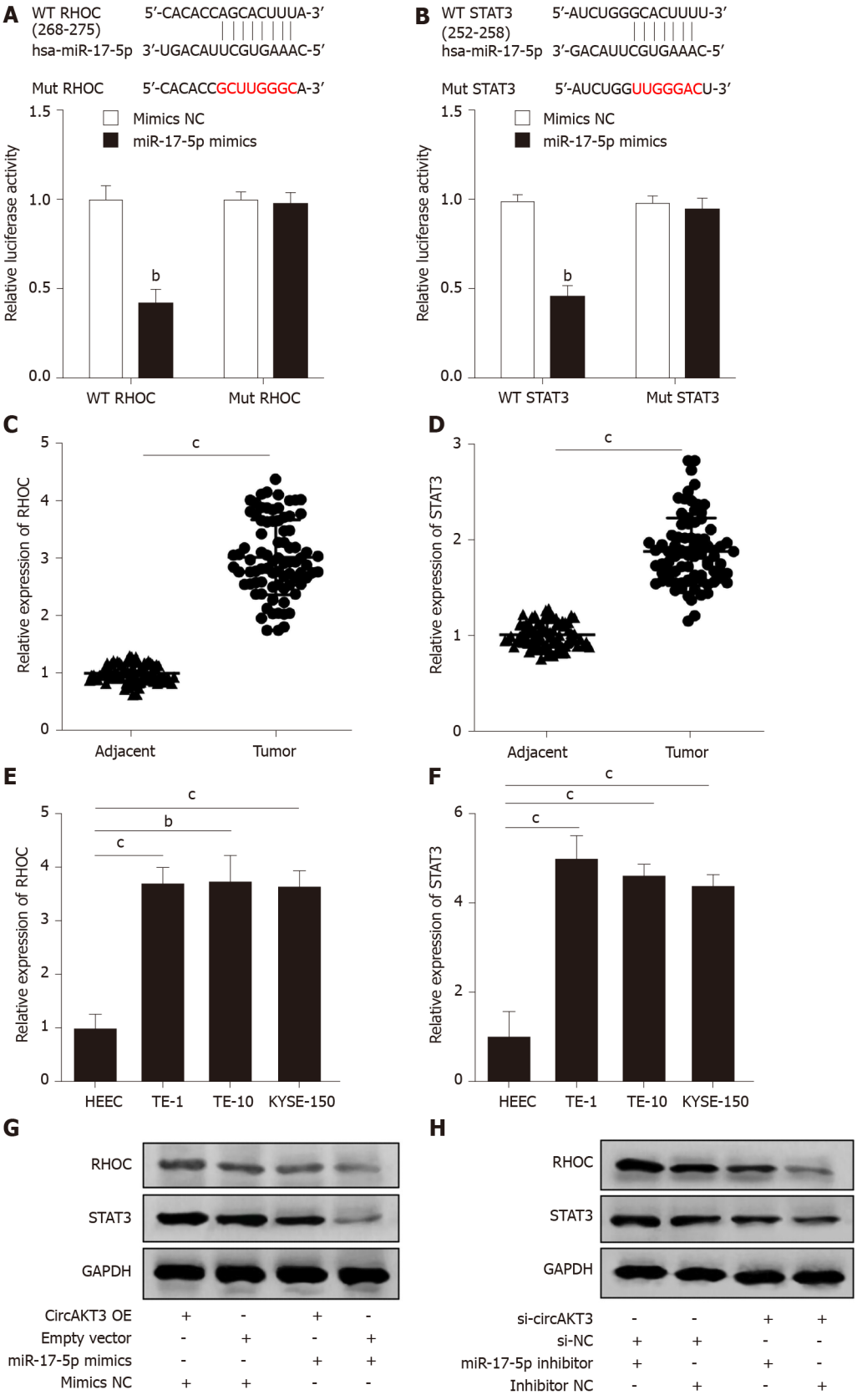

Figure 3 RHOC and STAT3 were modulated by the circular RNA AKT3/miR-17-5p axis. A: Schematic of the miR-17-5p binding sites in wild-type (WT) *RHOC* and the mutant (Mut) *RHOC* (up). Luciferase reporter assay was performed in HEK-293T cells to determine the binding ability between miR-17-5p and RHOC (down); B: Schematic of the miR-17-5p binding site in WT *STAT3* and the Mut *STAT3* (up). Luciferase reporter assay was performed in HEK-293T cells to determine the binding ability between miR-17-5p and STAT3 (down); C and D: The expression of *RHOC* (C) and *STAT3* (D) in tissue samples; E and F: The expression of *RHOC* (E) and *STAT3* (F) in indicated cell lines; G and H: Protein level of RHOC and STAT3 in TE-1 cells with indicated transfection. $^{b}P < 0.01$; $^{c}P < 0.001$. circAKT3: Circular RNA AKT3; HEEC: Human normal esophageal epithelial cell line; NC: Negative control; OE: Overexpression.

progression of clear cell renal cell carcinoma[20]. These findings, combined with our results, indicate a tumor specificity of circAKT3. Moreover, we identified miR-17-5p as a downstream molecule of circAKT3 to suppress the effects of circAKT3 on esophageal cancer cells by evaluating proliferation, migration, and invasion of TE-1 cells and found that esophageal cancer tissue samples and cell lines showed a significantly lower level of miR-17-5p. It has been reported that the expression of *miR-17-5p* decreased esophageal cancer stem-like cells and mediated radiation resistance[13], which further reinforced our findings.

Additionally, we screened two protumor molecules RHOC and STAT3 as the direct downstream targets of miR-17-5p. RHOC is one of the Ras homolog family members and functions as a protumor molecule in multiple tumors[21,22]. Clinical data shows that RHOC is positively expressed in esophageal cancer tissue samples and could be regarded as a predictor for patients with a poor prognosis of esophageal cancer[23,24]. The *in vitro* and *in vivo* experiments manifest that RHOC enhanced the proliferative and invasive capacity of esophageal cancer cells[25]. Similar to RHOC, STAT3 is a pivotal molecule that accelerates development and progression of malignant tumors[26,27]. In esophageal cancer cells, activation of STAT3 dramatically reduced apoptotic rate and contributed to increased proliferative ability[28]. Moreover, STAT3 promoted the expression of programmed death ligand 1 to mediate immune evasion of esophageal cancer cells[29].

CONCLUSION

Taken together, our research discovered that circAKT3 enhanced proliferative, migratory, and invasive capacities of esophageal cancer cells by sponging miR-17-5p to exert protumor effects, and downregulation of circAKT3 inhibited xenograft tumor growth of esophageal cancer *in vivo*, providing a potential target for better understanding the underlying mechanism of esophageal cancer.

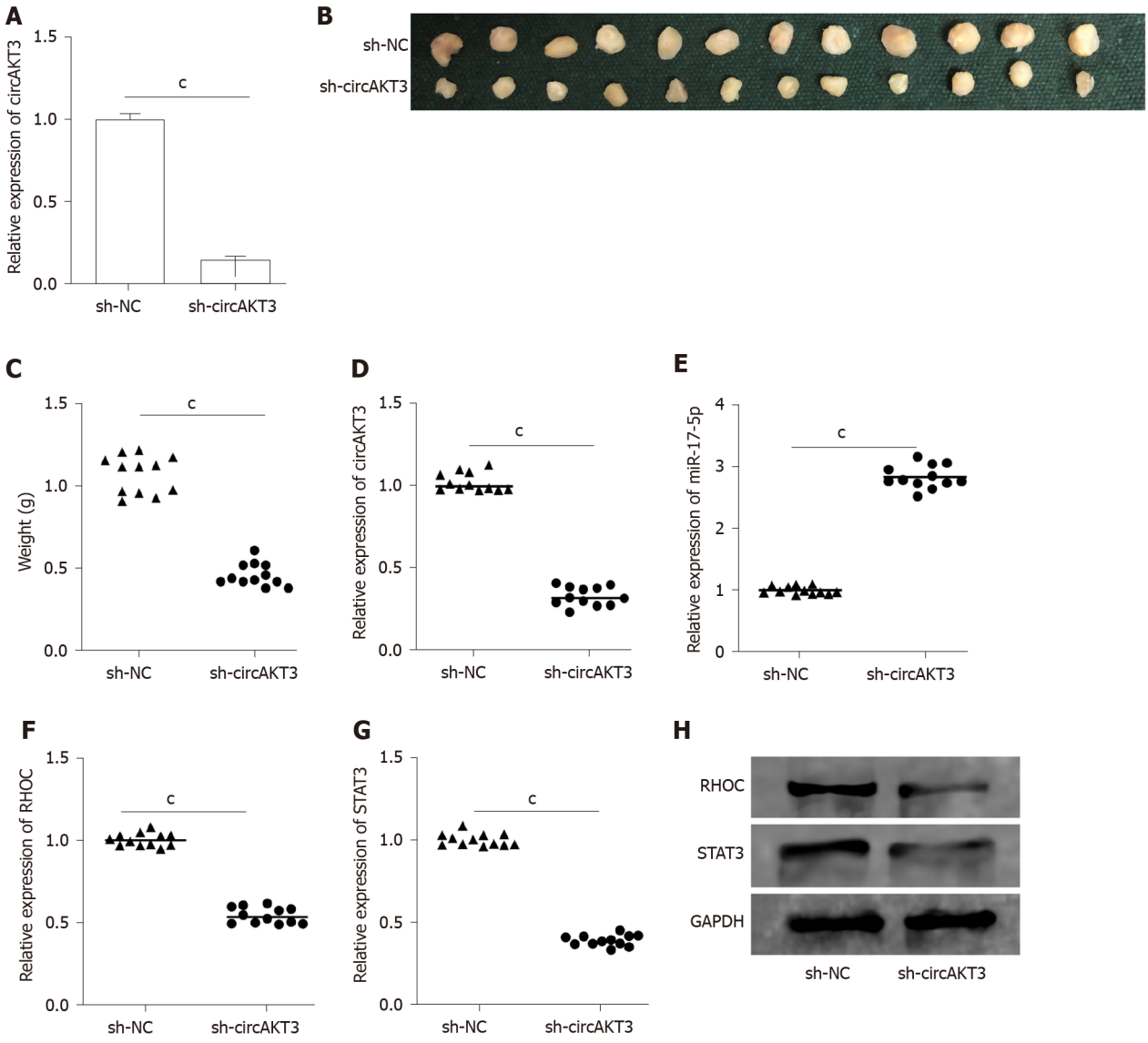

Figure 4 *Circular RNA AKT3* knockdown suppressed growth of esophageal cancer *in vivo*. A: The expression of *circular RNA AKT3* (*circAKT3*) in TE-1 cells with circAKT3 short hairpin (sh)RNA transfection; B and C: The size (B) and weight (C) of the xenograft tumor injected with circAKT3 shRNA-transfected TE-1 cells; D-G: The expression of *circAKT3* (D), *miR-17-5p* (E), *RHOC* (F) and *STAT3* (G) in the xenograft tumor injected with circAKT3 shRNA-transfected TE-1 cells by quantitative real time-polymerase chain reaction; H: The protein levels of RHOC and STAT3 in the xenograft tumor injected with circAKT3 shRNA-transfected TE-1 cells. $^{c}P < 0.001$. sh-NC: Negative control shRNA; sh-circAKT3: Circular RNA AKT3 shRNA.

ARTICLE HIGHLIGHTS

Research background

Esophageal cancer is one of the most malignant tumors in the digestive system and exploring the underlying mechanism is a key issue that needs to be addressed. Circular RNA AKT3 (circAKT3) is a novel noncoding RNA participating in the development and progression of multiple tumors.

Research motivation

To identify biomarkers for the diagnosis and treatment of esophageal cancer.

Research objectives

To explore the mechanism of the role of circAKT3 in the development of esophageal cancer.

Research methods

Cell Counting Kit-8, wound healing assay, Transwell assay, and fluorescence analysis

were used to evaluate the circAKT3 effect on proliferation, migration, invasion, and apoptosis of esophageal cancer cells.

Research results

In vitro assays results revealed that proliferative, migratory, and invasive capacities of esophageal cancer cells were significantly enhanced by *circAKT3* overexpression. miR-17-5p was screened as the target of circAKT3, and miR-17-5p antagonized the effects of circAKT3 on esophageal cancer cells. Moreover, we identified RHOC and STAT3 as the direct target molecules of miR-17-5p, and circAKT3 facilitated expression of *RHOC* and *STAT3* by inhibiting miR-17-5p. *In vivo* assays showed *circAKT3* knockdown inhibited growth of esophageal cancer.

Research conclusions

CircAKT3 enhanced proliferative, migratory, and invasive capacities of esophageal cancer cells by sponging miR-17-5p to exert protumor effects, and downregulation of circAKT3 inhibited xenograft tumor growth of esophageal cancer *in vivo*, providing a potential target for better understanding the underlying mechanism of esophageal cancer.

Research perspectives

The role of circAKT3 in other tumors may be uncovered in the future, and its application in anticancer therapy will be promoted.

REFERENCES

1 **Bray F**, Ferlay J, Soerjomataram I, Siegel RL, Torre LA, Jemal A. Global cancer statistics 2018: GLOBOCAN estimates of incidence and mortality worldwide for 36 cancers in 185 countries. *CA Cancer J Clin* 2018; **68**: 394-424 [PMID: 30207593 DOI: 10.3322/caac.21492]

2 **Lagergren J**, Smyth E, Cunningham D, Lagergren P. Oesophageal cancer. *Lancet* 2017; **390**: 2383-2396 [PMID: 28648400 DOI: 10.1016/S0140-6736(17)31462-9]

3 **van Rossum PSN**, Mohammad NH, Vleggaar FP, van Hillegersberg R. Treatment for unresectable or metastatic oesophageal cancer: current evidence and trends. *Nat Rev Gastroenterol Hepatol* 2018; **15**: 235-249 [PMID: 29235549 DOI: 10.1038/nrgastro.2017.162]

4 **Ohashi S**, Miyamoto S, Kikuchi O, Goto T, Amanuma Y, Muto M. Recent Advances From Basic and Clinical Studies of Esophageal Squamous Cell Carcinoma. *Gastroenterology* 2015; **149**: 1700-1715 [PMID: 26376349 DOI: 10.1053/j.gastro.2015.08.054]

5 **Kristensen LS**, Andersen MS, Stagsted LVW, Ebbesen KK, Hansen TB, Kjems J. The biogenesis, biology and characterization of circular RNAs. *Nat Rev Genet* 2019; **20**: 675-691 [PMID: 31395983 DOI: 10.1038/s41576-019-0158-7]

6 **Xia L**, Song M, Sun M, Wang F, Yang C. Circular RNAs as Biomarkers for Cancer. *Adv Exp Med Biol* 2018; **1087**: 171-187 [PMID: 30259366 DOI: 10.1007/978-981-13-1426-1_14]

7 **Qu S**, Yang X, Li X, Wang J, Gao Y, Shang R, Sun W, Dou K, Li H. Circular RNA: A new star of noncoding RNAs. *Cancer Lett* 2015; **365**: 141-148 [PMID: 26052092 DOI: 10.1016/j.canlet.2015.06.003]

8 **Zang J**, Lu D, Xu A. The interaction of circRNAs and RNA binding proteins: An important part of circRNA maintenance and function. *J Neurosci Res* 2020; **98**: 87-97 [PMID: 30575990 DOI: 10.1002/jnr.24356]

9 **Wang S**, Tang D, Wang W, Yang Y, Wu X, Wang L, Wang D. circLMTK2 acts as a sponge of miR-150-5p and promotes proliferation and metastasis in gastric cancer. *Mol Cancer* 2019; **18**: 162 [PMID: 31722712 DOI: 10.1186/s12943-019-1081-4]

10 **Lu H**, Yao B, Wen X, Jia B. FBXW7 circular RNA regulates proliferation, migration and invasion of colorectal carcinoma through NEK2, mTOR, and PTEN signaling pathways in vitro and in vivo. *BMC Cancer* 2019; **19**: 918 [PMID: 31519156 DOI: 10.1186/s12885-019-6028-z]

11 **Huang X**, Li Z, Zhang Q, Wang W, Li B, Wang L, Xu Z, Zeng A, Zhang X, Zhang X, He Z, Li Q, Sun G, Wang S, Li Q, Wang L, Zhang L, Xu H, Xu Z. Circular RNA AKT3 upregulates PIK3R1 to enhance cisplatin resistance in gastric cancer *via* miR-198 suppression. *Mol Cancer* 2019; **18**: 71 [PMID: 30927924 DOI: 10.1186/s12943-019-0969-3]

12 **Xia X**, Li X, Li F, Wu X, Zhang M, Zhou H, Huang N, Yang X, Xiao F, Liu D, Yang L, Zhang N. A novel tumor suppressor protein encoded by circular AKT3 RNA inhibits glioblastoma tumorigenicity by competing with active phosphoinositide-dependent Kinase-1. *Mol Cancer* 2019; **18**: 131 [PMID: 31470874 DOI: 10.1186/s12943-019-1056-5]

13 **Lynam-Lennon N**, Heavey S, Sommerville G, Bibby BA, Ffrench B, Quinn J, Gasch C, O'Leary JJ, Gallagher MF, Reynolds JV, Maher SG. MicroRNA-17 is downregulated in esophageal adenocarcinoma cancer stem-like cells and promotes a radioresistant phenotype. *Oncotarget* 2017; **8**: 11400-11413 [PMID: 28002789 DOI: 10.18632/oncotarget.13940]

14 **Zhan N**, Li B, Xu X, Xu J, Hu S. Inhibition of FASN expression enhances radiosensitivity in human non-small cell lung cancer. *Oncol Lett* 2018; **15**: 4578-4584 [PMID: 29541228 DOI: 10.3892/ol.2018.7896]

15 **Pastushenko I**, Blanpain C. EMT Transition States during Tumor Progression and Metastasis. *Trends Cell Biol* 2019; **29**: 212-226 [PMID: 30594349 DOI: 10.1016/j.tcb.2018.12.001]

16 **Liu Z**, Hu G, Zhao Y, Xiao Z, Yan M, Ren M. Silence of cZNF292 suppresses the growth, migration, and invasion of human esophageal cancer Eca-109 cells *via* upregulating miR-206. *J Cell Biochem* 2020; **121**: 2354-2362 [PMID: 31680303 DOI: 10.1002/jcb.29458]

17 **Shi N**, Shan B, Gu B, Song Y, Chu H, Qian L. Circular RNA circ-PRKCI functions as a competitive endogenous RNA to regulate AKT3 expression by sponging miR-3680-3p in esophageal squamous cell carcinoma. *J Cell Biochem* 2019; **120**: 10021-10030 [PMID: 30659640 DOI: 10.1002/jcb.28285]

18 **Zhang Y**, Wang Q, Zhu D, Rong J, Shi W, Cao X. Up-regulation of circ-SMAD7 inhibits tumor proliferation and migration in esophageal squamous cell carcinoma. *Biomed Pharmacother* 2019; **111**: 596-601 [PMID: 30611100 DOI: 10.1016/j.biopha.2018.12.116]

19 **Xing Y**, Zha WJ, Li XM, Li H, Gao F, Ye T, Du WQ, Liu YC. Circular RNA circ-Foxo3 inhibits esophageal squamous cell cancer progression *via* the miR-23a/PTEN axis. *J Cell Biochem* 2020; **121**: 2595-2605 [PMID: 31680314 DOI: 10.1002/jcb.29481]

20 **Xue D**, Wang H, Chen Y, Shen D, Lu J, Wang M, Zebibula A, Xu L, Wu H, Li G, Xia L. Circ-AKT3 inhibits clear cell renal cell carcinoma metastasis *via* altering miR-296-3p/E-cadherin signals. *Mol Cancer* 2019; **18**: 151 [PMID: 31672157 DOI: 10.1186/s12943-019-1072-5]

21 **Guan X**, Chen S, Zhao Y. The role of RhoC in malignant tumor invasion, metastasis and targeted therapy. *Histol Histopathol* 2018; **33**: 255-260 [PMID: 28664531 DOI: 10.14670/HH-11-915]

22 **Thomas P**, Pranatharthi A, Ross C, Srivastava S. RhoC: a fascinating journey from a cytoskeletal organizer to a Cancer stem cell therapeutic target. *J Exp Clin Cancer Res* 2019; **38**: 328 [PMID: 31340863 DOI: 10.1186/s13046-019-1327-4]

23 **Faried A**, Faried LS, Usman N, Kato H, Kuwano H. Clinical and prognostic significance of RhoA and RhoC gene expression in esophageal squamous cell carcinoma. *Ann Surg Oncol* 2007; **14**: 3593-3601 [PMID: 17896152 DOI: 10.1245/s10434-007-9562-x]

24 **Zhao ZH**, Tian Y, Yang JP, Zhou J, Chen KS. RhoC, vascular endothelial growth factor and microvascular density in esophageal squamous cell carcinoma. *World J Gastroenterol* 2015; **21**: 905-912 [PMID: 25624724 DOI: 10.3748/wjg.v21.i3.905]

25 **Faried A**, Faried LS, Kimura H, Nakajima M, Sohda M, Miyazaki T, Kato H, Usman N, Kuwano H. RhoA and RhoC proteins promote both cell proliferation and cell invasion of human oesophageal squamous cell carcinoma cell lines in vitro and in vivo. *Eur J Cancer* 2006; **42**: 1455-1465 [PMID: 16750623 DOI: 10.1016/j.ejca.2006.02.012]

26 **Huynh J**, Chand A, Gough D, Ernst M. Therapeutically exploiting STAT3 activity in cancer - using tissue repair as a road map. *Nat Rev Cancer* 2019; **19**: 82-96 [PMID: 30578415 DOI: 10.1038/s41568-018-0090-8]

27 **Thilakasiri PS**, Dmello RS, Nero TL, Parker MW, Ernst M, Chand AL. Repurposing of drugs as STAT3 inhibitors for cancer therapy. *Semin Cancer Biol* 2019 [PMID: 31711994 DOI: 10.1016/j.semcancer.2019.09.022]

28 **Liu Y**, Zhi Y, Song H, Zong M, Yi J, Mao G, Chen L, Huang G. S1PR1 promotes proliferation and inhibits apoptosis of esophageal squamous cell carcinoma through activating STAT3 pathway. *J Exp Clin Cancer Res* 2019; **38**: 369 [PMID: 31438989 DOI: 10.1186/s13046-019-1369-7]

29 **Zhang W**, Pang Q, Yan C, Wang Q, Yang J, Yu S, Liu X, Yuan Z, Wang P, Xiao Z. Induction of PD-L1 expression by epidermal growth factor receptor-mediated signaling in esophageal squamous cell carcinoma. *Onco Targets Ther* 2017; **10**: 763-771 [PMID: 28243112 DOI: 10.2147/OTT.S118982]

World Journal of Gastroenterology

Submit a Manuscript: https://www.f6publishing.com

World J Gastroenterol 2021 January 21; 27(3): 255-266

DOI: 10.3748/wjg.v27.i3.255

ISSN 1007-9327 (print) ISSN 2219-2840 (online)

ORIGINAL ARTICLE

Retrospective Study

Serum vitamin D and vitamin-D-binding protein levels in children with chronic hepatitis B

Cai-Zhi Huang, Jie Zhang, Lin Zhang, Cui-Hua Yu, Yi Mo, Li-Ya Mo

ORCID number: Cai-Zhi Huang 0000-0001-9122-1199; Jie Zhang 0000-0001-9637-8961; Lin Zhang 0000-0002-4273-0592; Cui-Hua Yu 0000-0002-9685-2990; Yi Mo 0000-0002-0623-9309; Li-Ya Mo 0000-0002-1154-6899.

Author contributions: All authors contributed to the conceptualization of the study; Mo LY designed the research; Huang CZ and Zhang J performed the research; Zhang L and Yu CH contributed to data collection; Huang CZ and Mo Y analyzed the data; Huang CZ and Mo LY wrote and revised the paper.

Supported by Hunan Provincial Health Commission Science Foundation of China, No. 20200017.

Institutional review board statement: This research was reviewed and approved by Ethics Committee of Hunan Children's Hospital.

Informed consent statement: Informed consent was obtained from all subjects.

Conflict-of-interest statement: All authors have no conflict of interest to declare.

Data sharing statement: No

Cai-Zhi Huang, Jie Zhang, Lin Zhang, Yi Mo, Li-Ya Mo, Department of Laboratory Medicine, Hunan Children's Hospital, Changsha 410007, Hunan Province, China

Cui-Hua Yu, Department of GCP Certified Sites, The Third Hospital of Changsha City, Changsha 410005, Hunan Province, China

Corresponding author: Li-Ya Mo, MBBS, Chief Technician, Director, Professor, Department of Laboratory Medicine, Hunan Children's Hospital, No. 86 Ziyuan Road, Changsha 410007, Hunan Province, China. 643183753@qq.com

Abstract

BACKGROUND

Vitamin D is an essential fat-soluble secosteroid hydroxylated by the liver to form the intermediate metabolite calcidiol {25-hydroxy vitamin D [25(OH)D]}, which is a reliable indicator to investigate individual vitamin D status. Vitamin-D-binding protein (VDBP) is a multifunctional glycoprotein mainly synthesized in the liver and the major transport protein for vitamin D and its metabolites. Serum vitamin D and VDBP are both associated with hepatitis B. However, few studies have reported the relationship and clinical significance of vitamin D and VDBP with hepatitis B virus (HBV) replication and hepatic fibrosis in children with chronic hepatitis B (CHB).

AIM

To explore vitamin D and VDBP serum levels in children with CHB and the association of vitamin D and VDBP with HBV replication and hepatic fibrosis.

METHODS

We enrolled 204 children with CHB admitted to Hunan Children' Hospital in summer and autumn between 2018 and 2019 and 170 healthy controls. CHB patients included: 164 hepatitis B e antigen (HBeAg) positive and 40 HBeAg negative; 193 hepatitis B surface antigen (HBsAg) positive and 11 HBsAg negative; 164 with detectable HBV deoxyribonucleic acid (DNA) and 40 with undetectable HBV DNA; 131 with HBV genotype B and 23 with HBV genotype C; and 27 without hepatic fibrosis and 97 with hepatic fibrosis. Serum levels of 25(OH)D, VDBP, liver function markers, and other clinical parameters were collected to analyze their association with vitamin D and VDBP. Mann-Whitney *U* test, Kruskal-Wallis *H* test, or *t* test was used to analyze serum 25(OH)D and VDBP levels in different groups. Spearman rank correlation test was utilized to

analyze the correlation of 25(OH)D and VDBP with other markers. Statistically significant factors determined by univariate analysis were further analyzed by binary multivariate logistic regression analysis. $P < 0.05$ was considered statistically significant.

RESULTS

Children with CHB had lower serum 25(OH)D (56.64 ± 17.89 nmoL/L) and VDBP [122.40 (70.74-262.84 μg/L)] levels than healthy controls had ($P < 0.001$). Serum 25(OH)D and VDBP levels were significantly different among the different grades of hepatic fibrosis ($P < 0.05$). VDBP levels in children with HBV genotype C, HBsAg, HBeAg, and detectable HBV DNA were significantly lower than those in children with HBV genotype B, no HBsAg, no HBeAg, and undetectable HBV DNA ($P < 0.05$). Serum 25(OH)D level was negatively correlated with age and serum total bilirubin level ($r = -0.396$ and -0.280, respectively, $P < 0.001$). Serum VDBP level was negatively correlated with HBV DNA ($\log_{10}$ IU/mL) ($r = -0.272$, $P < 0.001$). Serum 25(OH)D level was not correlated with VDBP level ($P > 0.05$). Univariate ($P < 0.05$) and multivariate logistic regression analysis showed that low level of 25(OH)D (odds ratio = 0.951, 95% confidence interval: 0.918-0.985) and high level of HBV DNA (odds ratio = 1.445, 95% confidence interval: 1.163-1.794) were independently correlated with hepatic fibrosis ($P < 0.01$).

CONCLUSION

Serum levels of 25(OH)D and VDBP are decreased in children with CHB. Serum VDBP level is negatively correlated with HBV replication. Low level of 25(OH)D is independently associated with hepatic fibrosis in children with CHB. There is no significant association between serum levels of 25(OH)D and VDBP.

Key Words: Chronic hepatitis B; Children; Vitamin D; Vitamin-D-binding protein; Hepatitis B virus

Core Tip: Serum vitamin D and vitamin-D-binding protein (VDBP) levels are associated with hepatitis B. The association of vitamin D and VDBP with hepatitis B virus replication and hepatic fibrosis in children with chronic hepatitis B (CHB) has rarely been reported. We found that low level of serum 25-hydroxy vitamin D is an independent factor associated with development of hepatic fibrosis, and it could be valuable for maintaining sufficient 25-hydroxy vitamin D level to prevent or delay hepatic fibrosis in children with CHB. VDBP is negatively correlated with hepatitis B virus replication, and VDBP analogs might be considered for management of CHB.

Citation: Huang CZ, Zhang J, Zhang L, Yu CH, Mo Y, Mo LY. Serum vitamin D and vitamin-D-binding protein levels in children with chronic hepatitis B. *World J Gastroenterol* 2021; 27(3): 255-266
URL: https://www.wjgnet.com/1007-9327/full/v27/i3/255.htm
DOI: https://dx.doi.org/10.3748/wjg.v27.i3.255

INTRODUCTION

Vitamin D is a fat-soluble secosteroid and is essential for humans. Vitamin D is mainly produced in the skin by means of sunlight exposure or retrieved from dietary components. In order to become biologically active, vitamin D needs to be combined with vitamin-D-binding protein (VDBP), which is the major transport protein of vitamin D and its metabolites, and it sequentially converts to its intermediate metabolite calcidiol {25-hydroxy vitamin D [25(OH)D]} and the final active form calcitriol (1,25-dihydroxy vitamin D) by hydroxylation in the liver and kidneys. Twenty-five (OH)D is the main metabolite of vitamin D and is relatively stable in serum. Precise quantification of calcitriol is problematic because of its short half-life and serum concentrations are 1000 times lower compared to those of 25(OH)D. In

additional data are available.

Manuscript source: Unsolicited manuscript

Specialty type: Gastroenterology and hepatology

Country/Territory of origin: China

Peer-review report's scientific quality classification
Grade A (Excellent): 0
Grade B (Very good): B, B
Grade C (Good): 0
Grade D (Fair): 0
Grade E (Poor): 0

Received: November 4, 2020
Peer-review started: November 4, 2020
First decision: December 24, 2020
Revised: December 29, 2020
Accepted: January 6, 2021
Article in press: January 6, 2021
Published online: January 21, 2021

P-Reviewer: Fraga RS
S-Editor: Fan JR
L-Editor: Filipodia
P-Editor: Ma YJ

contrast, 25(OH)D has a half-life of approximately 3 wk, making it a suitable and largely reliable indicator to investigate the individual vitamin D status. Vitamin D promotes absorption of calcium and regulates skeletal function. It is also a powerful modulator of the immune response and is closely associated with many diseases such as immune disease[1], inflammatory bowel disease[2], cancer[3], and metabolic disorders[4].

Hepatitis B virus (HBV) is a serious threat to human health and life. HBV infection is one of the major contributors to the development of chronic hepatitis, fibrosis, cirrhosis, and hepatocellular carcinoma. About 1 million people die from HBV infection every year[5,6]. One-third of the population around the world are infected by HBV, and it was estimated by the World Health Organization in 2015 that 257 million people were living with chronic hepatitis B infection. Newborn infants and children with acute HBV infection are prone to developing chronic hepatitis B (CHB), and the rate of chronicity in newborn infants, children aged < 6 years, and adults is 80%-90%, 25%-30%, and 1%-5%[7], respectively.

Immune and inflammatory responses participate in chronic liver injuries and fibrogenesis of CHB *via* activating hepatic stellate cells. Due to the heterogeneity of CHB, patients may have different levels of viral replication and severity of hepatic disease. Pathologically, patients infected with HBV are characterized by impairment of T-cell function. The elimination of HBV in CHB patients largely depends on the cellular immune response mediated by T helper (Th)1 cells. Combination of the active form of vitamin D and vitamin D receptor (VDR) may inhibit the proliferation of Th1 cells and the release of cytokines and concurrently activate Th2 cells, thus regulating the immune response. However, HBV-transfected cells downregulate VDR expression, thereby preventing vitamin D from inhibiting transcription and translation of HBV *in vitro*, and HBV might use this mechanism to avoid the immune system[8]. Therefore, it is believed that vitamin D is closely linked to hepatitis B. In recent years, it has been shown that vitamin D deficiency is related to CHB in adults, and vitamin D level might affect the antiviral effect and disease progression and prognosis[9,10]. Nevertheless, the association of HBV replication and vitamin D level is not consistent[11,12], and there have been few studies about the relationship among vitamin D, VDBP, and CHB in children. Thus, we carried out this study to investigate the association of vitamin D and VDBP with HBV replication and hepatic fibrosis in children with CHB.

MATERIALS AND METHODS

Study population

This research was approved by the Ethics Committee of Hunan Children's Hospital. The study protocol conformed to the provisions of the Declaration of Helsinki. The diagnostic criteria and definitions for CHB were in accordance with the American Association for the Study of Liver Diseases 2018 Hepatitis B Guidance[13]. Hepatic fibrosis was classified according to the Scheuer Scoring System: Grade 0, no fibrosis; grade 1, enlarged and fibrotic portal tracts; grade 2, periportal or portal-portal septal fibrosis but intact architecture; grade 3, fibrosis with architectural distortion but no obvious cirrhosis; and grade 4, probable or definite cirrhosis.

We selected 257 children with CHB who were admitted to Hunan Children's Hospital in summer and autumn between 2018 and 2019, along with 170 randomly selected healthy controls. Patients were excluded from the present analysis if they met the following exclusion criteria: (1) Patients with infectious liver disease caused by pathogens other than HBV and with other liver diseases such as autoimmune liver disease; (2) Patients with malignant tumors; (3) Patients who have received immunomodulatory therapy or taken vitamin D preparations in the past 4 wk; (4) Patients with comorbidities that may affect the serum levels of vitamin D and VDBP, including malnutrition, renal disease, and diabetes; and (5) Repeated patients during the study period. Lastly, 53 of the patients were excluded, and a total of 204 children were enrolled in the analysis.

The enrolled patients included: 193 hepatitis B surface antigen (HBsAg) positive and 11 HBsAg negative; 164 hepatitis B e antigen (HBeAg) positive and 40 HBeAg negative; 164 with detectable HBV deoxyribonucleic acid (DNA) and 40 with undetectable HBV DNA; 131 with HBV genotype B, 23 with HBV genotype C, and 50 without genotyping due to refusal of guardians; and 124 with histopathological determination of grade of hepatic fibrosis (27 grade 0, 74 grade 1, 12 grade 2, 9 grade 3, and 2 grade 4), and 80 without histopathological examination because of refusal of

guardians. The flow chart of the study is shown in Figure 1.

Data collection

All blood tests were provided by the Department of Laboratory Medicine of Hunan Children's Hospital. Serum 25(OH)D level was determined by chemiluminescent immunoassay (ADVIA Centaur XP; Siemens, Erlangen, Germany). Serum VDBP level was detected by ELISA (reagent kit from China). After collection, the human serum samples for 25(OH)D examination were stored at 4 °C and tested within 24 h, and the samples for VDBP examination were stored at -70 °C and tested within 1 wk. The definition of vitamin D levels in Hunan Children's Hospital included deficiency (< 37.50 nmoL/L), insufficiency (37.5-50.0 nmoL/L), and sufficiency (50.0-250.0 nmoL/L). Other clinical parameters including liver function tests, serum HBV DNA level, and serological markers of HBV, such as HBsAg and HBeAg, were collected for analysis of the association with 25(OH)D and VDBP levels.

Statistical analysis

Statistical analysis was performed using SPSS version 19.0 software (Armonk, NY, United States). Normal distribution measurement data were expressed as mean ± standard deviation and analyzed by the *t* test to determine the difference between two groups. Non-normal distribution measurement data were expressed as median (interquartile range) and analyzed by Mann-Whitney *U* test or Kruskal-Wallis *H* test. Numerical data were expressed as rate or percentage and analyzed by χ^2 test. The Spearman's rank correlation test was used to determine the correlation between the two groups. Binary multivariate logistic regression analysis was applied to analyze further the statistically significant factors determined by univariate analysis. Statistical analysis was based on the actual number of completed cases if values were missing. $P < 0.05$ by two-tailed tests was considered statistically significant for tests of all variables.

RESULTS

Analysis of serum levels of 25(OH)D and VDBP in patients with CHB and healthy controls

Serum levels of 25(OH)D, VDBP, calcium, and phosphorus and liver function test results in patients with CHB and healthy controls are shown in Table 1. Patients with CHB had higher serum levels of alanine aminotransferase (ALT), aspartate aminotransferase (AST), and total bilirubin (TBil); longer prothrombin time (PT); and lower serum levels of 25(OH)D, VDBP, calcium, and phosphorus. No difference in albumin (ALB) level was found between patients with CHB and healthy controls. There were 25 cases (12.25%) of vitamin D deficiency, 44 (21.57%) of vitamin D insufficiency, and 135 (66.18%) of vitamin D sufficiency in children with CHB. The cases of vitamin D deficiency, insufficiency, and sufficiency in healthy controls were 3 (1.76%), 12 (7.06%), and 155 (91.18%), respectively. The distribution frequency of vitamin D in CHB patients and healthy controls is shown in Figure 2.

Differences in serum levels of 25(OH)D and VDBP in CHB children with different conditions

Serum levels of 25(OH)D and VDBP in different groups of children with CHB are shown in Table 2. In children with CHB, no significant difference was found in serum 25(OH)D levels between HBeAg-positive and -negative ($P = 0.091$), between HBsAg-positive and -negative ($P = 0.076$), between patients with HBV genotype B and genotype C ($P = 0.753$), or between patients with detectable and undetectable HBV DNA ($P = 0.441$). Serum level of 25(OH)D was significantly different among groups with various grades of hepatic fibrosis ($P < 0.001$). The levels of serum 25(OH)D decreased successively in patients with grade 0, 1, 2, and 3 of hepatic fibrosis, and the difference between any two groups was significant ($P < 0.05$).

Serum levels of VDBP in children with HBeAg, HBsAg, HBV genotype C, and detectable HBV DNA were significantly lower than those in children without HBeAg and HBsAg and with HBV genotype B and undetectable HBV DNA. There was a significant difference in serum VDBP levels among patients with various grades of hepatic fibrosis ($P = 0.032$). Patients with grade 2 hepatic fibrosis had higher serum VDBP levels than those with grade 0 or 3 hepatic fibrosis ($P < 0.05$), and no significant difference was found between any other two groups. The data for hepatic fibrosis

Table 1 Serum levels of 25-hydroxy vitamin D and vitamin-D-binding protein in patients with chronic hepatitis B and healthy controls

Factor	CHB, *n* = 204	Healthy controls, *n* = 170	χ^2/Z/*t* value[1]	*P* value[1]
Sex, M/F	133/71	108/62	0.11	0.737
Age in mo	61.00 (37.0-97.75)	56.00 (32.75-82.25)	1.27	0.205
ALT in IU/L	30.22 (17.80-63.36)	15.00 (8.75-24.25)	9.37	< 0.001
AST in IU/L	38.25 (28.70-64.98)	25.00 (17.00-31.50)	10.44	< 0.001
TBil in μmoL/L	8.67 (6.61-12.65)	7.00 (5.60-9.25)	4.57	< 0.001
ALB in g/L	42.52 ± 3.53	42.10 ± 5.39	0.88	0.383
PT in s	13.34 ± 0.80	11.37 ± 0.91	22.22	< 0.001
25(OH)D, nmoL/L	56.64 ± 17.89	75.48 ± 28.28	7.52	< 0.001
VDBP, μg/L	122.40 (70.74-262.84)	643.25 (415.74-1034.43)	14.89	< 0.001
Calcium, mmoL/L	2.24 ± 0.15	2.44 ± 0.16	11.99	< 0.001
Phosphorus, mmoL/L	1.47 ± 0.12	1.69 ± 0.16	14.80	< 0.001

[1]Normal distribution measurement data were expressed as mean ± SD and analyzed by the *t* test to determine the difference between two groups. Non-normal distribution measurement data were expressed as median (interquartile range) and analyzed by Mann-Whitney *U* test to determine the difference between two groups. Numerical data were expressed as rate and analyzed by χ^2 test. 25(OH)D: 25-hydroxy vitamin D; ALB: Albumin; ALT: Alanine aminotransferase; AST: Aspartate aminotransferase; F: Female; M: Male; PT: Prothrombin time; TBil: Total bilirubin; VDBP: Vitamin-D-binding protein.

grade 4 were not involved in statistical analysis because there were only 2 cases.

Correlation between serum levels of 25(OH)D and VDBP and other clinical parameters in patients with CHB

Spearman's rank correlation test revealed that serum levels of 25(OH)D were negatively correlated with age and serum TBil level in children with CHB (r = -0.396, -0.280, P < 0.001), but serum 25(OH)D level was not correlated with sex or serum levels of ALT, AST, ALB, PT, calcium, phosphorus, HBV DNA, and VDBP. Serum VDBP level was negatively correlated with serum HBV DNA ($\log_{10}$ IU/mL) (r = -0.272, P < 0.001) in children with CHB (Figure 3). No significant correlation was found between VDBP levels and age, sex, or levels of ALT, AST, TBil, ALB, PT, calcium, and phosphorus.

Univariate and multivariate analyses of factors associated with hepatic fibrosis

Univariate analysis revealed that CHB patients with hepatic fibrosis had higher levels of TBil, VDBP, and HBV DNA, lower levels of 25(OH)D, and lower rate of HBeAg-positive to -negative than CHB patients without hepatic fibrosis. Multivariate logistic regression analysis showed that low level of serum 25(OH)D [odds ratio = 0.951, 95% confidence interval: 0.918-0.985] and high level of HBV DNA (odds ratio = 1.445, 95% confidence interval: 1.163-1.794) were both independently correlated with hepatic fibrosis in children with CHB (Table 3).

DISCUSSION

In the present study, the serum levels of 25(OH)D in children with CHB was investigated, along with its correlation with other factors. Children with CHB were found to have lower serum 25(OH)D levels than healthy controls; CHB patients with hepatic fibrosis had lower levels of 25(OH)D than patients without hepatic fibrosis; and low level of serum 25(OH)D was independently correlated with hepatic fibrosis. The results demonstrate the value of maintaining normal levels of 25(OH)D for the prevention and delay of hepatic fibrosis in children with CHB.

Compared with healthy controls, patients with CHB had higher rates of vitamin D deficiency and insufficiency. This may be due to the decrease of vitamin D hydroxylation in the liver in the context of impaired liver function and the increase of vitamin D consumption on account of immune response mediated by vitamin D in patients with CHB.

Table 2 Serum levels of 25-hydroxy vitamin D and vitamin-D-binding protein in different groups of children with chronic hepatitis B

Group (*n*)	25(OH)D, nmoL/L	*Z*/*t*/*H* value[1]	*P* value[1]	VDBP, μg/L	*Z*/*H* value[1]	*P* value[1]
HBeAg		1.70	0.091		3.81	< 0.001
Positive (164)	57.69 ± 18.06			106.95 (68.44-203.21)		
Negative (40)	52.35 ± 16.73			257.23 (135.61-342.96)		
HBV genotype[2]		0.32	0.753		2.51	0.012
Genotype B (131)	55.69 ± 17.63			105.00 (69.30-199.35)		
Genotype C (23)	56.93 ± 17.69			75.40 (42.75-123.10)		
HBsAg		1.77	0.076		4.32	< 0.001
Positive (193)	56.26 ± 18.17			113.87 (69.90-217.03)		
Negative (11)	56.60 (54.37-72.96)			439.65 (259.27-510.45)		
HBV DNA		0.77	0.441		4.75	< 0.001
Detectable (164)	57.12 ± 18.14			105.75 (66.39-193.73)		
Undetectable (40)	54.69 ± 16.91			284.18 (152.64-406.14)		
Fibrosis grades[2]		29.81	< 0.001		8.81	0.032
Grade 0 (27)	61.86 ± 13.63			90.00 (61.20-121.45)		
Grade 1 (74)	54.97 ± 13.63			117.03 (65.74-275.76)		
Grade 2 (12)	43.99 (35.79-55.15)			174.88 (121.34-292.94)		
Grade 3 (9)	32.95 (28.61-35.20)			78.13 (35.05-176.75)		

[1]Normal distribution measurement data were analyzed by *t* test to determine the difference between two groups. For non-normal distribution measurement data, Mann-Whitney *U* test was used to compare serum levels of 25-hydroxy vitamin D and vitamin-D-binding protein between two groups, and Kruskal-Wallis *H* test was applied to analyze the difference among multiple groups.
[2]Statistical analysis was based on the actual number of completed cases because of the missing values. 25(OH)D: 25-hydroxy vitamin D; HBeAg: Hepatitis B e antigen; HBsAg: Hepatitis B surface antigen; HBV: Hepatitis B virus; VDBP: Vitamin-D-binding protein.

Some investigations have indicated that serum 25(OH)D level is negatively correlated with HBV load, and low 25(OH)D level is associated with HBV genotype B, HBsAg, and HBeAg[11,14]. Other studies have shown inconsistent results[8,10,12]. In the present study, 25(OH)D was not correlated with HBV DNA in patients with CHB, and serum levels of 25(OH)D did not differ significantly between patients with or without HBeAg, patients with HBV genotype B or C, patients with or without HBsAg, and patients with or without detectable HBV DNA. These results indicate that serum 25(OH)D levels are not associated with HBV genotype and virus replication. The discrepancy between various studies may have been caused by the different disease course and stage and study population.

A previous study revealed that vitamin D can reduce profibrotic factors and collagen expression and that it has immunomodulatory effects on immune cells, including T cells[15]. Vitamin D has been found to have an antifibrotic effects on human primary transforming-growth-factor-β-stimulated hepatic stellate cells[16]. In the present study, serum levels of 25(OH)D in CHB children with hepatic fibrosis were markedly decreased, and the higher the grade of hepatic fibrosis, the lower the level of serum 25(OH)D. Multivariate logistic regression analysis also revealed that low level of 25(OH)D was independently associated with hepatic fibrosis, which suggested that maintaining normal levels of 25(OH)D in children with CHB may have a positive effect on the prevention and delay of hepatic fibrosis.

VDBP, also known as gc-globulin, is a plasma glycoprotein with a molecular weight of 56-58 kDa, composed of 458 amino acids. VDBP is primarily synthesized in the liver and expressed in several organs and tissues, including the liver, kidneys, gonads and fat, and neutrophils. Unlike serum vitamin D following seasonal variation, serum concentration of VDBP is stable during the year[17]. VDBP has numerous physiological roles, including transporting vitamin D and its metabolites, regulating bone development, scavenging actin, and regulating immune and inflammation process[18].

In the present study, serum VDBP levels in CHB children were significantly lower

Table 3 Univariate and multivariate analyses of hepatic fibrosis in children with chronic hepatitis B

Factor	Without hepatic fibrosis, *n* = 27	Hepatic fibrosis, *n* = 97	Univariate analysis		Multivariate analysis	
			Z/*t*/χ^2 value[1]	*P* value[1]	OR (95%CI)[1]	*P* value[1]
Age in mo	54.00 (32.0-98.0)	63.00 (40.00-95.00)	0.83	0.407		
Male/female	18/9	63/34	0.03	0.868		
ALT in IU/L	32.03 (16.40-57.0)	43.48 (20.15-88.64)	0.98	0.330		
AST in IU/L	39.11 (27.50-65.30)	47.30 (30.65-83.10)	1.14	0.254		
TBil in μmoL/L	6.77 (6.10-8.80)	9.20 (6.98-14.20)	2.86	0.004	1.053 (0.938-1.182)	0.384
ALB in g/L	42.98 ± 2.17	42.30 ± 3.27	1.27	0.209		
PT in s	13.29 ± 0.76	13.26 ± 0.78	0.18	0.860		
25(OH)D, nmoL/L	61.86 ± 13.63	51.22 ± 14.67	3.38	0.001	0.951 (0.918-0.985)	0.005
VDBP, μg/L	90.00 (61.20-121.45)	134.50 (71.25-267.18)	1.98	0.047	1.001 (0.999-1.003)	0.316
Calcium, mmoL/L	2.30 ± 0.16	2.27 ± 0.15	0.88	0.383		
Phosphorus, mmoL/L	1.48 ± 0.12	1.45 ± 0.12	1.19	0.237		
HBV DNA in $\log_{10}$ IU/mL	5.40 (2.00-7.31)	6.88 (5.53-7.64)	2.40	0.017	1.445 (1.163-1.794)	0.001
HBeAg positive/negative	26/1	73/24	5.81	0.016	0.138 (0.017-1.160)	0.068

[1]Normal distribution measurement data, non-normal distribution measurement data and numerical data were analyzed by *t* test, Mann-Whitney *U* test and χ^2 test to determine the difference between two groups, respectively. Binary multivariate logistic regression analysis was applied to further analyze the statistically significant factors determined by univariate analysis. 25(OH)D: 25-hydroxy vitamin D; ALB: Albumin; ALT: Alanine aminotransferase; AST: Aspartate aminotransferase; CI: Confidence interval; DNA: Deoxyribonucleic acid; HBeAg: Hepatitis B e antigen; HBV: Hepatitis B virus; OR: Odds ratio; PT: Prothrombin time; TBil: Total bilirubin; VDBP: Vitamin-D-binding protein.

than those in healthy controls, and the levels of VDBP were markedly decreased in patients with HBV genotype C, HBsAg, HBeAg, and detectable HBV DNA. VDBP levels were negatively correlated with HBV DNA levels in children with CHB. The results demonstrated that serum levels of VDBP were associated with HBV genotype and negatively correlated with HBV replication. The reasons for the decrease in VDBP may be lower production in impaired hepatic cells and greater consumption of scavenging actin, mediating monocyte and neutrophil chemotaxis to inflammatory foci caused by HBV replication[18].

Children with CHB and hepatic fibrosis had higher VDBP level, and VDBP levels increased in patients with grade 1 and 2 but decreased in patients with grade 3 fibrosis. Although it has been reported that hepatocytes are compensatory in the early stage of fibrosis and that the remaining normal hepatocytes produce more VDBP to replenish the shortage in the circulation caused by massive consumption[19], the detailed mechanism of VDBP variation in different stages of hepatic fibrosis is still unknown. The association between VDBP and hepatic fibrosis and the underlying mechanisms warrant further investigation.

Serum levels of 25(OH)D and VDBP were both decreased in children with CHB, but there was no significant correlation between the two markers. This may be due to the multifunctional property of VDBP. VDBP has many other important physiological functions other than being a transporter and < 5% of the binding sites on VDBP are occupied by 25(OH)D[18]. Most VDBP may be involved in the immune response and inflammatory process caused by HBV infection. The different biological functions of the two markers result in the incompletely consistent variation.

CONCLUSION

Both serum 25(OH)D and VDBP levels are significantly decreased in children with CHB, VDBP may be negatively correlated with HBV replication, and low level of serum 25(OH)D is an independent factor associated with the development of hepatic fibrosis. Therefore, maintaining sufficient 25(OH)D level in children with CHB could be valuable to prevent or delay the process of fibrosis, and the development and

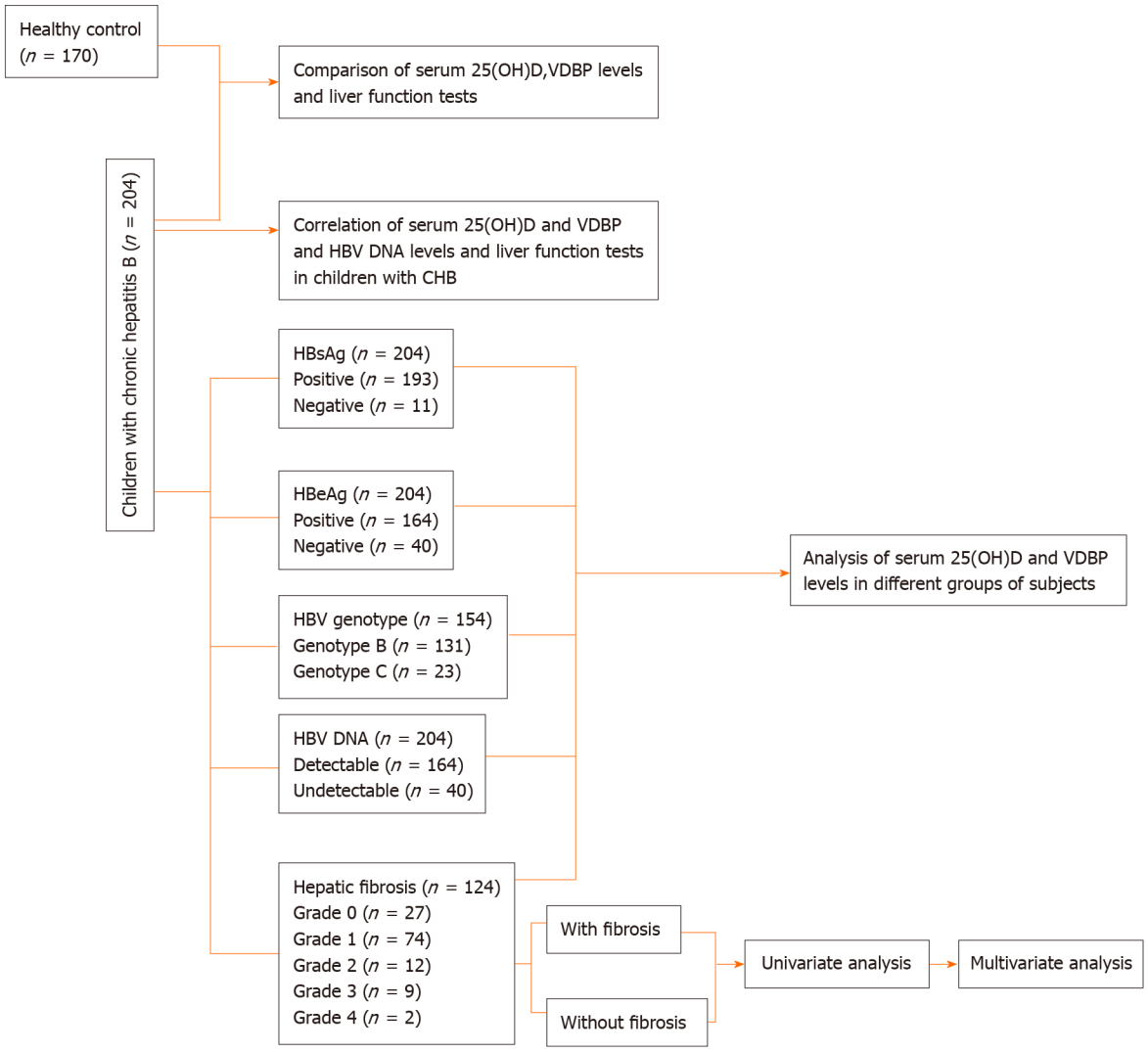

Figure 1 Flow chart of the study. 25(OH)D: 25-hydroxy vitamin D; CHB: Chronic hepatitis B; HBeAg: Hepatitis B e antigen; HBsAg: Hepatitis B surface antigen; HBV: Hepatitis B virus; VDBP: Vitamin D binding protein.

application of VDBP analogues might be a consideration for the management of CHB.

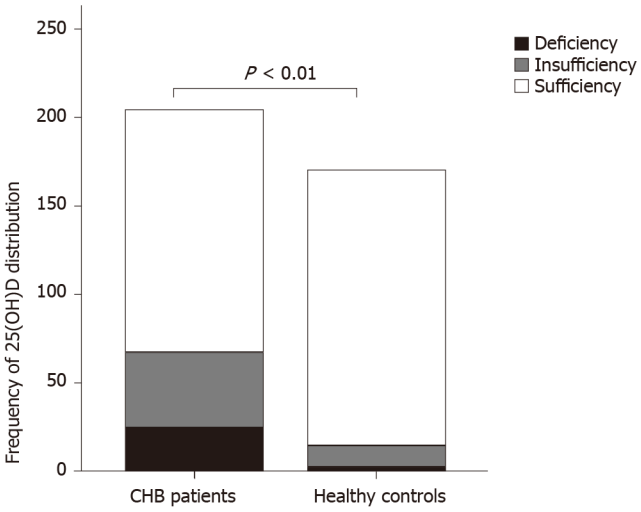

Figure 2 Distribution frequency of serum 25-hydroxy vitamin D in chronic hepatitis B patients and healthy controls. 25(OH)D: 25-hydroxy vitamin D; CHB: Chronic hepatitis B.

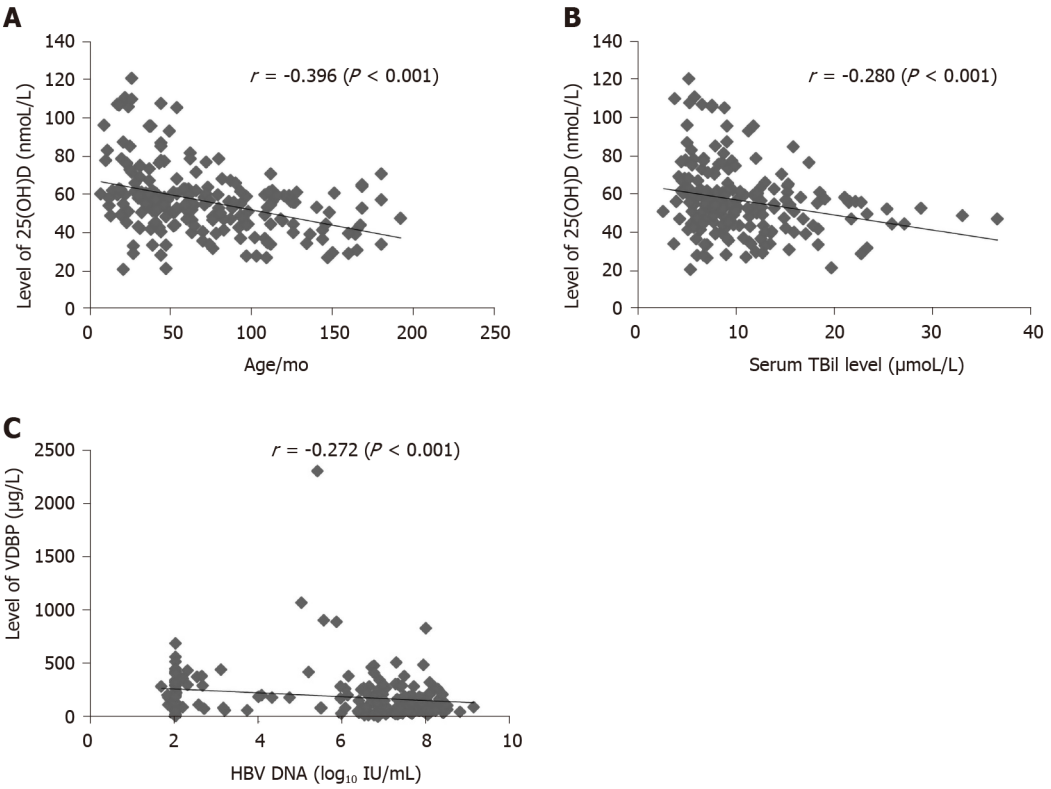

Figure 3 Distribution and correlation of serum 25-hydroxy vitamin D and vitamin-D-binding protein levels with other parameters in children with chronic hepatitis B. A: Correlation of serum 25-hydroxy vitamin D [25(OH)D] level with age; B: Correlation of serum 25(OH)D level with serum total bilirubin level; C: Correlation of serum vitamin-D-binding protein level with serum hepatitis B virus deoxyribonucleic acid. 25(OH)D: 25-hydroxy vitamin D; DNA: Deoxyribonucleic acid; HBV: Hepatitis B virus; TBil: Total bilirubin; VDBP: Vitamin-D-binding protein.

ARTICLE HIGHLIGHTS

Research background

Vitamin D is an essential fat-soluble secosteroid hydroxylated by the liver to form the intermediate metabolite {calcidiol, 25-hydroxy vitamin D [25(OH)D]}, which is a reliable indicator for investigating individual vitamin D status. Vitamin D is known to promote absorption of calcium and regulate skeletal function and is a powerful modulator of the immune response. Vitamin-D-binding protein (VDBP) as the major

transport protein of vitamin D and its metabolites is mainly synthesized by the liver, and VDBP has many other physiological roles, including regulation of bone development, scavenging actin, and regulation of immune and inflammatory processes. Immune and inflammatory responses are involved in chronic liver injuries and fibrogenesis of chronic hepatitis B (CHB). It has been demonstrated that serum levels of vitamin D and VDBP are associated with the development and progress of CHB. However, few studies have been reported about the relationship of vitamin D and VDBP with hepatitis B virus (HBV) replication and hepatic fibrosis in children with CHB. It is of interest to investigate the clinical significance of serum vitamin D and VDBP levels in children with CHB.

Research motivation

Few studies have been reported about the serum levels of vitamin D and VDBP and their clinical significance in children with CHB. Some studies have revealed that vitamin D can reduce profibrotic factors and collagen expression and that they have immunomodulatory effects on immune cells, including T cells. Patients infected with HBV is pathologically characterized as the functional impairment of T cells. The elimination of HBV in CHB patients largely depends on the cellular immune response mediated by T helper (Th)1 cells. Combination of the active form of vitamin D and vitamin D receptor may inhibit the proliferation of Th1 cells and the release of cytokines, and concurrently activate Th2 cells, thus regulating immune responses. Vitamin D and its metabolites in the circulation are mainly transported by VDBP, which is a multifunctional plasma glycoprotein that can mediate monocyte and neutrophil chemotaxis to inflammatory foci caused by HBV replication. The present study aimed at exploring the clinical significance of serum 25(OH)D and VDBP levels in children with CHB. The results will help to illustrate whether vitamin D and VDBP levels are associated with HBV replication and hepatic fibrosis.

Research objectives

The main objective of this study was to investigate the serum levels of vitamin D and VDBP in children with CHB and analyze the association of vitamin D and VDBP with HBV replication and hepatic fibrosis.

Research methods

We enrolled 204 children with CHB who were admitted to Hunan Children's Hospital in summer and autumn between 2018 and 2019 and 170 healthy controls. Children with CHB included: 164 hepatitis B e antigen (HBeAg) positive and 40 HBeAg negative; 193 hepatitis B surface antigen (HBsAg) positive and 11 HBsAg negative; 164 with detectable HBV DNA and 40 with undetectable HBV DNA; 131 with HBV genotype B and 23 with HBV genotype C; and 97 with hepatic fibrosis and 27 without hepatic fibrosis. Serum levels of 25(OH)D, VDBP, liver function markers, and other clinical parameters were collected for analysis of the association with vitamin D and VDBP. Mann-Whitney *U* test, Kruskal-Wallis *H* test, or *t* test was used to analyze serum 25(OH)D and VDBP levels in different groups of subjects. Spearman rank correlation test was utilized to analyze the correlation of 25(OH)D and VDBP with other markers. Finally, statistically significant factors for hepatic fibrosis determined by univariate analysis were further analyzed by binary multivariate logistic regression analysis.

Research results

Children with CHB had lower serum 25(OH)D (56.64 ± 17.89 nmoL/L) and VDBP [122.40 (70.74-262.84 μg/L)] levels than healthy controls had ($P < 0.001$). Serum 25(OH)D and VDBP levels were significantly different among the stages of hepatic fibrosis ($P < 0.05$). Patients with HBV genotype C, HBsAg, HBeAg, and detectable HBV DNA had lower VDBP levels than patients with HBV genotype B, without HBsAg and HBeAg, and undetectable HBV DNA ($P < 0.05$). Serum 25(OH)D level was negatively correlated with age and serum total bilirubin level ($r = -0.396$ and -0.280, respectively, $P < 0.001$). Serum VDBP level was negatively associated with HBV DNA ($\log_{10}$ IU/mL) ($r = -0.272$, $P < 0.001$). Serum 25(OH)D level was not correlated with VDBP level ($P > 0.05$). Univariate ($P < 0.05$) and multivariate logistic regression analysis showed that low level of 25(OH)D (odds ratio = 0.951, 95% confidence interval: 0.918-0.985) and high level of HBV DNA (odds ratio = 1.445, 95% confidence interval: 1.163-1.794) were independently associated with hepatic fibrosis ($P < 0.01$).

Research conclusions

Children with CHB have lower serum levels of 25(OH)D and VDBP. Serum VDBP level is negatively correlated with replication of HBV. Low level of 25(OH)D is independently associated with hepatic fibrosis in CHB children. There is no significant association between serum levels of 25(OH)D and VDBP.

Research perspectives

Previous studies and our data indicate that vitamin D and VDBP are involved in the inflammatory response and immunological regulation in children with CHB. Vitamin D may play an antifibrotic role by reducing stimulation of hepatic stellate cells, profibrotic factors, and collagen expression. VDBP may have a positive effect on alleviating liver injury caused by HBV replication. We speculate that sufficient concentration of vitamin D and VDBP in children with CHB may be beneficial for the progress and prognosis of the disease. The potential value of vitamin D detection in monitoring hepatic fibrosis development and VDBP detection in evaluating the degree of inflammation and liver injury, more detailed mechanism of vitamin D and VDBP on the progression of CHB, and whether VDBP analogs may become a treatment measure for children with CHB warrant further investigation.

ACKNOWLEDGEMENTS

The authors thank Professor Lian Tang from the Department of Liver Disease in Hunan Children's Hospital, China for her advice and language modification of this manuscript.

REFERENCES

1 **Vanherwegen AS**, Gysemans C, Mathieu C. Regulation of Immune Function by Vitamin D and Its Use in Diseases of Immunity. *Endocrinol Metab Clin North Am* 2017; **46**: 1061-1094 [PMID: 29080635 DOI: 10.1016/j.ecl.2017.07.010]

2 **Barbalho SM**, Goulart RA, Gasparini RG. Associations between inflammatory bowel diseases and vitamin D. *Crit Rev Food Sci Nutr* 2019; **59**: 1347-1356 [PMID: 29236523 DOI: 10.1080/10408398.2017.1406333]

3 **Hu K**, Callen DF, Li J, Zheng H. Circulating Vitamin D and Overall Survival in Breast Cancer Patients: A Dose-Response Meta-Analysis of Cohort Studies. *Integr Cancer Ther* 2018; **17**: 217-225 [PMID: 28589744 DOI: 10.1177/1534735417712007]

4 **Schmitt EB**, Nahas-Neto J, Bueloni-Dias F, Poloni PF, Orsatti CL, Petri Nahas EA. Vitamin D deficiency is associated with metabolic syndrome in postmenopausal women. *Maturitas* 2018; **107**: 97-102 [PMID: 29169589 DOI: 10.1016/j.maturitas.2017.10.011]

5 **Terrault NA**, Bzowej NH, Chang KM, Hwang JP, Jonas MM, Murad MH; American Association for the Study of Liver Diseases. AASLD guidelines for treatment of chronic hepatitis B. *Hepatology* 2016; **63**: 261-283 [PMID: 26566064 DOI: 10.1002/hep.28156]

6 **Nannini P**, Sokal EM. Hepatitis B: changing epidemiology and interventions. *Arch Dis Child* 2017; **102**: 676-680 [PMID: 27986700 DOI: 10.1136/archdischild-2016-312043]

7 **Komatsu H**, Inui A. Hepatitis B virus infection in children. *Expert Rev Anti Infect Ther* 2015; **13**: 427-450 [PMID: 25724218 DOI: 10.1586/14787210.2015.1019867]

8 **Gotlieb N**, Tachlytski I, Lapidot Y, Sultan M, Safran M, Ben-Ari Z. Hepatitis B virus downregulates vitamin D receptor levels in hepatoma cell lines, thereby preventing vitamin D-dependent inhibition of viral transcription and production. *Mol Med* 2018; **24**: 53 [PMID: 30326825 DOI: 10.1186/s10020-018-0055-0]

9 **Hoan NX**, Tong HV, Song LH, Meyer CG, Velavan TP. Vitamin D deficiency and hepatitis viruses-associated liver diseases: A literature review. *World J Gastroenterol* 2018; **24**: 445-460 [PMID: 29398866 DOI: 10.3748/wjg.v24.i4.445]

10 **Yu R**, Tan D, Ning Q, Niu J, Bai X, Chen S, Cheng J, Yu Y, Wang H, Xu M, Shi G, Wan M, Chen X, Tang H, Sheng J, Dou X, Shi J, Ren H, Wang M, Zhang H, Gao Z, Chen C, Ma H, Jia J, Hou J, Xie Q, Sun J. Association of baseline vitamin D level with genetic determinants and virologic response in patients with chronic hepatitis B. *Hepatol Res* 2018; **48**: E213-E221 [PMID: 28834607 DOI: 10.1111/hepr.12972]

11 **Hu YC**, Wang WW, Jiang WY, Li CQ, Guo JC, Xun YH. Low vitamin D levels are associated with high viral loads in patients with chronic hepatitis B: a systematic review and meta-analysis. *BMC Gastroenterol* 2019; **19**: 84 [PMID: 31185932 DOI: 10.1186/s12876-019-1004-2]

12 **Zhao XY**, Li J, Wang JH, Habib S, Wei W, Sun SJ, Strobel HW, Jia JD. Vitamin D serum level is associated with Child-Pugh score and metabolic enzyme imbalances, but not viral load in chronic hepatitis B patients. *Medicine (Baltimore)* 2016; **95**: e3926 [PMID: 27399065 DOI:

10.1097/MD.0000000000003926]
13 **Terrault NA**, Lok ASF, McMahon BJ, Chang KM, Hwang JP, Jonas MM, Brown RS Jr, Bzowej NH, Wong JB. Update on prevention, diagnosis, and treatment of chronic hepatitis B: AASLD 2018 hepatitis B guidance. *Hepatology* 2018; **67**: 1560-1599 [PMID: 29405329 DOI: 10.1002/hep.29800]
14 **Chen EQ**, Bai L, Zhou TY, Fe M, Zhang DM, Tang H. Sustained suppression of viral replication in improving vitamin D serum concentrations in patients with chronic hepatitis B. *Sci Rep* 2015; **5**: 15441 [PMID: 26486883 DOI: 10.1038/srep15441]
15 **Artaza JN**, Norris KC. Vitamin D reduces the expression of collagen and key profibrotic factors by inducing an antifibrotic phenotype in mesenchymal multipotent cells. *J Endocrinol* 2009; **200**: 207-221 [PMID: 19036760 DOI: 10.1677/JOE-08-0241]
16 **Beilfuss A**, Sowa JP, Sydor S, Beste M, Bechmann LP, Schlattjan M, Syn WK, Wedemeyer I, Mathé Z, Jochum C, Gerken G, Gieseler RK, Canbay A. Vitamin D counteracts fibrogenic TGF-β signalling in human hepatic stellate cells both receptor-dependently and independently. *Gut* 2015; **64**: 791-799 [PMID: 25134788 DOI: 10.1136/gutjnl-2014-307024]
17 **Oleröd G**, Hultén LM, Hammarsten O, Klingberg E. The variation in free 25-hydroxy vitamin D and vitamin D-binding protein with season and vitamin D status. *Endocr Connect* 2017; **6**: 111-120 [PMID: 28179376 DOI: 10.1530/EC-16-0078]
18 **Lisowska-Myjak B**, Jóźwiak-Kisielewska A, Łukaszkiewicz J, Skarżyńska E. Vitamin D-binding protein as a biomarker to confirm specific clinical diagnoses. *Expert Rev Mol Diagn* 2020; **20**: 49-56 [PMID: 31795772 DOI: 10.1080/14737159.2020.1699064]
19 **Schiødt FV**, Clemmesen JO, Bondesen S, Dahl B, Ott P. Increased turnover of Gc-globulin in patients with hepatic encephalopathy. *Scand J Gastroenterol* 2001; **36**: 998-1003 [PMID: 11521994 DOI: 10.1080/00365520175030555 8]

World Journal of Gastroenterology

Submit a Manuscript: https://www.f6publishing.com

World J Gastroenterol 2021 January 21; 27(3): 267-280

DOI: 10.3748/wjg.v27.i3.267

ISSN 1007-9327 (print) ISSN 2219-2840 (online)

ORIGINAL ARTICLE

Retrospective Study

Trends in the management of anorectal melanoma: A multi-institutional retrospective study and review of the world literature

Josh Bleicher, Jessica N Cohan, Lyen C Huang, William Peche, T Bartley Pickron, Courtney L Scaife, Tawnya L Bowles, John R Hyngstrom, Elliot A Asare

ORCID number: Josh Bleicher 0000-0001-6137-4426; Jessica N Cohan 0000-0002-5461-4716; Lyen C Huang 0000-0002-8605-2631; William Peche 0000-0001-9770-2137; T Bartley Pickron 0000-0002-0880-1959; Courtney L Scaife 0000-0003-2497-4961; Tawnya L Bowles 0000-0002-1883-1510; John R Hyngstrom 0000-0002-4833-3838; Elliot A Asare 0000-0002-0176-3865.

Author contributions: Bleicher J, Bowles TL, Hyngstrom JR and Asare EA designed the study and created the methodology; Bleicher J and Asare EA performed data analysis; Bleicher J created the first draft of the manuscript; Asare EA supervised the research; all authors participated in data acquisition and provided edits and helped with subsequent writing.

Institutional review board statement: The Institutional Review Boards of the University of Utah and Intermountain Health Care approved this study.

Conflict-of-interest statement: I confirm that I have no financial disclosures to declare. As the corresponding author for this manuscript, I also declare that none of my co-authors have financial disclosures to declare.

Josh Bleicher, Jessica N Cohan, Lyen C Huang, William Peche, T Bartley Pickron, Courtney L Scaife, Tawnya L Bowles, John R Hyngstrom, Elliot A Asare, Department of Surgery, Huntsman Cancer Institute at the University of Utah, Salt Lake City, UT 84114, United States

William Peche, John R Hyngstrom, Department of Surgery, George E Wahlen Department of Veterans Affairs Medical Center, Salt Lake City, UT 84114, United States

Tawnya L Bowles, Elliot A Asare, Department of Surgery, Intermountain Medical Center, Murray, UT 84107, United States

Corresponding author: Elliot A Asare, MD, MS, Assistant Professor, Surgical Oncologist, Department of Surgery, Huntsman Cancer Institute at the University of Utah, 1950 Circle of Hope Drive, Suite N6345, Salt Lake City, UT 84114, United States. elliot.asare@hci.utah.edu

Abstract

BACKGROUND

Anorectal melanoma (ARM) is a rare disease with a poor prognosis. Evidence on optimal treatment is limited and surgical management varies widely. We hypothesized that the frequency of abdominoperineal resection used as primary treatment of ARM has decreased over the past several decades.

AIM

To update our understanding of outcomes for patients with ARM and analyze management trends around the world.

METHODS

This is a multi-institutional, retrospective study of patients treated for ARM at 7 hospitals. Hospitals included both large, academic, tertiary care centers and smaller, general community hospitals. Using prospectively maintained institutional tumor registries, we identified 24 patients diagnosed with ARM between January 2000 and May 2019. We analyzed factors prognostic for recurrence and survival. We then used Cox regression to measure overall survival (OS) and melanoma-specific survival. We also performed a literature review to assess trends in surgical management and outcomes.

RESULTS

Of the 24 patients diagnosed with ARM, 12 (50.0%) had local, 8 (33.3%) regional,

Data sharing statement: Because of the small number of participants involved in this cohort and the inability to obtain informed consent, it is difficult to ensure patient anonymity in our dataset and this will not be made available. Statistical code is available from the first author at josh.bleicher@hsc.utah.edu.

Manuscript source: Unsolicited manuscript

Specialty type: Gastroenterology and hepatology

Country/Territory of origin: United States

Peer-review report's scientific quality classification

Grade A (Excellent): 0
Grade B (Very good): B, B, B, B
Grade C (Good): 0
Grade D (Fair): 0
Grade E (Poor): 0

Received: December 1, 2020
Peer-review started: December 1, 2020
First decision: December 21, 2020
Revised: December 28, 2020
Accepted: January 7, 2021
Article in press: January 7, 2021
Published online: January 21, 2021

P-Reviewer: Gong N, Taher M
S-Editor: Fan JR
L-Editor: A
P-Editor: Li JH

and 4 (16.7%) distant disease at diagnosis. Median time to recurrence was 10.4 mo [interquartile range (IQR) 7.5-17.2] with only 2 patients (9.3%) not developing recurrence following surgical resection. Median OS was 18.8 mo (IQR 13.5-33.9). One patient is still alive without recurrence at 21.4 mo from diagnosis; no other patient survived 5 years. Primary surgical management with abdominoperineal resection (APR) *vs* wide excision (WE) did not lead to differences in OS [hazard ratio = 1.4 (95%CI: 0.3-6.8)]. Review of the literature revealed geographic differences in surgical management of ARM, with increased use of WE in the United States and Europe over time and more frequent use of APR in Asia and India. There was no significant improvement in survival over time.

CONCLUSION

There is wide variation in the management of ARM and survival outcomes remain poor regardless of approach. Surgical management should aim to minimize morbidity.

Key Words: Melanoma; Anorectal melanoma; Literature review; Melanoma surgery; Surgical oncology; Colorectal surgery

Core Tip: This is a retrospective study to evaluate current trends in management of anorectal melanoma (ARM). On review of 24 patients from 7 hospitals in Utah, we found that ARM is a highly lethal disease with overall survival of 18.8 mo (interquartile range 13.5-33.9) and no 5-year survivors. Only 2 patients underwent abdominoperineal resection (APR) as primary surgical management. Review of the literature demonstrated wide variation in surgical management of ARM over time and around the world. Whether APR or wide excision was used, outcomes remained poor. With this data, we recommend that surgical management should aim to minimize morbidity.

Citation: Bleicher J, Cohan JN, Huang LC, Peche W, Pickron TB, Scaife CL, Bowles TL, Hyngstrom JR, Asare EA. Trends in the management of anorectal melanoma: A multi-institutional retrospective study and review of the world literature. *World J Gastroenterol* 2021; 27(3): 267-280
URL: https://www.wjgnet.com/1007-9327/full/v27/i3/267.htm
DOI: https://dx.doi.org/10.3748/wjg.v27.i3.267

INTRODUCTION

Anorectal melanoma (ARM) is a rare malignancy with a poor prognosis. The estimated annual incidence in the United States is less than 5 cases per 10 million[1]. Overall 5-year survival is between 10% and 20%[2]. This low survival is due to the late diagnosis of most tumors and aggressive biology of ARM[3]. Most tumors are first recognized from symptoms such as bleeding, obstruction, pain, or changes in bowel habits[4-6]. When these tumors are recognized, they are often misdiagnosed as hemorrhoids or other benign anorectal pathology[7].

National Clinical Cancer Network (NCCN) guidelines on melanoma do not currently include recommendations for treatment of ARM[8]. Without guidelines, and due to the rare nature of the tumor, treatment is highly variable. Controversy exists over optimal primary surgical therapy. Some advocate abdominoperineal resection (APR) for initial treatment, while others report similar oncologic outcomes with wide excision (WE) alone[9,10]. As outcomes are universally poor, many providers recommend the less invasive and lower morbidity WE as primary treatment[11]. Optimal primary nodal management strategy is also unknown. Non-surgical therapy is even more varied. Radiotherapy, chemotherapy, and targeted therapies (including interferon, checkpoint-inhibitors, anti-BRAF therapy, and tyrosine kinase inhibitors) have all been used alone or in various combinations[12-17]. No clear treatment strategy has emerged as the gold standard for treatment of this rare but aggressive disease.

Given the lack of guidelines and variability in reported practice patterns, we analyzed outcomes from a multi-institutional cohort of patients with ARM. We also provide an updated review of the literature to compare outcomes from across the decades and around the world. This review allows for analysis of overall trends to help guide treatment decisions for patients with ARM.

MATERIALS AND METHODS

Study design

We retrospectively reviewed patients diagnosed with ARM between January 1, 2000 and January 1, 2019. This allowed for at least 12 mo of follow-up for all patients. Patients were identified using international classification of diseases-9/10 codes in prospectively maintained institutional tumor registries at 7 centers near Salt Lake City, Utah. These centers included the University of Utah Huntsman Cancer Institute and 6 hospitals affiliated with Intermountain Health Care. All names were linked across institutions to ensure only unique patients were included in the study.

Data Collection

We abstracted data from the electronic medical record and institutional tumor registries. Manual chart review was performed for all records to verify data and obtain additional information. Data abstracted includes patient demographics, primary tumor characteristics, treatment details, and cancer-related outcomes. Both adjuvant therapy and therapy at time of relapse were recorded. Specific chemotherapy and immunotherapy agents were noted. Vital status was available for all but one patient.

Extent of disease was categorized into local, regional, or distant depending on whether disease was confined to the anorectum, involved regional lymph nodes, or other organs[3]. Extent of disease classification was based on clinical documentation. The extent of primary surgical therapy was also determined by clinical documentation. The Institutional Review Boards of the University of Utah and Intermountain Health Care approved this study.

Statistical analyses

Statistical analyses were performed using Stata Version 15.1 (Stata Corp, College Station, TX, United States). We analyzed patient demographics, initial tumor characteristics, and treatment details using descriptive statistics. We calculated median time to recurrence, melanoma-specific survival (MSS), and overall survival (OS) for the cohort and determined MSS and OS at 2, 3, and 5-year intervals. Patients with unknown survival outcomes were excluded from OS analysis and patients with unknown cause of death were excluded from MSS analysis. We graphically evaluated these outcomes using the Kaplan-Meier method. Time-zero for all time-to-event outcomes was the date of diagnosis. Recurrence was defined as re-appearance of disease on physical exam or radiographically in patients who had been initially rendered free of disease after initial treatment. Patients were determined to be free of disease following initial therapy based on intention to treat, as described in clinical documentation.

Cox regression was used to assess for any factors associated with survival. Results were considered statistically significant if the two-sided $P < 0.05$. Analysis of outcomes associated with different surgical and non-surgical treatment options was performed in a similar fashion. Multivariable analysis was not performed because of the small sample size of this cohort.

Review of the literature

We performed a literature review using the PubMed database. The 2009 PRISMA checklist was used to ensure transparent reporting of search and review methodology[18]. The search term used was "ARM." Search results did not differ significantly when "anal melanoma" or "rectal melanoma" were considered separately. All English language articles were included. Articles were excluded if they did not describe outcomes of a unique cohort of at least 10 patients. When multiple articles described overlapping patient cohorts, the most recent and inclusive article was used. Studies describing patient outcomes from national databases in the United States were excluded, as these patients are often represented in other institutional studies. National database studies from other countries were included when other cohorts from these countries did not exist. All titles and abstracts were reviewed for

inclusion.

Once this review was complete, all full-length articles were reviewed. Outcomes of interest were surgical management of patients, median OS, and 5-year OS. No summary of outcomes was performed because of the significant heterogeneity among the various studies.

RESULTS

Twenty-four patients met inclusion criteria. Two-thirds of patients were female, with median age of 65.5 [interquartile range (IQR) 54-76] (Table 1). Patients were from five different states (UT, ID, WY, NV, CO) and approximately 20% of patients were from rural communities. Of 13 patients with information on Breslow depth, 7 (53.8%) were > 5 mm. There were 9 (37.5%) patients whose melanoma exhibited ulceration (Table 1). Half of the patients had advanced disease at diagnosis; 8 with nodal disease and 4 with distant metastases.

Fifteen patients (62.5%) underwent WE at diagnosis and 2 patients (8.3%) underwent APR (Table 2). Seven patients (29.2%) received biopsy alone, including 2/4 patients with distant disease at diagnosis. The primary operation took place at a median of 27 d after diagnosis (IQR 0-47). Sentinel lymph node biopsy (SLNB) was performed in 6 (25%) patients. Of those with local or nodal disease, nearly half of patients received surgery alone as primary management. The remainder of patients received systemic therapy of some form following surgical resection. There was wide variation in adjuvant treatment. Some patients received chemotherapy, radiation, interferon, or checkpoint-inhibitor therapy alone; others received these in various combinations (Table 2).

Of 21 patients with complete follow-up data, only 2 (9.5%) remained free of disease after resection. One of these patients died of metastatic colon adenocarcinoma 13.9 mo after ARM diagnosis. The other patient was alive at last follow-up with no evidence of disease 21.4 mo from diagnosis. Excluding the 4 patients with distant disease at diagnosis, 3 (20.0%) of the remaining 15 patients were never free of disease and the remaining 12 (80.0%) recurred after initial treatment. One patient who was never free of disease underwent APR as salvage therapy. Median time to recurrence was 10.4 mo (IQR 7.5-17.2). At the time of recurrence, 4 patients (33.3%) opted not to pursue further therapy given their age, comorbidities, and/or overall prognosis. Of those who received further treatment (n = 8), only 1 patient had surgery (repeat WE and bilateral inguinal lymph node dissection). Use of systemic therapy was highly variable. Individual patient treatments and outcomes are shown in Supplementary Table 1.

Survival status was known for all but 1 patient. Of these 23 patients, 1 (4.3%) was alive at last follow-up (21.4 mo from diagnosis). Fourteen (60.9%) died from ARM. The cause of death was unknown for 7 (30.4%) patients. Median OS was 18.8 mo (IQR 13.5-33.9) with 0 survivors at 5 years (Figure 1A). Two-year OS was 21.0% (95%CI: 6.8%-40.3%) and 3-year OS was 10.4% (95%CI: 1.8%-27.9%). Median MSS was 19.5 mo (IQR 14.8-35.1) (Figure 1B). Two-year MSS was 29.1% (95%CI: 9.1%-53.0%) and 3-year MSS was 14.6% (95%CI: 2.4%-37.0%). Excluding patients with distant disease at diagnosis, median OS was 19.9 mo (IQR 16.0-35.1) with 2-year OS of 25.5% (95%CI: 8.2%-47.3%) and 3-year OS of 12.7% (95%CI: 2.2%-33.0%). Median MSS was 19.9 mo (IQR 16.4-39.8) with 2-year MSS of 36.4% (95%CI: 11.2%-62.7%) and 3-year MSS of 18.2% (95%CI: 2.9%-44.2%).

Age, sex, rural location, mitoses, ulceration, and Breslow depth were not prognostic of OS. Patients with distant disease at diagnosis had higher risk of mortality than patients with local disease [hazard ratio (HR) = 14.6 (95%CI: 2.5-86.7)] or nodal disease [HR = 14.4 (95%CI: 2.2-92.1)]. No differences in OS were noted for patients who underwent APR *vs* WE as their primary operation [HR = 1.4 (95%CI: 0.3-6.8)]. There was no significant difference in OS between patients who underwent nodal surgery [SLNB or completion lymph node dissection (CLND)] and those who did not [HR = 0.4 (95%CI: 0.1-1.1)]. Exclusion of patients with distant disease at diagnosis did not alter these results. No individual adjuvant therapy (immunotherapy, radiation, or chemotherapy) demonstrated a benefit over another therapy for patients with local or nodal disease treated with surgery as initial treatment.

Review of the literature

This search revealed 360 unique articles, of which 33 were included for review (Figure 2). Cohorts differed across studies, with some including all patients diagnosed with ARM and others limited to only patients with local or nodal disease or patients

Table 1 Demographics and primary tumor characteristics for cohort with anorectal melanoma (*n* = 24)

Classification		*n*
Age, years (median, IQR)		65.5 (54-76)
	≤ 50	3 (12.5)
	51–60	7 (29.2)
	61–70	6 (25.0)
	71–80	6 (25.0)
	> 80	2 (8.3)
Sex	M	8 (33.3)
	F	16 (66.7)
Race	White	23 (95.8)
	Latino	1 (4.2)
Rural	Yes	5 (20.8)
	No	19 (79.2)
Breslow depth (mm)	≤ 5	6 (25.0)
	> 5	7 (29.2)
	Unknown	11 (45.8)
Ulceration	Present	9 (37.5)
	Absent	2 (8.3)
	Unknown	13 (54.2)
Mitoses	> 1	7 (29.2)
	Unknown	17 (70.8)
Stage	I	12 (50.0)
	II	8 (33.3)
	III	4 (16.7)

IQR: Interquartile range.

treated with curative intent. Twenty-five studies reported median OS (Table 3). Median OS ranged from 7-49.5 mo and 21 (84%) studies had median OS < 25 mo. There was wide variation in the type of surgical management across studies. At some centers, all patients received WE while other centers treated all patients with APR[10,19,20].

Eight studies achieved a 5-year OS rate of 20%. Three of these studies included patients diagnosed before 1980, with 1 study including patients from the 1930s[10,21,22]. The other five study cohorts spanned into the 2000s. Surgical management of patients was mixed in this subset of studies. In a study of 54 patients with ARM treated at MD Anderson Cancer Center (MDACC) from 1989-2008, all patients with local disease underwent WE followed by radiation therapy and a 5-year OS of 30% was reported[10]. In another study from South Korea, authors described 12 patients who underwent APR and 7 who underwent WE with significantly improved OS with APR compared to WE[9]. In the remainder of studies, 3 studies reported no significant differences between APR and WE and 3 did not report results of this comparison[7,21-24]. No other dominant themes in surgical or non-surgical treatment were noted across these studies with superior survival outcomes.

Across all studies, the number of APRs was similar to WEs. In total, 427 patients had APR and 436 underwent WE. Studies from the same institution at different time points showed a trend towards performing fewer APRs with time. In two studies from Memorial Sloan Kettering Cancer Center (MSKCC) looking at cohorts from 1950-1977 and 1984-2003, 73.3% of patients underwent APR in the older cohort compared to 41.3% in the more recent cohort[25,26]. At MDACC, Ross *et al*[27] reported APR in 53.8% of patients from 1952-1988 while Kelly *et al*[10] reported exclusive treatment with WE

Table 2 Treatment details for cohort with anorectal melanoma (*n* = 24)

	Treatment	
Primary operation, *n*	WE	15 (62.5)
	APR	2 (8.3)
	Biopsy alone	7 (29.2)
Primary nodal operation, *n*	SLNB	6 (25.0)
	CLND	3 (12.5)
	None	15 (62.5)
Adjuvant therapy, *n*[1]	Chemotherapy alone	0 (0)
	Radiation alone	1 (4.2)
	Interferon alone	3 (12.5)
	Checkpoint Inhibitor	3 (12.5)
	Combination chemotherapy/radiation	2 (8.3)
	Combination chemotherapy/immunotherapy	3 (12.5)
	Combination radiation/immunotherapy	1 (4.2)
	None	11 (45.8)
Surgery at recurrence[2]	APR	1 (9.1)
	WE	1 (9.1)
Non-operative therapies at recurrence[2]	Chemotherapy	1 (9.1)
	Radiation	0 (0)
	Interferon	0 (0)
	Checkpoint Inhibitor	2 (18.2)
	Combination chemotherapy/radiation	4 (26.7)
	Combination chemotherapy/immunotherapy	2 (13.3)
	Combination radiation/immunotherapy	2 (13.3)

[1]Excluding patients with distant disease at diagnosis (*n* = 4).
[2]Percentages calculated from total patients with recurrence who underwent treatment (*n* = 8).
APR: Abdominoperineal resection; WE: Wide excision; SLNB: Sentinel lymph node biopsy; CLND: Completion lymph node dissection.

between 1989-2008, as noted previously[10,27].

Geographic variation in surgical management exists. In United States cohorts, 45.7% (132/289) of surgical patients underwent APR, down to 24.3% over the past 40 years (35/144). European cohorts were similar with 45.1% of patients undergoing APR (123/273). Asian (China, South Korea, Japan, and Taiwan) and Indian cohorts had higher rates of APR with 69.9% (200/286) and 79.7% (51/64) of patients receiving APR as primary surgical therapy respectively. Das *et al*[19] and Ranjith *et al*[20] report cohorts from India with 100% of patients undergoing APR[19,20].

DISCUSSION

Dr. George Pack wrote in 1967, "cures are possible although they do not occur with encouraging frequency[19]". This study confirms the dismal prognosis associated with ARM. Only 1 patient from our study cohort was alive at last follow up, and there were no 5-year survivors. Only 6/33 studies reviewed reported a 5-year OS > 20%, and some of these studies included only patients with local disease. Most studies reported median OS of less than 2 years, and many less than 1 year. There is no compelling evidence from this review that a significant improvement in survival has been made for patients with ARM since 1967.

This study also demonstrates the wide variation in surgical treatment for ARM, both

Table 3 Studies included in literature review and select outcomes

Ref.	Date published	Location	Dates included	Sample size	Median age	M/F (*n*)	APR/WE (*n*)	Median OS	APR *vs* WE (% survival to 5 yr)	Overall 5 yr survival (%)
Pack *et al*[40]	1967	Pack Medical Foundation, United States	1930-1965	20	53.5[1]	5/15	11/3	-	-	5
Abbas *et al*[41]	1980	Roswell Park Memorial Institute, United States	1930-1979	20	61.7	4/16	11/7	18.8[1]	20.1 mo *vs* 8.5 mo[3]	7
Ward *et al*[42]	1986	St. Mark's Hospital, United Kingdom	1932-1982	21	-	12/9	9/6	8.8[1]	-	0
Thibault *et al*[21]	1996	Mayo Clinic, United States	1939-1993	50	63[1]	15/35	26/10	26[1,2]	18 *vs* 19	22
Wanebo *et al*[25]	1990	Memorial Sloan Kettering Cancer Center, United States	1950-1977	36	60	15/21	22/8	14	16/7 mo *vs* 21.5 mo[3,4]	8
Ross *et al*[27]	1990	MD Anderson Cancer Center, United States	1952-1988	32	-	-	14/12	18.6	19.5 mo *vs* 18.9 mo[3]	3
Dodds *et al*[43]	2019	Melanoma Institute Australia, Australia	1958-2016	43	61	21/22	20/15	24	-	16
Siegal *et al*[44]	1983	Sheba Medical Center, Israel	1960-1981	30	64[1]	13/17	15/9	10.5[1]	-	7
Roumen *et al*[45]	1996	Eindhoven Cancer Registry, Netherlands	1960-1995	63	66	27/36	21/18	-	-	6
Nilsson *et al*[46]	2010	Swedish National Cancer Registry, Sweden	1960-1999	251	73	101/150	66/86	11.2	7 *vs* 15, *P* = 0.08	
Podnos *et al*[47]	2006	City of Hope National Medical Center, United States	1973-2001	126	69.2[1]	39/87	-	15	-	19
Slingluff *et al*[48]	1990	Duke University Medical Center, United States	1974-1988	24	64[1]	7/17	13/8	18	18 *vs* 12	8
Belli *et al*[49]	2008	National Institute of Cancer, Italy	1975-2006	40	63	19/21	13/18	17	18.5 *vs* 18.5, *P* = 0.97	-
Che *et al*[22]	2011	Peking Union Medical College, China	1975-2008	56	-	22/34	36/20	21	24.6 *vs* 9.9, *P* = 0.65	20
Pessaux *et al*[50]	2004	Institut Gustave Roussy, France	1977-2002	30	58.1	7/23	9/21	17	16 *vs* 33	17
Ramakrishnan *et al*[51]	2008	Cancer Institue (WIA), India	1980-2004	63	-	34/29	3/8	9.5[2]	-	5
Yeh *et al*[26]	2006	Memorial Sloan Kettering Cancer Center, United States	1984-2003	46	59	18/28	19/27	39[5]	32 *vs* 35, *P* = 0.66[5]	-
Homsi *et al*[52]	2007	H. Lee Moffitt Cancer Center, United States	1987-2004	12	67	3/9	5/6	-	-	-
Bullard *et al*[53]	2003	University of Minnesota, United States	1988-2002	15	65[1]	6/9	4/11	18[6]	14 mo *vs* 19 mo[3]	-
Kelly *et al*[10]	2010	MD Anderson Cancer Center, United States	1989-2008	54	61	19/35	0/54	29	-	30
Das *et al*[19]	2003	Tata Memorial Hospital, India	1990-2001	72	49[1]	20/52	24/0	13[2,5]	-	8[2]
Hicks *et al*[28]	2014	John Hopkins Hospital, United States	1991-2012	18	64	10/8	7/11	15.5	11.5 mo *vs* 13.5 mo, *P* = 0.75[3]	-
Yen *et al*[54]	2013	Chang Gung Memorial Hospital, China	1993-2011	22	58.4[1]	8/14	12/8	-	0 *vs* 28.6, *P* = 0.06	9
Zhang *et al*[7]	2010	First Affiliated Hospital of Guangxi Medical University, China	1995-2007	54	54	21/33	39/15	25	30 *vs* 16, *P* = 0.28	26

Aytac *et al*[55]	2010	Uludag University, Turkey	1997-2004	14	58	8/6	11/3	7.5	-	0
Ishizone *et al*[32]	2008	Shinshu University Hospital, Japan	1997-2006	79	65.8[1]	34/45	63/14	22	-	29
Belbaraka *et al*[56]	2012	National Institute of Oncology, Morocco	1998-2007	17	58[1]	12/5	7/3	8	-	-
Choi *et al*[9]	2010	Samsung Medical Center, South Korea	1999-2008	19	61	8/11	12/7	45.9	50 *vs* 0	32
Miguel *et al*[23]	2015	IPOFG, Portugal	2000-2011	10	70.5	2/8	5/1	9.3	-	20
Ranjith *et al*[20]	2018	Regional Cancer Center Thiruvanathapuram, India	2001-2013	31	56	12/19	9/0	9	-	0
Ren *et al*[24]	2018	Fudan University Shanghai Cancer Center, China	2005-2017	60	61	18/42	38/22	-	-	33.3[5]
Nusrath *et al*[57]	2018	Basavatakrakam Indo American Cancer Hospital, India	2010-2015	30	50	15/15	15/5	13	13 *vs* 36, P = 0.48	-
Sahu *et al*[58]	2017	Tata Memorial Hospital, India	2013-2015	37	54	25/12	-	7	-	-

[1]Mean reported instead of median.
[2]Only cases treated with curative intent included in analysis.
[3]Median overall survival (OS) [abdominoperineal resection (APR) *vs* wide excision].
[4]APR OS grouped as lymph node negative/lymph node positive.
[5]Melanoma specific survival.
[6]Mean OS of deceased patients only.
APR: Abdominoperineal resection; WE: Wide excision; mo: Month; OS: Overall survival.

within and between medical centers. Geographic variation also exists, with United States and European centers more likely to perform WE and Asian and Indian centers more likely to perform APR. This finding was true in our cohort, with few patients undergoing APR. While low sample size limits analysis, there was no difference in survival outcomes between patients undergoing WE *vs* APR. Multiple other groups have demonstrated similar or better outcomes with WE compared to APR[10,28]. This same conclusion has been reached using larger cohorts from Surveillance, Epidemiology, and End Results and National Cancer Database (NCDB)[1,11,12]. A prior systematic review concluded that while APR may reduce local recurrence, there is no improvement in OS or recurrence-free survival compared to WE[29].

WE allows for avoidance of a colostomy and significantly reduced morbidity compared to APR. A study of 49 patients undergoing WE demonstrated the safety of this procedure; 3 patients had minor infections requiring antibiotics and 1 patient required a second operation for postoperative bleeding. No other complications from surgery occurred[10]. While most studies of APR for ARM have not reported complication rates, APR for other indications is known to be associated with significant morbidities. Perineal wound complications occur in up to 40% of patients and 50% of patients develop genitourinary and/or sexual dysfunction postoperatively[30]. No studies currently exist in ARM that compare quality of life between WE and APR[31]. Some centers continue to routinely perform APR for ARM patients; however, we did not find evidence in this review to support this practice[9,19,20,32].

Nodal management also differs widely. In our cohort, there were no significant differences in survival outcomes between patients who underwent initial nodal surgery (SLNB or CLND) and those who did not. Nearly 2/3 of patients did not receive any nodal staging or treatment. Older studies hypothesized that the benefit of APR was largely secondary to the mesorectal lymphadenectomy performed with this procedure[25]. However, Yeh *et al*[26] found that the presence of lymph node metastases had no prognostic significance on survival in 19 patients who underwent APR at MSKCC[26]. Many patients in this cohort received local surgery alone and did not receive additional therapy until the time of recurrence. Some of these patients likely had unidentified nodal disease at the time of initial surgery. If patients had undergone SLNB and were found to have positive nodal disease, adjuvant systemic therapy could have been initiated sooner. The impact this may have had on survival is unknown. This review did not find studies with large enough patient numbers to make

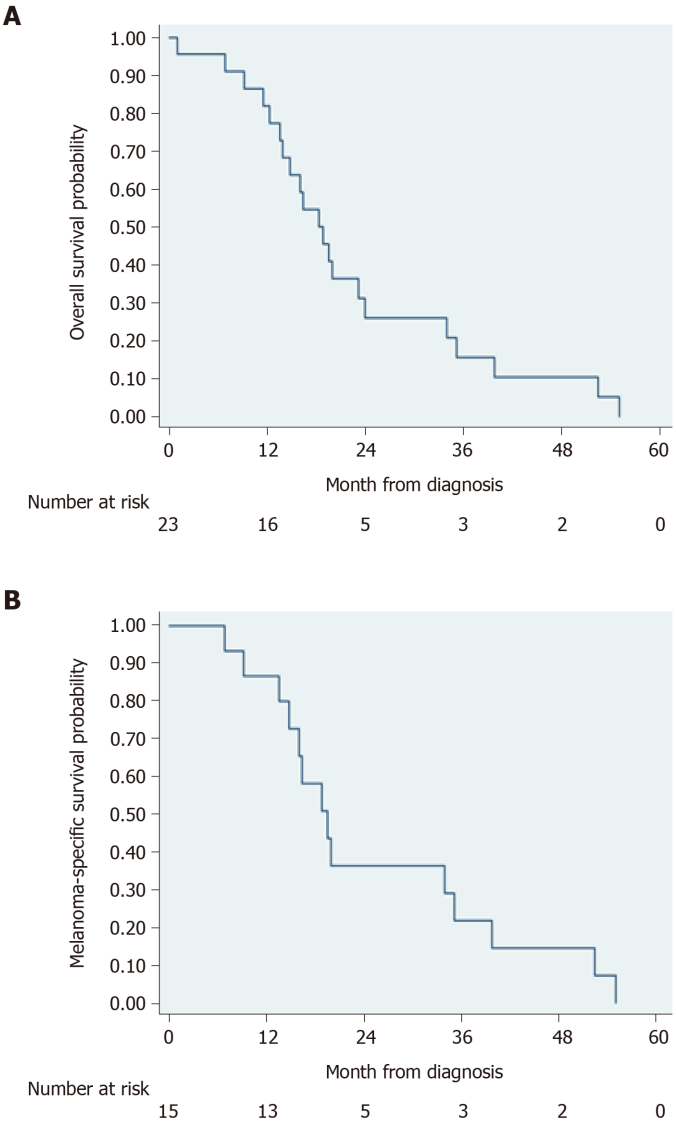

Figure 1 Overall mortality and melanoma-specific mortality in cohort of patients with anorectal melanoma. A: Overall mortality; B: Melanoma-specific mortality.

conclusions regarding the benefits of nodal surgery.

Use of immune checkpoint inhibitors and targeted therapies is also controversial and evidence is lacking to help with decision making. While checkpoint inhibitors, tyrosine kinase inhibitors, and BRAF/MEK inhibitors have significantly improved outcomes for cutaneous melanoma over the past decade, their role in treatment of ARM remains unknown[33-36]. Results of immune checkpoint inhibitor therapy for ARM are limited and show mixed outcomes. Tokuhara *et al*[13] reported a case of a 67-year-old male with ARM who had no oncologic progression of disease for 17 mo after initiation of anti- programmed death 1 (PD-1) therapy[13]. Conversely, Faure *et al*[37] reported a case of a 77 year-old male with ARM who progressed rapidly on anti-PD-1 therapy[37]. Higher level evidence of the effectiveness of immune checkpoint inhibitor therapy in treating ARM is lacking[13,38]. While immune checkpoint inhibitor therapy has helped individual patients with ARM, the efficacy of this treatment in most ARMs has been questioned as most ARMs do not exhibit 1-PD-ligand expression and few have tumor-infiltrating lymphocytes[25]. Evidence for other targeted therapies is similarly poor[2]. The genomic profiles of ARMs differ from cutaneous melanomas, with very low BRAF expression and few NRAS and KIT mutations[39]. ARM likely has different drivers of metastases with fewer targetable mutations. Although a rare disease, clinical trials are necessary to determine what therapies are most useful for ARM.

This study is limited by its retrospective nature and small cohort size. ARM is an extremely rare disease and only 24 cases were identified over a 20-year period. Additionally, the lack of a synoptic report for this disease has resulted in many

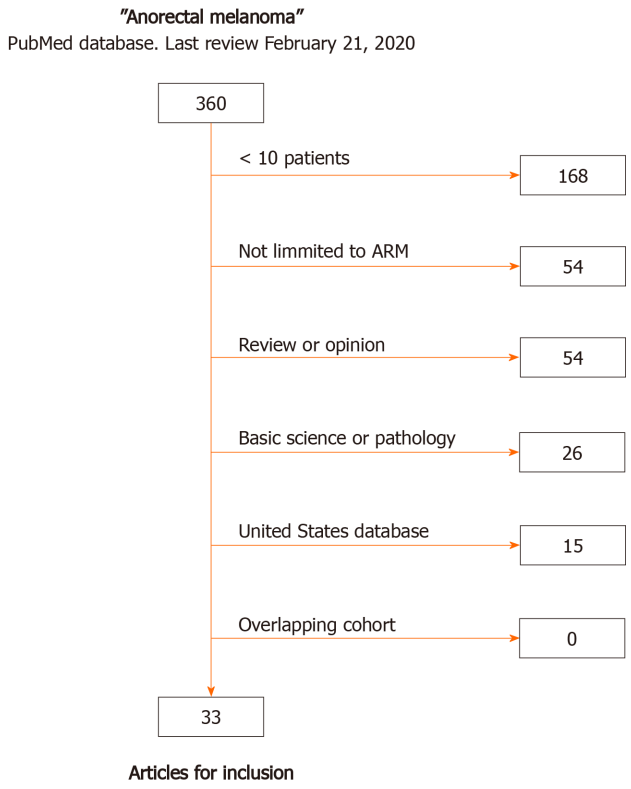

Figure 2 Flow diagram of selection of articles for literature review. ARM: Anorectal melanoma.

missing pertinent variables which would have strengthened this study.

CONCLUSION

ARM is a highly lethal disease. Over the past 50 years, outcomes have remained largely unchanged. Without good evidence to drive treatment decisions, surgical and non-surgical management remains highly variable across the United States and the world. Even within our own cohort, management differed between patients. Review of the literature was also unable to resolve many questions on ARM. There does not appear to be survival benefit of APR over WE. With no clear advantage to APR, surgical management should aim to minimize morbidity. Many other questions on ARM management remain unanswered. Improving the quality of data on ARM is necessary. A consensus meeting of experts aimed at the identification of pertinent variables to collect would be a good first step. Additionally, clinical trials to assess the role of sentinel lymph node biopsy, targeted therapies, radiation therapy, and treatment sequencing are needed.

ARTICLE HIGHLIGHTS

Research background

Anorectal melanoma (ARM) is a rare disease with poor outcomes. 5-year survival remains < 20%.

Research motivation

Optimal surgical management of ARM remains unknown. Abdominoperineal resection (APR) and wide excision (WE) are both used and no gold standard for primary tumor management currently exists. Understanding trends in management and outcomes is critical to determining appropriate surgical management.

Research objectives

We aimed to update our understanding of treatment outcomes for patients with ARM

and analyze trends across countries and time.

Research methods

We performed a retrospective study of patients who were diagnosed with ARM at 7 hospitals in the Salt Lake City, UT region. We analyzed factors prognostic for recurrence and survival. We also performed a review of the literature to assess regional and temporal trends in ARM management.

Research results

We identified 24 patients diagnosed with ARM between 2000-01 and 2019-05. 12 (50.0%) had local, 8 (33.3%) regional, and 4 (16.7%) distant disease at diagnosis. Only 2 patients who had surgical resection of their primary tumor with curative intent failed to recur. Median time to recurrence was 10.4 mo [interquartile range (IQR) 7.5–17.2] and median overall survival was 18.8 mo (IQR 13.5–33.9). No patients survived to 5 years. No survival differences were noted for patients managed with WE *vs* APR. Review of the literature demonstrated regional trends in surgical management of ARM, with WE favored in the United States and Europe and APR used more frequently in Asia.

Research conclusions

ARM remains a highly lethal disease regardless of surgical treatment. Patients who undergo WE and APR have poor outcomes. No convincing evidence exists to favor APR over WE. Despite this, APR continues to be used for primary surgical management, although with decreasing frequency in the United States and Europe in recent years. We feel that surgical management should aim to minimize morbidity. WE should be favored over APR for primary surgical treatment.

Research perspectives

Further research should focus on better risk stratification and the role of targeted therapies, radiation therapy, and treatment sequencing. Improving non-surgical therapies will be critical to improving survival for patients with ARM.

ACKNOWLEDGEMENTS

We thank Emily Z. Keung, MD, MD Anderson Cancer Center, Houston, TX, United States.

REFERENCES

1 **Chen H**, Cai Y, Liu Y, He J, Hu Y, Xiao Q, Hu W, Ding K. Incidence, Surgical Treatment, and Prognosis of Anorectal Melanoma From 1973 to 2011: A Population-Based SEER Analysis. *Medicine (Baltimore)* 2016; **95**: e2770 [PMID: 26886623 DOI: 10.1097/MD.0000000000002770]

2 **Paolino G**, Didona D, Macrì G, Calvieri S, Mercuri SR. Anorectal Melanoma. In: Scott JF, Gerstenblith MR, editors. Noncutaneous Melanoma [Internet]. *Brisbane (AU): Codon Publications* 2018; **6**: 83-98 [PMID: 29874013 DOI: 10.15586/codon.noncutaneousmelanoma.2018.ch6]

3 **Patrick RJ**, Fenske NA, Messina JL. Primary mucosal melanoma. *J Am Acad Dermatol* 2007; **56**: 828-834 [PMID: 17349716 DOI: 10.1016/j.jaad.2006.06.017]

4 **Mihajlovic M**, Vlajkovic S, Jovanovic P, Stefanovic V. Primary mucosal melanomas: a comprehensive review. *Int J Clin Exp Pathol* 2012; **5**: 739-753 [PMID: 23071856]

5 **van Schaik PM**, Ernst MF, Meijer HA, Bosscha K. Melanoma of the rectum: a rare entity. *World J Gastroenterol* 2008; **14**: 1633-1635 [PMID: 18330962 DOI: 10.3748/wjg.14.1633]

6 **Khan M**, Bucher N, Elhassan A, Barbaryan A, Ali AM, Hussain N, Mirrakhimov AE. Primary anorectal melanoma. *Case Rep Oncol* 2014; **7**: 164-170 [PMID: 24748866 DOI: 10.1159/000360814]

7 **Zhang S**, Gao F, Wan D. Effect of misdiagnosis on the prognosis of anorectal malignant melanoma. *J Cancer Res Clin Oncol* 2010; **136**: 1401-1405 [PMID: 20130908 DOI: 10.1007/s00432-010-0793-z]

8 **National Comprehensive Cancer Network**. Cutaneous Melanoma: Clinical Practice Guidelines in Oncology. 2019

9 **Choi BM**, Kim HR, Yun HR, Choi SH, Cho YB, Kim HC, Yun SH, Lee WY, Chun HK. Treatment outcomes of anorectal melanoma. *J Korean Soc Coloproctol* 2011; **27**: 27-30 [PMID: 21431094 DOI: 10.3393/jksc.2011.27.1.27]

10 **Kelly P**, Zagars GK, Cormier JN, Ross MI, Guadagnolo BA. Sphincter-sparing local excision and hypofractionated radiation therapy for anorectal melanoma: a 20-year experience. *Cancer* 2011; **117**: 4747-4755 [PMID: 21446049 DOI: 10.1002/cncr.26088]

11 **Ciarrocchi A**, Pietroletti R, Carlei F, Amicucci G. Extensive surgery and lymphadenectomy do not improve survival in primary melanoma of the anorectum: results from analysis of a large database (SEER). *Colorectal Dis* 2017; **19**: 158-164 [PMID: 27317493 DOI: 10.1111/codi.13412]

12 **Taylor JP**, Stem M, Yu D, Chen SY, Fang SH, Gearhart SL, Safar B, Efron JE. Treatment Strategies and Survival Trends for Anorectal Melanoma: Is it Time for a Change? *World J Surg* 2019; **43**: 1809-1819 [PMID: 30830243 DOI: 10.1007/s00268-019-04960-w]

13 **Tokuhara K**, Nakatani K, Tanimura H, Yoshioka K, Kiyohara T, Kon M. A first reported case of metastatic anorectal amelanotic melanoma with a marked response to anti-PD-1 antibody nivolumab: A case report. *Int J Surg Case Rep* 2017; **31**: 188-192 [PMID: 28171845 DOI: 10.1016/j.ijscr.2017.01.028]

14 **Knowles J**, Lynch AC, Warrier SK, Henderson M, Heriot AG. A case series of anal melanoma including the results of treatment with imatinib in selected patients. *Colorectal Dis* 2016; **18**: 877-882 [PMID: 26546509 DOI: 10.1111/codi.13209]

15 **Shoushtari AN**, Bluth MJ, Goldman DA, Bitas C, Lefkowitz RA, Postow MA, Munhoz RR, Buchar G, Hester RH, Romero JA, Fitzpatrick LJ, Weiser MR, Panageas KS, Wolchok JD, Chapman PB, Carvajal RD. Clinical features and response to systemic therapy in a historical cohort of advanced or unresectable mucosal melanoma. *Melanoma Res* 2017; **27**: 57-64 [PMID: 27792058 DOI: 10.1097/CMR.0000000000000306]

16 **Kim KB**, Sanguino AM, Hodges C, Papadopoulos NE, Eton O, Camacho LH, Broemeling LD, Johnson MM, Ballo MT, Ross MI, Gershenwald JE, Lee JE, Mansfield PF, Prieto VG, Bedikian AY. Biochemotherapy in patients with metastatic anorectal mucosal melanoma. *Cancer* 2004; **100**: 1478-1483 [PMID: 15042682 DOI: 10.1002/cncr.20113]

17 **Lian B**, Si L, Cui C, Chi Z, Sheng X, Mao L, Li S, Kong Y, Tang B, Guo J. Phase II randomized trial comparing high-dose IFN-α2b with temozolomide plus cisplatin as systemic adjuvant therapy for resected mucosal melanoma. *Clin Cancer Res* 2013; **19**: 4488-4498 [PMID: 23833309 DOI: 10.1158/1078-0432.CCR-13-0739]

18 PRISMA. Systematic Review and Meta-analysis Checklist. 2009

19 **Das G**, Gupta S, Shukla PJ, Jagannath P. Anorectal melanoma: a large clinicopathologic study from India. *Int Surg* 2003; **88**: 21-24 [PMID: 12731727]

20 **Ranjith S**, Muralee M, Sajeed A, Arun PM, Cherian K, Nair CK, Augustine P, Ahamed I. Anorectal melanoma: experience from a tertiary cancer care centre in South India. *Ann R Coll Surg Engl* 2018; **100**: 185-189 [PMID: 29046101 DOI: 10.1308/rcsann.2017.0184]

21 **Thibault C**, Sagar P, Nivatvongs S, Ilstrup DM, Wolff BG. Anorectal melanoma--an incurable disease? *Dis Colon Rectum* 1997; **40**: 661-668 [PMID: 9194459 DOI: 10.1007/BF02140894]

22 **Che X**, Zhao DB, Wu YK, Wang CF, Cai JQ, Shao YF, Zhao P. Anorectal malignant melanomas: retrospective experience with surgical management. *World J Gastroenterol* 2011; **17**: 534-539 [PMID: 21274385 DOI: 10.3748/wjg.v17.i4.534]

23 **Miguel I**, Freire J, Passos MJ, Moreira A. Anorectal malignant melanoma: retrospective analysis of management and outcome in a single Portuguese Institution. *Med Oncol* 2015; **32**: 445 [PMID: 25502089 DOI: 10.1007/s12032-014-0445-2]

24 **Ren M**, Lu Y, Lv J, Shen X, Kong J, Dai B, Kong Y. Prognostic factors in primary anorectal melanoma: a clinicopathological study of 60 cases in China. *Hum Pathol* 2018; **79**: 77-85 [PMID: 29763716 DOI: 10.1016/j.humpath.2018.05.004]

25 **Wanebo HJ**, Woodruff JM, Farr GH, Quan SH. Anorectal melanoma. *Cancer* 1981; **47**: 1891-1900 [PMID: 6164474 DOI: 10.1002/1097-0142(19810401)47:7<1891::aid-cncr2820470730>3.0.co;2-k]

26 **Yeh JJ**, Shia J, Hwu WJ, Busam KJ, Paty PB, Guillem JG, Coit DG, Wong WD, Weiser MR. The role of abdominoperineal resection as surgical therapy for anorectal melanoma. *Ann Surg* 2006; **244**: 1012-1017 [PMID: 17122627 DOI: 10.1097/01.sla.0000225114.56565.f9]

27 **Ross M**, Pezzi C, Pezzi T, Meurer D, Hickey R, Balch C. Patterns of failure in anorectal melanoma. A guide to surgical therapy. *Arch Surg* 1990; **125**: 313-316 [PMID: 2306178 DOI: 10.1001/archsurg.1990.01410150035007]

28 **Hicks CW**, Pappou EP, Magruder JT, Gazer B, Fang S, Wick EC, Gearhart SL, Ahuja N, Efron JE. Clinicopathologic Presentation and Natural History of Anorectal Melanoma: A Case Series of 18 Patients. *JAMA Surg* 2014; **149**: 608-611 [PMID: 24848283 DOI: 10.1001/jamasurg.2013.4643]

29 **Matsuda A**, Miyashita M, Matsumoto S, Takahashi G, Matsutani T, Yamada T, Kishi T, Uchida E. Abdominoperineal resection provides better local control but equivalent overall survival to local excision of anorectal malignant melanoma: a systematic review. *Ann Surg* 2015; **261**: 670-677 [PMID: 25119122 DOI: 10.1097/SLA.0000000000000862]

30 **Peterson CY**, Garcia-Aguilar J. Abdominoperineal resection for rectal cancer. In: Fischer's Mastery of Surgery. 2019: 1841-1852

31 **Smith HG**, Glen J, Turnbull N, Peach H, Board R, Payne M, Gore M, Nugent K, Smith MJF. Less is more: A systematic review and meta-analysis of the outcomes of radical *vs* conservative primary resection in anorectal melanoma. *Eur J Cancer* 2020; **135**: 113-120 [PMID: 32563895 DOI: 10.1016/j.ejca.2020.04.041]

32 **Ishizone S**, Koide N, Karasawa F, Akita N, Muranaka F, Uhara H, Miyagawa S. Surgical treatment for anorectal malignant melanoma: report of five cases and review of 79 Japanese cases. *Int J Colorectal Dis* 2008; **23**: 1257-1262 [PMID: 18633625 DOI: 10.1007/s00384-008-0529-6]

33 **Freeman M**, Laks S. Surveillance imaging for metastasis in high-risk melanoma: importance in individualized patient care and survivorship. *Melanoma Manag* 2019; **6**: MMT12 [PMID: 31236204

DOI: 10.2217/mmt-2019-0003]
34 **Joseph RW**, Elassaiss-Schaap J, Kefford R, Hwu WJ, Wolchok JD, Joshua AM, Ribas A, Hodi FS, Hamid O, Robert C, Daud A, Dronca R, Hersey P, Weber JS, Patnaik A, de Alwis DP, Perrone A, Zhang J, Kang SP, Ebbinghaus S, Anderson KM, Gangadhar TC. Baseline Tumor Size Is an Independent Prognostic Factor for Overall Survival in Patients with Melanoma Treated with Pembrolizumab. *Clin Cancer Res* 2018; **24**: 4960-4967 [PMID: 29685882 DOI: 10.1158/1078-0432.CCR-17-2386]
35 **Long GV**, Flaherty KT, Stroyakovskiy D, Gogas H, Levchenko E, de Braud F, Larkin J, Garbe C, Jouary T, Hauschild A, Chiarion-Sileni V, Lebbe C, Mandalà M, Millward M, Arance A, Bondarenko I, Haanen JBAG, Hansson J, Utikal J, Ferraresi V, Mohr P, Probachai V, Schadendorf D, Nathan P, Robert C, Ribas A, Davies MA, Lane SR, Legos JJ, Mookerjee B, Grob JJ. Dabrafenib plus trametinib *vs* dabrafenib monotherapy in patients with metastatic BRAF V600E/K-mutant melanoma: long-term survival and safety analysis of a phase 3 study. *Ann Oncol* 2017; **28**: 1631-1639 [PMID: 28475671 DOI: 10.1093/annonc/mdx176]
36 **Kaufman H**, Amatruda T, Nemunaitis JJ, Chesney JA, Delman KA, Spitler LE, Collichio FA, Ross MI, Zhang Y, Shilkrut M, Andtbacka RHI. Tumor size and clinical outcomes in melanoma patients (MEL pts) treated with talimogene laherparepvec (T-VEC). *J Clin Oncol* 2015; **33**: 9074 [DOI: 10.1200/jco.2015.33.15_suppl.9074]
37 **Faure M**, Rochigneux P, Olive D, Taix S, Brenot-Rossi I, Gilabert M. Hyperprogressive Disease in Anorectal Melanoma Treated by PD-1 Inhibitors. *Front Immunol* 2018; **9**: 797 [PMID: 29725330 DOI: 10.3389/fimmu.2018.00797]
38 **Cai YT**, Cao LC, Zhu CF, Zhao F, Tian BX, Guo SY. Multiple synchronous anorectal melanomas with different colors: A case report. *World J Clin Cases* 2019; **7**: 1337-1343 [PMID: 31236398 DOI: 10.12998/wjcc.v7.i11.1337]
39 **Yang HM**, Hsiao SJ, Schaeffer DF, Lai C, Remotti HE, Horst D, Mansukhani MM, Horst BA. Identification of recurrent mutational events in anorectal melanoma. *Mod Pathol* 2017; **30**: 286-296 [PMID: 27739435 DOI: 10.1038/modpathol.2016.179]
40 **Pack GT**, Oropeza R. A comparative study of melanoma and epidermoid carcinoma of the anal canal: A review of 20 melanomas and 29 epidermoid carcinomas (1930 to 1965). *Dis Colon Rectum* 1967; **10**: 161-176 [PMID: 6026797 DOI: 10.1007/BF02617173]
41 **Abbas JS**, Karakousis CP, Holyoke ED. Anorectal melanoma: clinical features, recurrence and patient survival. *Int Surg* 1980; **65**: 423-426 [PMID: 7451062]
42 **Ward MW**, Romano G, Nicholls RJ. The surgical treatment of anorectal malignant melanoma. *Br J Surg* 1986; **73**: 68-69 [PMID: 3947881 DOI: 10.1002/bjs.1800730127]
43 **Dodds TJ**, Wilmott JS, Jackett LA, Lo SN, Long GV, Thompson JF, Scolyer RA. Primary anorectal melanoma: clinical, immunohistology and DNA analysis of 43 cases. *Pathology* 2019; **51**: 39-45 [PMID: 30497801 DOI: 10.1016/j.pathol.2018.09.060]
44 **Siegal B**, Cohen D, Jacob ET. Surgical treatment of anorectal melanomas. *Am J Surg* 1983; **146**: 336-338 [PMID: 6614323 DOI: 10.1016/0002-9610(83)90410-5]
45 **Roumen RM**. Anorectal melanoma in The Netherlands: a report of 63 patients. *Eur J Surg Oncol* 1996; **22**: 598-601 [PMID: 9005147 DOI: 10.1016/S0748-7983(96)92346-X]
46 **Nilsson PJ**, Ragnarsson-Olding BK. Importance of clear resection margins in anorectal malignant melanoma. *Br J Surg* 2010; **97**: 98-103 [PMID: 20013935 DOI: 10.1002/bjs.6784]
47 **Podnos YD**, Tsai NC, Smith D, Ellenhorn JD. Factors affecting survival in patients with anal melanoma. *Am Surg* 2006; **72**: 917-920 [PMID: 17058735]
48 **Slingluff CL Jr**, Vollmer RT, Seigler HF. Anorectal melanoma: clinical characteristics and results of surgical management in twenty-four patients. *Surgery* 1990; **107**: 1-9 [PMID: 2296748]
49 **Belli F**, Gallino GF, Lo Vullo S, Mariani L, Poiasina E, Leo E. Melanoma of the anorectal region: the experience of the National Cancer Institute of Milano. *Eur J Surg Oncol* 2009; **35**: 757-762 [PMID: 18602790 DOI: 10.1016/j.ejso.2008.05.001]
50 **Pessaux P**, Pocard M, Elias D, Duvillard P, Avril MF, Zimmerman P, Lasser P. Surgical management of primary anorectal melanoma. *Br J Surg* 2004; **91**: 1183-1187 [PMID: 15449271 DOI: 10.1002/bjs.4592]
51 **Ramakrishnan AS**, Mahajan V, Kannan R. Optimizing local control in anorectal melanoma. *Indian J Cancer* 2008; **45**: 13-19 [PMID: 18453735 DOI: 10.4103/0019-509x.40641]
52 **Homsi J**, Garrett C. Melanoma of the anal canal: a case series. *Dis Colon Rectum* 2007; **50**: 1004-1010 [PMID: 17468984 DOI: 10.1007/s10350-007-0242-5]
53 **Bullard KM**, Tuttle TM, Rothenberger DA, Madoff RD, Baxter NN, Finne CO, Spencer MP. Surgical therapy for anorectal melanoma. *J Am Coll Surg* 2003; **196**: 206-211 [PMID: 12595048 DOI: 10.1016/S1072-7515(02)01538-7]
54 **Yen CI**, Chen HH, Chiang SF, Yeh CY, Chen JS, Hsieh PS, Chiang JM, Tsai WS, Tang R, Changchien CR, Wang JY. Anorectal melanoma: review of 22 consecutive cases. *Hepatogastroenterology* 2013; **60**: 89-93 [PMID: 22829553 DOI: 10.5754/hge12453]
55 **Aytac B**, Adim SB, Yerci O, Yilmazlar T. Anorectal malignant melanomas: experience of Uludag University. *Kaohsiung J Med Sci* 2010; **26**: 658-662 [PMID: 21186014 DOI: 10.1016/S1607-551X(10)70100-5]
56 **Belbaraka R**, Elharroudi T, Ismaili N, Fetohi M, Tijami F, Jalil A, Errihani H. Management of anorectal melanoma: report of 17 cases and literature review. *J Gastrointest Cancer* 2012; **43**: 31-35 [PMID: 20886311 DOI: 10.1007/s12029-010-9216-2]

57 **Nusrath S**, Thammineedi SR, Patnaik SC, Raju KVVN, Pawar S, Goel V, Chavali RN, Murthy S. Anorectal Malignant Melanoma-Defining the Optimal Surgical Treatment and Prognostic Factors. *Indian J Surg Oncol* 2018; **9**: 519-523 [PMID: 30538382 DOI: 10.1007/s13193-018-0791-1]

58 **Sahu A**, Ramaswamy A, Singhal N, Doshi V, Mirani J, Desouza A, Banavali S, Saklani A, Ostwal V. Metastatic anorectal melanomas - An exploratory retrospective analysis on the benefits of systemic therapy *vs* best supportive care in a resource-limited setting from India. *South Asian J Cancer* 2017; **6**: 147-150 [PMID: 29404289 DOI: 10.4103/sajc.sajc_276_16]

World Journal of Gastroenterology

Submit a Manuscript: https://www.f6publishing.com

World J Gastroenterol 2021 January 21; 27(3): 281-293

DOI: 10.3748/wjg.v27.i3.281

ISSN 1007-9327 (print) ISSN 2219-2840 (online)

ORIGINAL ARTICLE

Observational Study

Comparative study on artificial intelligence systems for detecting early esophageal squamous cell carcinoma between narrow-band and white-light imaging

Bing Li, Shi-Lun Cai, Wei-Min Tan, Ji-Chun Li, Ayimukedisi Yalikong, Xiao-Shuang Feng, Hon-Ho Yu, Pin-Xiang Lu, Zhen Feng, Li-Qing Yao, Ping-Hong Zhou, Bo Yan, Yun-Shi Zhong

ORCID number: Bing Li 0000-0001-9802-5860; Shi-Lun Cai 0000-0002-5000-9658; Wei-Min Tan 0000-0001-7677-4772; Ji-Chun Li 0000-0003-4906-8244; Ayimukedisi Yalikong 0000-0002-7328-8354; Xiao-Shuang Feng 0000-0002-7933-3996; Hon-Ho Yu 0000-0002-9580-345X; Pin-Xiang Lu 0000-0001-5941-9584; Zhen Feng 0000-0003-0424-4726; Li-Qing Yao 0000-0001-6900-6791; Ping-Hong Zhou 0000-0002-5434-0540; Bo Yan 0000-0003-0256-9682; Yun-Shi Zhong 0000-0002-3128-3168.

Author contributions: Zhong YS and Yan B conceived the study design; Li B, Cai SL, Tan WM, Li JC, Yalikong A, Yu HH, Lu PX, and Feng Z acquired the data; Li B, Cai SL, Yalikong A, Tan WM, Feng XS, Yao LQ, Zhou PH, and Zhong YS analyzed and interpreted the data; Li B, Tan WM, and Cai SL drafted the manuscript; Zhong YS critically revised the manuscript for important intellectual content; Li B, Cai SL, Tan WM, Li JC, Yalikong A, Feng XS, Yu HH, Lu PX, Feng Z, Yao LQ, Zhou PH, Yan B, and Zhong YS approved the final version of the manuscript; Li B, Cai SL and Tan WM contributed equally to this article.

Supported by National Key R&D

Bing Li, Shi-Lun Cai, Ayimukedisi Yalikong, Li-Qing Yao, Ping-Hong Zhou, Yun-Shi Zhong, Department of Endoscopy Center, Zhongshan Hospital of Fudan University, Shanghai 200032, China

Wei-Min Tan, Ji-Chun Li, Bo Yan, School of Computer Science, Fudan University, Shanghai 200433, China

Xiao-Shuang Feng, Clinical Statistical Center, Shanghai Cancer Center of Fudan University, Shanghai 200032, China

Hon-Ho Yu, Department of Gastroenterology, Kiang Wu Hospital, Macau SAR 999078, China

Pin-Xiang Lu, Zhen Feng, Department of Endoscopy Center, Xuhui Hospital, Zhongshan Hospital of Fudan University, Shanghai 200031, China

Corresponding author: Yun-Shi Zhong, MD, PhD, Professor, Department of Endoscopy Center, Zhongshan Hospital of Fudan University, No. 180 Fenglin Road, Shanghai 200032, China. zhongyunshi@yahoo.com

Abstract

BACKGROUND

Non-magnifying endoscopy with narrow-band imaging (NM-NBI) has been frequently used in routine screening of esophagus squamous cell carcinoma (ESCC). The performance of NBI for screening of early ESCC is, however, significantly affected by operator experience. Artificial intelligence may be a unique approach to compensate for the lack of operator experience.

AIM

To construct a computer-aided detection (CAD) system for application in NM-NBI to identify early ESCC and to compare it with our previously reported CAD system with endoscopic white-light imaging (WLI).

METHODS

A total of 2167 abnormal NM-NBI images of early ESCC and 2568 normal images were collected from three institutions (Zhongshan Hospital of Fudan University,

Program of China, No. 2018YFC1315000, No. 2018YFC1315005, No. 2019YFC1315800, and No. 2019YFC1315802; National Natural Science Foundation of China, No. 81861168036 and No. 81702305; Science and Technology Commission Foundation of Shanghai Municipality, No. 19411951600, and No. 19411951601; Macao SAR Science and Technology Development Foundation, No. 0023/2018/AFJ; and Dawn Program of Shanghai Education Commission, No. 18SG08.

Institutional review board statement: This study was reviewed and approved by the Ethics Committee of Zhongshan Hospital, Fudan University.

Informed consent statement: Patients were not required to give informed consent to the study because the analysis used anonymous clinical data that were obtained after each patient agreed to undergo treatment by written consent.

Conflict-of-interest statement: The authors declare that they have no competing interests.

Data sharing statement: The datasets used and analyzed during the current study are available from the corresponding author on reasonable request.

STROBE statement: The authors have read the STROBE Statement checklist of items, and the manuscript was prepared and revised according to the STROBE Statement-checklist of items.

Xuhui Hospital, and Kiang Wu Hospital) as the training dataset, and 316 pairs of images, each pair including images obtained by WLI and NBI (same part), were collected for validation. Twenty endoscopists participated in this study to review the validation images with or without the assistance of the CAD systems. The diagnostic results of the two CAD systems and improvement in diagnostic efficacy of endoscopists were compared in terms of sensitivity, specificity, accuracy, positive predictive value, and negative predictive value.

RESULTS

The area under receiver operating characteristic curve for CAD-NBI was 0.9761. For the validation dataset, the sensitivity, specificity, accuracy, positive predictive value, and negative predictive value of CAD-NBI were 91.0%, 96.7%, 94.3%, 95.3%, and 93.6%, respectively, while those of CAD-WLI were 98.5%, 83.1%, 89.5%, 80.8%, and 98.7%, respectively. CAD-NBI showed superior accuracy and specificity than CAD-WLI ($P = 0.028$ and $P \leq 0.001$, respectively), while CAD-WLI had higher sensitivity than CAD-NBI ($P = 0.006$). By using both CAD-WLI and CAD-NBI, the endoscopists could improve their diagnostic efficacy to the highest level, with accuracy, sensitivity, and specificity of 94.9%, 92.4%, and 96.7%, respectively.

CONCLUSION

The CAD-NBI system for screening early ESCC has higher accuracy and specificity than CAD-WLI. Endoscopists can achieve the best diagnostic efficacy using both CAD-WLI and CAD-NBI.

Key Words: Computer-aided detection; Esophageal squamous cell carcinoma; Endoscopy; Screening; Narrow-band imaging; White-light imaging

Core Tip: The computer-assisted diagnosis (CAD) system under conventional endoscopic white-light imaging (WLI) for screening of early esophagus squamous cell carcinoma (ESCC) has high accuracy. However, few studies have examined different characteristics of CAD application in WLI and narrow-band imaging (NBI) models. In this study, the CAD system we constructed under the NBI model for screening of early ESCC had higher accuracy and specificity than the CAD-WLI system. Endoscopists could achieve the best diagnostic efficacy by using both CAD-WLI and CAD-NBI. The two CAD systems have different advantages in avoiding missed diagnosis and excessive biopsy, which could help endoscopists, especially those with less experience, in more efficient screening of early ESCC.

Citation: Li B, Cai SL, Tan WM, Li JC, Yalikong A, Feng XS, Yu HH, Lu PX, Feng Z, Yao LQ, Zhou PH, Yan B, Zhong YS. Comparative study on artificial intelligence systems for detecting early esophageal squamous cell carcinoma between narrow-band and white-light imaging. *World J Gastroenterol* 2021; 27(3): 281-293
URL: https://www.wjgnet.com/1007-9327/full/v27/i3/281.htm
DOI: https://dx.doi.org/10.3748/wjg.v27.i3.281

INTRODUCTION

Upper gastrointestinal endoscopy combined with biopsy is the method of choice to diagnose esophagus squamous cell carcinoma (ESCC), and it has been widely adopted in population screening for ESCC[1,2]. However, it is not always easy to identify early-stage ESCC, especially for unexperienced doctors, during examination with white-light imaging (WLI)[3,4]. The narrow-band imaging (NBI) system improves the visualization of microvasculature and mucosal patterns in the alimentary tract[5]. Non-magnifying endoscopy with NBI (NM-NBI) has been used frequently in routine screening examinations with higher accuracy and specificity[6,7]. However, the sensitivity of NBI for screening of mucosal high-grade neoplasia is significantly

Manuscript source: Unsolicited manuscript

Specialty type: Gastroenterology and hepatology

Country/Territory of origin: China

Peer-review report's scientific quality classification

Grade A (Excellent): A
Grade B (Very good): 0
Grade C (Good): C
Grade D (Fair): 0
Grade E (Poor): 0

Received: October 9, 2020
Peer-review started: October 9, 2020
First decision: November 23, 2020
Revised: December 5, 2020
Accepted: December 22, 2020
Article in press: December 22, 2020
Published online: January 21, 2021

P-Reviewer: Kishida Y, Zavras N
S-Editor: Fan JR
L-Editor: Filipodia
P-Editor: Liu JH

different between experienced and less experienced endoscopists[8,9]. Early lesions missed at screening may not be identified until they become more advanced and less amenable to treatment. Thus, the experience of the operator plays a critical role in the screening result for early ESCC.

Artificial intelligence (AI) may be uniquely poised to compensate for the lack of operator experience. Studies have demonstrated the ability of AI to meet or exceed the performance of human experts as a triage or screening tool for gastrointestinal diseases[10,11]. In our previous research, we reported a novel system of computer-aided detection (CAD) to localize and identify early ESCC under conventional endoscopic WLI with sensitivity above 97%[12]. Here, another system of CAD for application in NM-NBI for screening of early ESCC was constructed and validated. More importantly, we compared the effectiveness of the two systems based on WLI or NM-NBI in helping endoscopists to detect early ESCC. On the basis of the results, we can determine which technique is most effective to help endoscopists, *i.e.* whether to use CAD-NBI or CAD-WLI alone or both.

MATERIALS AND METHODS

Study design

This study was performed at the Endoscopy Center of three general hospitals (Zhongshan Hospital of Fudan University, Xuhui Hospital, and Kiang Wu Hospital) in partnership with the School of Computer Science of Fudan University. Patient data were anonymized, and any personal identifying information was excluded. This study was approved by the Institutional Review Board of Zhongshan Hospital, Fudan University (approval No. B2019-141R). All authors had access to the study data and reviewed and approved the final manuscript.

Datasets used for training and validation of the CAD-NBI system

First, we retrospectively obtained esophagoscopic NM-NBI images for the development of the CAD system for NBI images (CAD-NBI system). In the training dataset, a total of 2167 abnormal NM-NBI images of early ESCCs in 235 cases and 2568 normal NM-NBI images in 412 cases were collected between January 2016 and April 2018 from three institutions. Then, we collected 316 pairs of images (133 abnormal and 183 normal), each pair including WLI and NBI at the same location and at the same angle, from 112 consecutive cases. The purpose of establishing this paired image dataset includes: (1) All NBI images are used to test our newly established CAD-NBI system; (2) White light images paired with NBI in the same situation are used to test the CAD system for WLI (CAD-WLI system)[12] that has been reported previously to compare the differences between the two CAD systems; and (3) Endoscopists are asked to review all the images from this validation dataset to evaluate their diagnostic ability with or without the help of these two CAD systems.

The criteria for normal and abnormal images refer to the previous study on CAD for screening of early ESCC from our team[12]. The criteria for choosing normal image data were as follows: (1) The initial endoscopic inspection results for the esophagus were negative; (2) The abovementioned patients had no newly detected lesions until September 2019; and (3) The normal images were confirmed by endoscopists with ≥ 15 years of experience in endoscopy, and all the endoscopists believed that the image is normal. All patients with abnormal endoscopic images underwent endoscopic submucosal dissection procedures, and three gastrointestinal pathologists (two with > 10 years of experience and one with > 15 years of experience) conducted histological assessments in the pathology departments of both centers. Early ESCC includes low-grade and high-grade intraepithelial neoplasia and esophageal cancer (EC) that has invaded mucosal or superficial submucosal layer.

Design and development of the CAD-NBI system

In this study, we consider the esophagus lesions in endoscopic images to be semantic objects. We demonstrate the development and validation of an endoscopist-level CAD-NBI system based on deep learning algorithm for screening esophagus lesions. We propose to use fully convolutional neural network based on Visual Geometry Group model for semantic segmentation, where semantics denote the esophagus lesions. Therefore, the CAD-NBI system is used to predict the location and irregular shape of esophagus lesions, which is helpful for endoscopists to judge the size, area, and location of lesions more effectively.

To obtain an accurate predictor based on limited esophagoscopic images, some

preprocessing is conducted on the esophagoscopic images before training. First, some irrelevant regions for lesion detection, such as black background, are cropped automatically using a simple image processing algorithm developed by us. Second, we randomly flip the esophagoscopic images horizontally and vertically to augment data diversity. Third, for further data augmentation, esophagoscopic images and the corresponding lesion masks are resized to 300 × 300 and randomly cropped to 224 × 224. During training, the network parameters are updated with the initial learning rate of 0.0001 and decayed every 2000 iterations with a decay rate of 0.9 in the staircase mode. During inference, given an esophagoscopic image that the CAD-NBI system has never seen previously, the system outputs the segmentation result of esophagoscopic lesion directly.

Comparison of the improvement of diagnostic capability of endoscopists under CAD-WLI and CAD-NBI

The accuracy of the CAD-NBI system was evaluated by the validation dataset established previously. We invited 20 endoscopists with varying experience from three centers to participate in this study in order to compare diagnostic performance between the CAD system and endoscopists. Moreover, we wanted to know the effectiveness of the two systems, CAD-WLI and CAD-NBI, for the improvement of diagnostic capabilities of endoscopists. Among the endoscopists, four were classified as highly experienced endoscopists who had performed more than 10000 conventional endoscopy examinations and 5000 NBI endoscopy examinations, eight were classified as mid-level endoscopists who had performed more than 5000 conventional endoscopy examinations and 2500 NBI endoscopy examinations, and eight were classified as junior endoscopists who had performed more than 2000 conventional endoscopy examinations and 1000 NBI endoscopy examinations.

To test the effectiveness of the two CAD systems, we designed a four-phase trial. In the first phase, the 20 endoscopists were asked to review every pair image of the validation dataset in digital format on a laptop. All of them were blinded to the histological data and asked to review the esophagoscopic images independently. The CAD-NBI system scanned and analyzed each NM-NBI image of every pair saved in JPEG/PNG format on the hard drive, and the CAD-WLI system did the same for NM-WLI images. In the second phase, after the WLI images had been marked using the CAD-WLI system (NBI images were not marked), we invited these endoscopists to again screen every pair of images in the validation dataset. This action was noteworthy as the review sequence of images was altered randomly by computer to minimize the impact of impression from the last performance in each phase. In the third phase, endoscopists were asked to review every pair of images in the validation dataset once again, after all NBI images were marked by the CAD-NBI system while WLI images were not. In the last phase, the endoscopists completed their final diagnosis for the validation paired images by referring to the results from both CAD-WLI and CAD-NBI systems. Between each two continuous phases, we set the wash-out phase as 1-1-2 mo, respectively. Moreover, these 20 endoscopists were unaware of the performance of the CAD-WLI and CAD-NBI systems. A flowchart depicting the processes used during the study is shown in Figure 1.

Outcome measures

The ability of the CAD-NBI system to identify early ESCC was mathematically assessed by the area under the curve of the receiver operating characteristic curve, and the sensitivity, specificity, accuracy, positive predictive value (PPV), and negative predictive value (NPV) were determined. The accuracy, sensitivity, specificity, PPV, and NPV were also compared between CAD-NBI, CAD-WLI, and the endoscopists.

Statistical analysis

The chi-square test and t test were used wherever applicable. A P value of < 0.05 was considered to be statistically significant. A two-sided McNemar test with a significance level of 0.05 was used to compare differences in accuracy, sensitivity, specificity, PPV, and NPV. All statistical analyses were performed using SPSS version 18.0 (SPSS Inc., Chicago, IL, United States).

RESULTS

The detailed characteristics of the patients and lesions in the validation image dataset

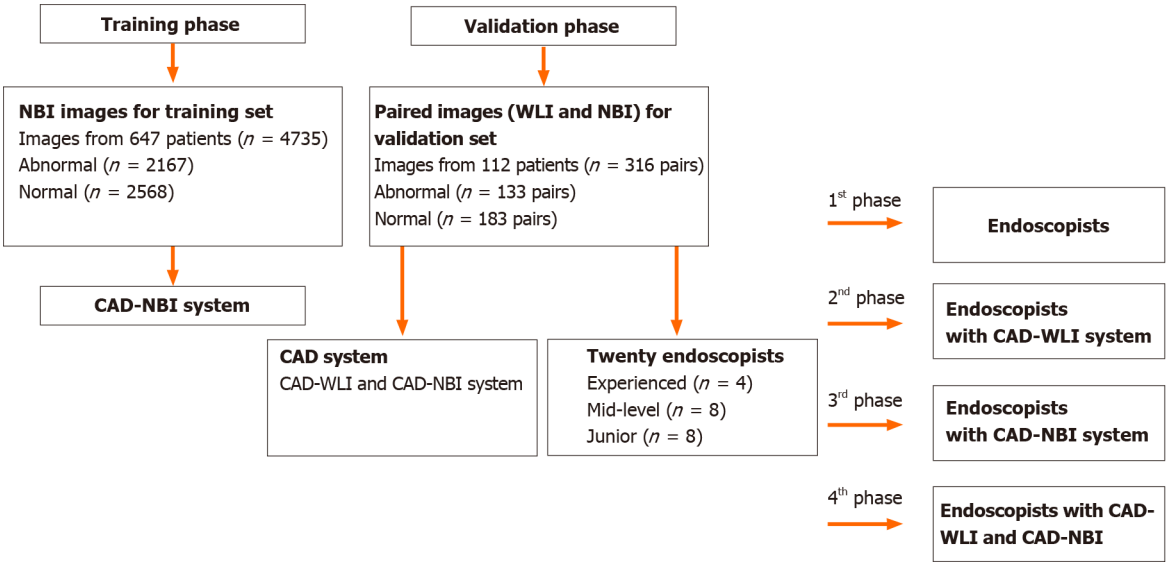

Figure 1 Flowchart of the procedures. CAD: Computer-assisted detection; NBI: Narrow-band imaging; WLI: White -light imaging.

are listed in Table 1.

Performance of the CAD-NBI and CAD-WLI systems

The receiver operating characteristic curve of the CAD-NBI system is shown in Figure 2, and the area under the curve was 0.9761. For 316 NBI images in the validation dataset, the sensitivity, specificity, accuracy, PPV, and NPV of CAD-NBI were 91.0%, 96.7%, 94.3%, 95.3%, and 93.6%, respectively. For 316 WLI images in the validation dataset, CAD-WLI correctly identified 131 of the 133 early ESCC lesions, with sensitivity, specificity, and accuracy of 98.5%, 83.1%, and 89.5%, respectively. The PPV and NPV of the CAD-WLI system were 80.8% and 98.7%, respectively.

Comparison of the two CAD systems (Figure 3) revealed that the accuracy and specificity of CAD-NBI were superior to those of CAD-WLI ($P = 0.028$ and $P \leq 0.001$). However, the sensitivity of the CAD-WLI system was higher than that of the CAD-NBI system ($P = 0.006$). The CAD-WLI and CAD-NBI system recognized and marked the lesion with a blue square in paired images (Figure 4A and B). In addition, when CAD-WLI mistakenly identified the normal mucosa as lesion (blue square) in WLI, CAD-NBI with high specificity could correct it in NBI (Figure 4C and D).

Comparison between CAD systems and the endoscopists

Table 2 compares the performance of the two CAD systems and the endoscopists for diagnosing early ESCC. The overall accuracy, sensitivity, specificity, PPV, and NPV of the 20 endoscopists were 73.9%, 87.7%, 81.9%, 81.7%, and 82.7%, respectively. Apparently, the experienced endoscopists achieved significantly better diagnostic results than the less experienced ones, including mid-level and junior endoscopists. The average accuracy value of the experienced endoscopists for early ESCC was 93.6%, which was similar to that of the CAD-NBI system and higher than that of the CAD-WLI system. CAD-WLI achieved the highest sensitivity (98.5%), whereas its specificity was lower than that of CAD-NBI with the highest value of 96.7% and the average value of all the endoscopists (87.7%).

Improvement after referring to the results from CAD-WLI and CAD-NBI

With the assistance of either CAD-WLI or CAD-NBI, all the three groups of endoscopists showed improvement in accurately diagnosing early ESCC (Figure 5). Table 3 shows the average diagnostic performance of endoscopists in the detection of early ESCC after referring to the results from the CAD-WLI system in the second phase and from the CAD-NBI system in the third phase. Next, we compared the advantages of the two systems in different aspects. The CAD-NBI system helped the endoscopists to achieve higher value than that achieved with the assistance of CAD-WLI system, especially in the mid-level group with a significant difference (85.3% *vs* 88.4%, $P = 0.012$). Experienced and mid-level endoscopists showed no significant differences in their sensitivity for lesions in the two phases, while the CAD-WLI system helped junior endoscopists to achieve higher sensitivity than that achieved

Table 1 Patient and lesion characteristics in the validation image set

Patient characteristics, *n* = 112	Value
Median age, yr (range)	59 (19-86)
Sex, male/female	67/45
Lesion characteristics, *n* = 42	
Median size, mm (range)	23 (9-42)
Location, Ce/Ut/Mt/Lt/Ae	0/3/24/15/0
Pathological diagnosis	
LGIN/HGIN	6/18
Cancer, M/SM1	15/3

Ae: Abdominal esophagus; Ce: Cervical esophagus; HGIN: High-grade intraepithelial neoplasia; LGIN: Low-grade intraepithelial neoplasia; Lt: Lower thoracic esophagus; M: Mucosal; Mt: Middle thoracic esophagus; SM1: Submucosal; Ut: Upper thoracic esophagus.

Table 2 Diagnostic performance of computer-assisted detection systems *vs* endoscopists

	CAD systems		Endoscopists			
	CAD-NBI	CAD-WLI	All, *n* = 20	Experienced, *n* = 4	Mid-level, *n* = 8	Junior, *n* = 8
Sensitivity, % (95%CI)	91.0	98.5	73.9 (68.1-79.7)	94.7 (85.0-100)	73.9 (71.9-75.8)	63.5 (59.7-67.3)
Specificity, % (95%CI)	96.7	83.1	87.7 (84.9-90.5)	92.8 (81.2-100)	83.4 (81.1-85.7)	89.4 (85.0-93.8)
Accuracy, % (95%CI)	94.3	89.5	81.9 (78.9-84.8)	93.6 (89.1-98.1)	79.4 (78.3-80.5)	78.5 (76.6-80.4)
PPV, % (95%CI)	95.3	80.8	81.7 (78.0-85.5)	91.4 (78.0-100)	76.5 (74.2-78.8)	82.2 (76.1-88.2)
NPV, % (95%CI)	93.6	98.7	82.7 (79.2-86.3)	96.4 (90.1-100)	81.5 (80.5-82.4)	77.2 (75.8-78.6)

CAD: Computer-assisted detection; CI: Confidence interval; NBI: Narrow-band imaging; NPV: Negative predictive value; PPV: Positive predictive value; WLI: White-light imaging.

using the CAD-NBI system (83.0% *vs* 77.3%, P = 0.008). In addition, there were no significant differences in the specificity of experienced endoscopists when using CAD-WLI or CAD-NBI. However, a significant improvement in diagnostic specificity was shown by mid-level (85.9% *vs* 92.6%, P = 0.000) and junior endoscopists (88.6% *vs* 94.9%, P = 0.003).

Table 4 shows the average diagnostic performance of endoscopists after referring to the results from both the CAD-WLI and CAD-NBI systems. In the fourth phase, the diagnostic capability of all the endoscopists improved to the highest level, with the accuracy, sensitivity, and specificity of 94.9%, 92.4%, and 96.7%, respectively. The accuracy of junior endoscopists was 92.9%, and it was significantly higher than that in the first (*vs* 78.5%, P = 0.000), second (*vs* 86.2%, P = 0.000), and third (*vs* 87.5%, P = 0.000) phases. The accuracy of mid-level endoscopists was 94.8%, and it was significantly higher than that in the first (*vs* 79.4%, P = 0.000), second (*vs* 85.3%, P = 0.000), and third (*vs* 88.4%, P = 0.000) phases. In the experienced endoscopist group, the average accuracy value was 98.8%, and it was also significantly higher than that in the first (*vs* 93.6%, P = 0.011), second (*vs* 95.5%, P = 0.015), and third (*vs* 96.5%, P = 0.049) phases (Figure 6A). In terms of sensitivity and specificity for lesions, the average values of the mid-level and junior groups also increased to the highest value after using CAD-WLI and CAD-NBI (Figure 6B and C).

DISCUSSION

CAD has been developed to overcome the limitation of less experience of diagnosis in young doctors. A recent study presented an AI system that can surpass human experts in breast cancer prediction[13]. In the field of gastroenterology, several CAD systems have shown excellent diagnostic potential compared with human endoscopists in

Table 3 Comparison of the improvement of endoscopists under computer-assisted detection-white-light imaging and computer-assisted detection-narrow-band imaging

	2nd phase CAD-WLI assistance	3rd phase CAD-NBI assistance	*P* value
Sensitivity, % (95%CI)			
All, *n* = 20	86.4 (83.1-89.6)	83.1 (79.6-86.6)	0.162
Experienced, *n* = 4	96.8 (94.4-99.2)	95.7 (91.8-99.5)	0.454
Mid-level, *n* = 8	84.5 (80.0-89.0)	82.6 (79.4-85.9)	0.435
Junior, *n* = 8	83.0 (79.3-86.6)	77.3 (74.9-79.7)	0.008
Specificity, % (95%CI)			
All, *n* = 20	88.7 (86.5-90.8)	94.4 (93.0-95.8)	0.000
Experienced, *n* = 4	94.5 (87.9-100)	97.2 (93.6-100)	0.310
Mid-level, *n* = 8	85.9 (84.3-87.4)	92.6 (90.7-94.5)	0.000
Junior, *n* = 8	88.6 (85.1-92.1)	94.9 (92.5-97.2)	0.003
Accuracy, % (95%CI)			
All, *n* = 20	87.7 (85.5-89.9)	89.7 (87.8-91.5)	0.156
Experienced, *n* = 4	95.5 (92.4-98.6)	96.5 (93.6-99.4)	0.469
Mid-level, *n* = 8	85.3 (83.1-87.5)	88.4 (87.1-89.7)	0.012
Junior, *n* = 8	86.2 (84.2-88.3)	87.5 (86.0-89.0)	0.261
PPV, % (95%CI)			
All, *n* = 20	84.9 (82.2-87.5)	91.6 (89.7-93.6)	0.000
Experienced, *n* = 4	93.0 (85.1-100)	96.1 (91.4-100)	0.325
Mid-level, *n* = 8	81.3 (79.4-83.2)	89.2 (86.7-91.7)	0.000
Junior, *n* = 8	84.4 (80.5-88.2)	91.8 (88.4-95.2)	0.004
NPV, % (95%CI)			
All, *n* = 20	90.1 (87.9-92.3)	88.7 (86.5-90.9)	0.361
Experienced, *n* = 4	97.7 (96.0-99.3)	96.9 (94.2-99.6)	0.465
Mid-level, *n* = 8	88.5 (85.6-91.4)	88.1 (86.2-89.9)	0.755
Junior, *n* = 8	87.8 (85.6-90.1)	85.2 (83.9-86.5)	0.031

CAD: Computer-assisted detection; CI: Confidence interval; NBI: Narrow-band imaging; NPV: Negative predictive value; PPV: Positive predictive value; WLI: Whit-light imaging.

colorectal polyp classification, determination of the invasion depth of gastric cancer, and identification of small bowel diseases[14-16]. The application of AI in automatically detecting and classifying lesions, especially in the context of medical imaging, is expected to help physicians provide more accurate diagnoses[17].

Squamous cell carcinoma is the predominant histologic subtype of EC in Asia, where the rate of EC is quite high[18]. Several research studies on CAD for improving the screening efficiency for ESCC have been reported. Horie *et al*[19] first evaluated the ability of the CNN to detect EC in endoscopic images of superficial and advanced cancer and achieved a sensitivity of 98%. Zhao *et al*[20] developed a deep learning model based on magnifying NBI images to investigate the automated classification of intrapapillary capillary loops and assist endoscopic diagnosis of early ESCC. In a recent study by Guo *et al*[21], the authors developed a CAD system for real-time automated diagnosis of precancerous lesions and ESCC. In 2019, our team reported a novel system using deep neural network (DNN) to localize and identify early ESCC under endoscopic WLI with high accuracy and sensitivity[12]. Moreover, after referring to the results of DNN-CAD, the average diagnostic ability of the endoscopists improved significantly. However, this CAD system could only identify early ESCC in WLI, and the specificity was only 85.4%, which may lead to unnecessary biopsies. As NBI is also an accurate diagnostic tool for early ESCC, a better CAD system that can be

Table 4 Diagnostic performance of endoscopists in screening of esophagus squamous cell carcinoma after referring to the results from computer-assisted detection-white-light imaging and computer-assisted detection-narrow-band imaging

	Sensitivity, % (95%CI)	Specificity, % (95%CI)	Accuracy, % (95%CI)	PPV, % (95%CI)	NPV, % (95%CI)
All, *n* = 20	92.4 (90.3-94.5)	96.7 (95.7-97.7)	94.9 (93.6-96.1)	95.3 (93.9-96.7)	94.7 (93.2-96.1)
Experienced, *n* = 4	98.5 (96.3-100)	99.1 (97.5-100)	98.8 (98.2-99.4)	98.7 (96.7-100)	98.9 (97.4-100)
Mid-level, *n* = 8	93.2 (91.3-95.1)	96.0 (94.5-97.6)	94.8 (93.7-95.9)	94.5 (92.5-96.6)	95.2 (93.8-96.5)
Junior, *n* = 8	88.5 (86.2-90.8)	96.1 (94.3-97.9)	92.9 (91.2-94.6)	94.3 (91.8-96.8)	92.0 (90.5-93.6)

CI: Confidence interval; NPV: Negative predictive value; PPV: Positive predictive value.

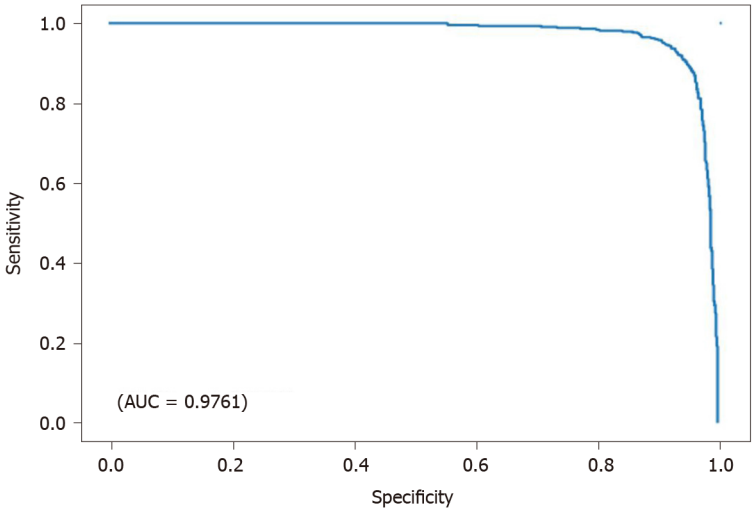

Figure 2 Receiver operating characteristic curve for the test dataset. The area under the curve (AUC) was above 97%.

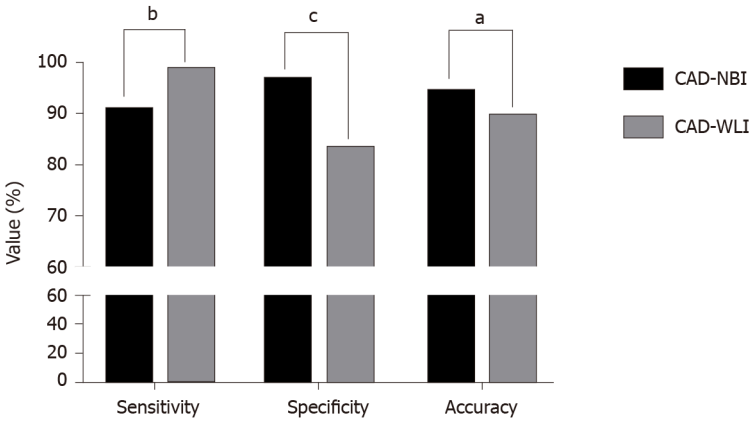

Figure 3 A comparison between the computer-assisted detection-narrow-band imaging and computer-assisted detection-white-light imaging systems in detecting early esophageal squamous cell carcinoma. [a]*P* < 0.05; [b]*P* < 0.01; [c]*P* < 0.001. CAD: Computer-assisted detection; NBI: Narrow-band imaging; WLI: White-light imaging.

used in the NBI model of endoscopy needs to be developed. In addition, a comparative study of AI application in WLI and NBI models is lacking.

In the present study, we developed a CAD system to detect early ESCC under the NBI model of endoscopy. Considering our previously developed CAD system for WLI, we wanted to compare the different characteristics of CAD-NBI and CAD-WLI systems to validate the usefulness of CAD-NBI. Therefore, 316 pairs of images, each pair including WLI and NBI at the same location and at the same angle, were collected from three institutions. The results showed that CAD for NM-NBI images of the esophagus had a good ability to diagnose early ESCC, with an accuracy of 94.3%. For

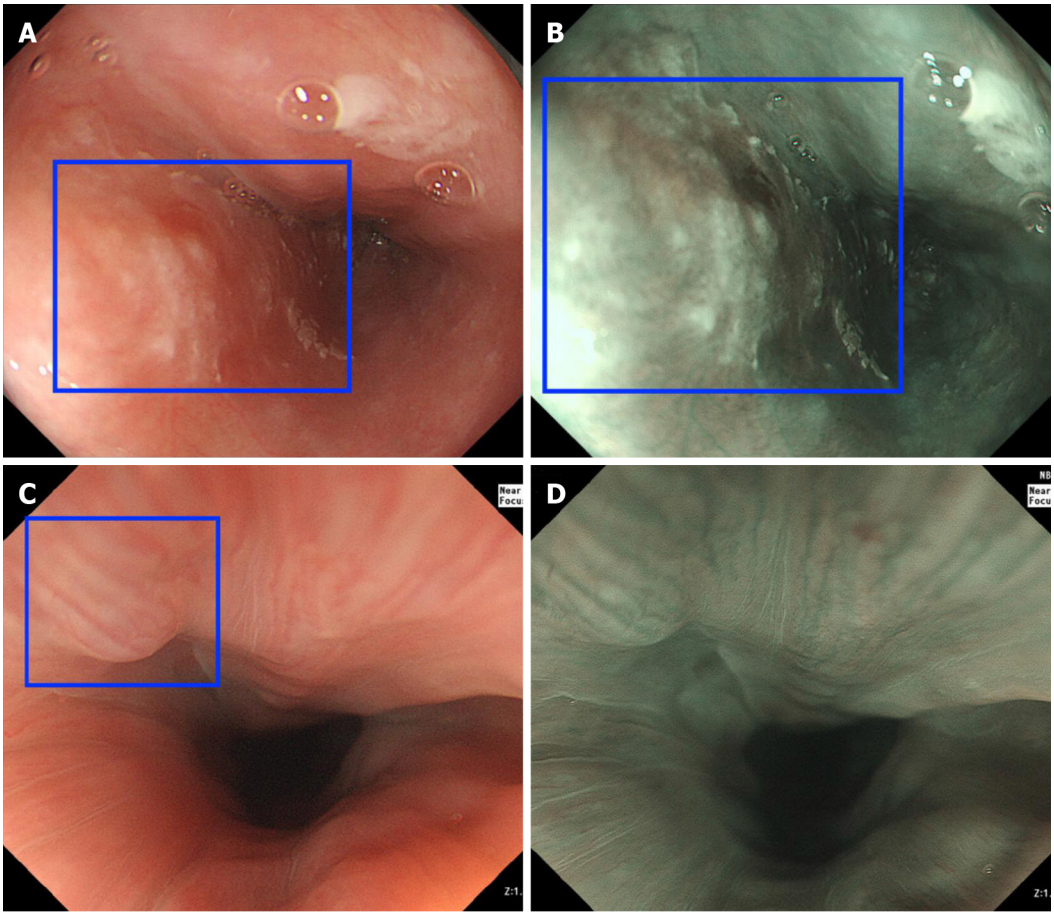

Figure 4 Examples of computer-assisted detection system-diagnosed images. A and B: under white-light imaging (WLI) and narrow-band imaging (NBI), computer-assisted detection (CAD)-WLI and CAD-NBI recognized the esophageal cancer lesion (blue square); C and D: CAD-WLI mistakenly identified the normal mucosa as a lesion (blue square) in WLI, while CAD-NBI corrected it in NBI.

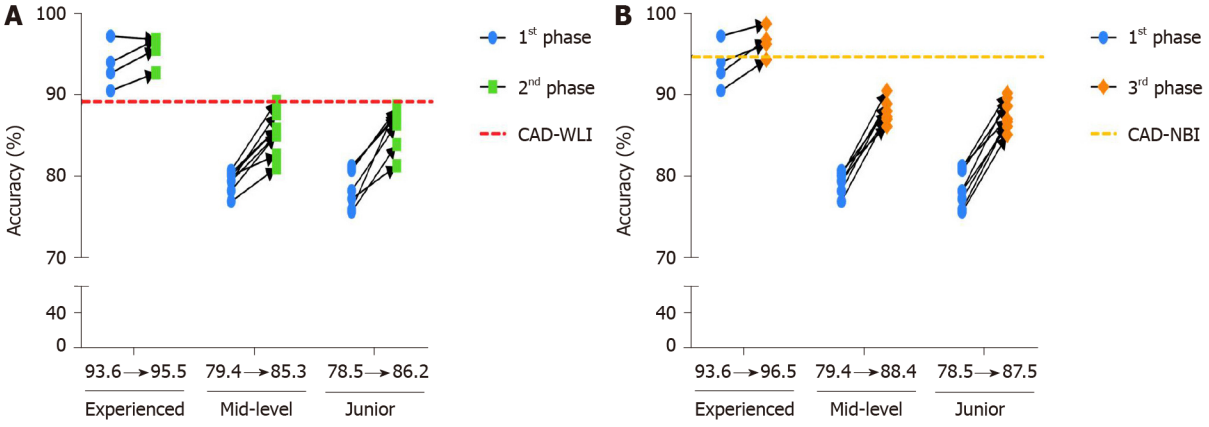

Figure 5 Improved accuracy of diagnosis with the assistance of the two computer-assisted detection systems according to the groups. A: Improvement of endoscopists' accuracy in the second phase with the assistance of computer-assisted detection (CAD)-white-light imaging; B: Improvement of endoscopists' accuracy in the third phase with the assistance of CAD-narrow-band imaging. WLI: White-light imaging.

WLI images in the validation dataset, CAD-WLI correctly identified 131 of the 133 lesions. The diagnostic ability of CAD-WLI for this validation image dataset was similar to that reported in our previous study[12]. Comparison of the two systems showed that CAD-NBI had superior accuracy and specificity compared to CAD-WLI, while the CAD-WLI system had higher sensitivity than the CAD-NBI system. The results showed that CAD-NBI may compensate for the feature of low specificity of CAD-WLI and make the overall accuracy higher, but its own sensitivity still needs to be improved further.

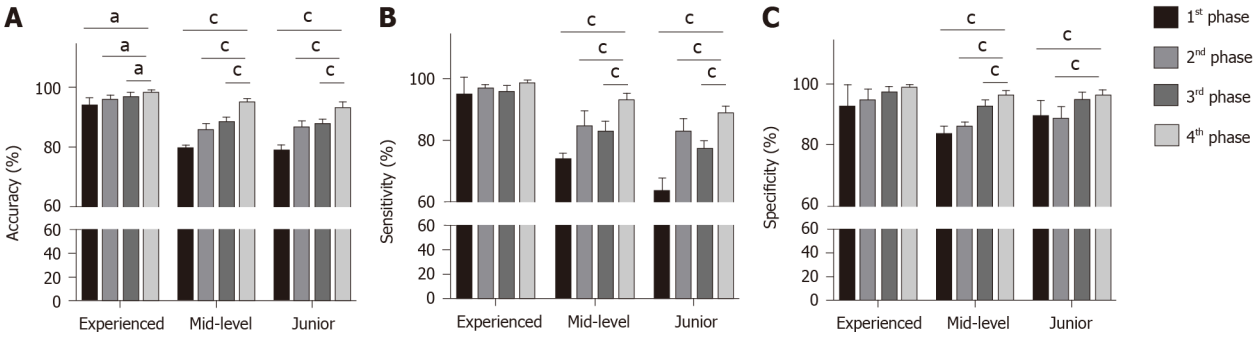

Figure 6 Average diagnostic performance of the three groups of endoscopists in four phases. A: Accuracy; B: Sensitivity; C: Specificity. $^{a}P < 0.05$; $^{c}P < 0.001$.

Endoscopists were asked to review the images from this validation dataset to evaluate their diagnostic ability. In the first phase, the average accuracy value of the experienced endoscopists for early ESCC was 93.6%, which was similar to that of the CAD-NBI system and higher than that of the CAD-WLI system. However, the average diagnostic accuracy of the less experienced endoscopists, including the mid-level (79.4%) and junior groups (78.5%), was lower. Subsequently, the less experienced endoscopists in particular showed improvement in their diagnostic ability with the help of both CAD-WLI in the second phase and CAD-NBI in the third phase. Junior endoscopists made a greater improvement in terms of sensitivity with the CAD-WLI system when their diagnostic specificity was further improved after referring to the results from CAD-NBI. In addition, mid-level endoscopists showed higher values of specificity and accuracy with the assistance of the CAD-NBI system than with the CAD-WLI system. In the fourth phase, by using both CAD-WLI and CAD-NBI, the average values of the three groups increased to the highest value. After simulating the clinical use of the two CAD systems through four different situations, we found that the two systems had different advantages in terms of avoiding missed diagnosis and performing excessive biopsy, and thus, endoscopists could achieve the best diagnostic efficacy by using both CAD-WLI and CAD-NBI.

The sensitivity of a previous system reported by Horie *et al*[19] for the diagnosis of ESCC on WLI and NBI was 72% and 86%, respectively, and our CAD-WLI and CAD-NBI systems provided higher sensitivity of 98.5% and 91.0%, respectively. We have continuously developed the two CAD systems for WLI and NBI based on DNN and conducted for the first time a comparative study to reveal the respective advantages of both systems. The ultimate goal is to integrate the two systems into one to meet the needs of different equipment in a hospital at all levels from different regions. Although Guo *et al*[21] reported that their system for the automated diagnosis of early ESCC under NBI had sensitivity and specificity of 98.04% and 95.03%, respectively, the sensitivity of CAD-WLI and specificity of CAD-NBI were similar to their reported values. In addition, our study invited 20 endoscopists to review the images of the validation dataset with or without the help of the two CAD systems; 10 of the 20 endoscopists (2 mid-level and 8 junior) are from Xuhui Hospital, which is a secondary hospital where the number of patients is much less than that in the tertiary hospital. As secondary hospitals have lower capability to diagnose and treat ESCC than tertiary hospitals, we wanted to assess fully the effectiveness of our CAD system in helping less experienced endoscopists to detect early ESCC, especially doctors in basic hospitals. Our results confirmed that the improvement of diagnosis capability was most pronounced in less experienced endoscopists.

Next, we will explain the reasons for the differences in the diagnostic characteristics of the two CAD systems. CAD-WLI and CAD-NBI are based on different concepts. CAD-WLI uses a bounding box method to detect the location of esophagus lesions in endoscopic images. The detection result of the CAD-WLI system unavoidably includes unnecessary areas such as background regions and parts of other lesions. In contrast, CAD-NBI uses the object semantic segmentation method based on the FCN model, which only outputs the regions of esophagus lesions. Therefore, the accuracy of the CAD-NBI system is higher than that of the CAD-WLI system. In addition, the CAD-NBI system is developed by an end-to-end trainable approach, which is different from the sliding window approach of the CAD-WLI system that densely generates a large number of candidate boxes with different sizes and ratios on a given image. Thus, the CAD-NBI system has the advantage of computational speed when compared with the

CAD-WLI system. Finally, NBI and WLI have different characteristics, which can help us obtain high accuracy, sensitivity, and specificity simultaneously. On the basis of the key observation, we can develop a multichannel DNN to extract and fuse the features of NBI and WLI simultaneously in future studies.

The present study has several limitations. First, the sample size, including images in the training and validation datasets, was small. The low detection rate of early ESCC limits our ability to obtain more images. In addition, our work on CAD for the early detection of ESCC was validated only on still images with a limited scale. Second, the performance of endoscopists in the latter phase may be slightly affected by the image impression of the previous phase. Third, the CAD diagnosis was based on high-quality images, and bias might occur with poor-quality images such as out-of-focus images or blurred images caused by mucus during real-time gastroscopy.

CONCLUSION

In conclusion, we have constructed a CAD system under the NBI model for screening early ESCC, and this CAD-NBI system has higher accuracy and specificity than the CAD-WLI system reported previously. Endoscopists could achieve the best diagnostic efficacy by using both CAD-WLI and CAD-NBI. Therefore, a novel system combining the characteristics of these two systems under WLI and NBI is needed.

ARTICLE HIGHLIGHTS

Research background

Non-magnifying endoscopy with narrow-band imaging (NM-NBI) has been frequently used in routine screening of esophagus squamous cell carcinoma (ESCC). The performance of NBI for screening of early ESCC is, however, significantly affected by operator experience. Artificial intelligence may be a unique approach to compensate for the lack of operator experience.

Research motivation

In our previous research, we reported a novel system of computer-aided detection (CAD) to localize and identify early ESCC under conventional endoscopic white-light imaging (WLI) with sensitivity of above 97%. The construction of another CAD system for application in NM-NBI was the next step in the continuation of our research.

Research objectives

To construct a CAD system for application in NM-NBI to identify early ESCC and compare it with our previously reported CAD system with endoscopic WLI.

Research methods

We collected a total of 2167 abnormal NM-NBI images of early ESCC and 2568 normal images from three institutions (Zhongshan Hospital of Fudan University, Xuhui Hospital, and Kiang Wu Hospital) as the training dataset, and 316 pairs of images, each pair including images obtained with WLI and NBI (same part), were collected for validation. Twenty endoscopists participated in this study to review the validation images with or without the assistance of the CAD systems. The diagnostic results of the two CAD systems and the improvement in the diagnostic efficacy of endoscopists were compared in terms of sensitivity, specificity, accuracy, positive predictive value, and negative predictive value.

Research results

The area under receiver operating characteristic curve for CAD-NBI was 0.9761. For the validation dataset, the sensitivity, specificity, accuracy, positive predictive value, and negative predictive value of CAD-NBI were 91.0%, 96.7%, 94.3%, 95.3%, and 93.6%, respectively, while those of CAD-WLI were 98.5%, 83.1%, 89.5%, 80.8%, and 98.7%, respectively. CAD-NBI showed superior accuracy and specificity than CAD-WLI (P = 0.028 and $P \leq 0.001$, respectively), while CAD-WLI had higher sensitivity than CAD-NBI (P = 0.006). By using both CAD-WLI and CAD-NBI, the endoscopists could improve their diagnostic efficacy to the highest level, with accuracy, sensitivity, and specificity of 94.9%, 92.4%, and 96.7%, respectively.

Research conclusions

The CAD-NBI system for screening early ESCC has higher accuracy and specificity than CAD-WLI. Endoscopists can achieve the best diagnostic efficacy by using both CAD-WLI and CAD-NBI.

Research perspectives

According to the results, the two CAD systems had different advantages in avoiding missed diagnosis and excessive biopsy, which could help endoscopists, especially those with less experience, in screening of early ESCC more efficiently. As the two CAD systems have unique characteristics, we plan to develop a multichannel deep neural network to extract and combine the features of NBI and WLI simultaneously in our future work.

REFERENCES

1 **Wei WQ**, Chen ZF, He YT, Feng H, Hou J, Lin DM, Li XQ, Guo CL, Li SS, Wang GQ, Dong ZW, Abnet CC, Qiao YL. Long-Term Follow-Up of a Community Assignment, One-Time Endoscopic Screening Study of Esophageal Cancer in China. *J Clin Oncol* 2015; **33**: 1951-1957 [PMID: 25940715 DOI: 10.1200/JCO.2014.58.0423]

2 **He Z**, Liu Z, Liu M, Guo C, Xu R, Li F, Liu A, Yang H, Shen L, Wu Q, Duan L, Li X, Zhang C, Pan Y, Cai H, Ke Y. Efficacy of endoscopic screening for esophageal cancer in China (ESECC): design and preliminary results of a population-based randomised controlled trial. *Gut* 2019; **68**: 198-206 [PMID: 29306867 DOI: 10.1136/gutjnl-2017-315520]

3 **Lee YC**, Wang CP, Chen CC, Chiu HM, Ko JY, Lou PJ, Yang TL, Huang HY, Wu MS, Lin JT, Hsiu-Hsi Chen T, Wang HP. Transnasal endoscopy with narrow-band imaging and Lugol staining to screen patients with head and neck cancer whose condition limits oral intubation with standard endoscope (with video). *Gastrointest Endosc* 2009; **69**: 408-417 [PMID: 19019362 DOI: 10.1016/j.gie.2008.05.033]

4 **Morita FH**, Bernardo WM, Ide E, Rocha RS, Aquino JC, Minata MK, Yamazaki K, Marques SB, Sakai P, de Moura EG. Narrow band imaging versus lugol chromoendoscopy to diagnose squamous cell carcinoma of the esophagus: a systematic review and meta-analysis. *BMC Cancer* 2017; **17**: 54 [PMID: 28086818 DOI: 10.1186/s12885-016-3011-9]

5 **Muto M**, Katada C, Sano Y, Yoshida S. Narrow band imaging: a new diagnostic approach to visualize angiogenesis in superficial neoplasia. *Clin Gastroenterol Hepatol* 2005; **3**: S16-S20 [PMID: 16012987 DOI: 10.1016/s1542-3565(05)00262-4]

6 **Nagami Y**, Tominaga K, Machida H, Nakatani M, Kameda N, Sugimori S, Okazaki H, Tanigawa T, Yamagami H, Kubo N, Shiba M, Watanabe K, Watanabe T, Iguchi H, Fujiwara Y, Ohira M, Hirakawa K, Arakawa T. Usefulness of non-magnifying narrow-band imaging in screening of early esophageal squamous cell carcinoma: a prospective comparative study using propensity score matching. *Am J Gastroenterol* 2014; **109**: 845-854 [PMID: 24751580 DOI: 10.1038/ajg.2014.94]

7 **Muto M**, Minashi K, Yano T, Saito Y, Oda I, Nonaka S, Omori T, Sugiura H, Goda K, Kaise M, Inoue H, Ishikawa H, Ochiai A, Shimoda T, Watanabe H, Tajiri H, Saito D. Early detection of superficial squamous cell carcinoma in the head and neck region and esophagus by narrow band imaging: a multicenter randomized controlled trial. *J Clin Oncol* 2010; **28**: 1566-1572 [PMID: 20177025 DOI: 10.1200/JCO.2009.25.4680]

8 **Ishihara R**, Takeuchi Y, Chatani R, Kidu T, Inoue T, Hanaoka N, Yamamoto S, Higashino K, Uedo N, Iishi H, Tatsuta M, Tomita Y, Ishiguro S. Prospective evaluation of narrow-band imaging endoscopy for screening of esophageal squamous mucosal high-grade neoplasia in experienced and less experienced endoscopists. *Dis Esophagus* 2010; **23**: 480-486 [PMID: 20095991 DOI: 10.1111/j.1442-2050.2009.01039.x]

9 **Rodríguez de Santiago E**, Hernanz N, Marcos-Prieto HM, De-Jorge-Turrión MÁ, Barreiro-Alonso E, Rodríguez-Escaja C, Jiménez-Jurado A, Sierra-Morales M, Pérez-Valle I, Machado-Volpato N, García-Prada M, Núñez-Gómez L, Castaño-García A, García García de Paredes A, Peñas B, Vázquez-Sequeiros E, Albillos A. Rate of missed oesophageal cancer at routine endoscopy and survival outcomes: A multicentric cohort study. *United European Gastroenterol J* 2019; **7**: 189-198 [PMID: 31080603 DOI: 10.1177/2050640618811477]

10 **Topol EJ**. High-performance medicine: the convergence of human and artificial intelligence. *Nat Med* 2019; **25**: 44-56 [PMID: 30617339 DOI: 10.1038/s41591-018-0300-7]

11 **Mori Y**, Kudo SE, Misawa M, Saito Y, Ikematsu H, Hotta K, Ohtsuka K, Urushibara F, Kataoka S, Ogawa Y, Maeda Y, Takeda K, Nakamura H, Ichimasa K, Kudo T, Hayashi T, Wakamura K, Ishida F, Inoue H, Itoh H, Oda M, Mori K. Real-Time Use of Artificial Intelligence in Identification of Diminutive Polyps During Colonoscopy: A Prospective Study. *Ann Intern Med* 2018; **169**: 357-366 [PMID: 30105375 DOI: 10.7326/M18-0249]

12 **Cai SL**, Li B, Tan WM, Niu XJ, Yu HH, Yao LQ, Zhou PH, Yan B, Zhong YS. Using a deep learning system in endoscopy for screening of early esophageal squamous cell carcinoma (with video). *Gastrointest Endosc* 2019; **90**: 745-753. e2 [PMID: 31302091 DOI:

10.1016/j.gie.2019.06.044]
13 **McKinney SM**, Sieniek M, Godbole V, Godwin J, Antropova N, Ashrafian H, Back T, Chesus M, Corrado GS, Darzi A, Etemadi M, Garcia-Vicente F, Gilbert FJ, Halling-Brown M, Hassabis D, Jansen S, Karthikesalingam A, Kelly CJ, King D, Ledsam JR, Melnick D, Mostofi H, Peng L, Reicher JJ, Romera-Paredes B, Sidebottom R, Suleyman M, Tse D, Young KC, De Fauw J, Shetty S. International evaluation of an AI system for breast cancer screening. *Nature* 2020; **577**: 89-94 [PMID: 31894144 DOI: 10.1038/s41586-019-1799-6]
14 **Chen PJ**, Lin MC, Lai MJ, Lin JC, Lu HH, Tseng VS. Accurate Classification of Diminutive Colorectal Polyps Using Computer-Aided Analysis. *Gastroenterology* 2018; **154**: 568-575 [PMID: 29042219 DOI: 10.1053/j.gastro.2017.10.010]
15 **Zhu Y**, Wang QC, Xu MD, Zhang Z, Cheng J, Zhong YS, Zhang YQ, Chen WF, Yao LQ, Zhou PH, Li QL. Application of convolutional neural network in the diagnosis of the invasion depth of gastric cancer based on conventional endoscopy. *Gastrointest Endosc* 2019; **89**: 806-815. e1 [PMID: 30452913 DOI: 10.1016/j.gie.2018.11.011]
16 **Ding Z**, Shi H, Zhang H, Meng L, Fan M, Han C, Zhang K, Ming F, Xie X, Liu H, Liu J, Lin R, Hou X. Gastroenterologist-Level Identification of Small-Bowel Diseases and Normal Variants by Capsule Endoscopy Using a Deep-Learning Model. *Gastroenterology* 2019; **157**: 1044-1054. e5 [PMID: 31251929 DOI: 10.1053/j.gastro.2019.06.025]
17 **He J**, Baxter SL, Xu J, Xu J, Zhou X, Zhang K. The practical implementation of artificial intelligence technologies in medicine. *Nat Med* 2019; **25**: 30-36 [PMID: 30617336 DOI: 10.1038/s41591-018-0307-0]
18 **Arnold M**, Soerjomataram I, Ferlay J, Forman D. Global incidence of oesophageal cancer by histological subtype in 2012. *Gut* 2015; **64**: 381-387 [PMID: 25320104 DOI: 10.1136/gutjnl-2014-308124]
19 **Horie Y**, Yoshio T, Aoyama K, Yoshimizu S, Horiuchi Y, Ishiyama A, Hirasawa T, Tsuchida T, Ozawa T, Ishihara S, Kumagai Y, Fujishiro M, Maetani I, Fujisaki J, Tada T. Diagnostic outcomes of esophageal cancer by artificial intelligence using convolutional neural networks. *Gastrointest Endosc* 2019; **89**: 25-32 [PMID: 30120958 DOI: 10.1016/j.gie.2018.07.037]
20 **Zhao YY**, Xue DX, Wang YL, Zhang R, Sun B, Cai YP, Feng H, Cai Y, Xu JM. Computer-assisted diagnosis of early esophageal squamous cell carcinoma using narrow-band imaging magnifying endoscopy. *Endoscopy* 2019; **51**: 333-341 [PMID: 30469155 DOI: 10.1055/a-0756-8754]
21 **Guo L**, Xiao X, Wu C, Zeng X, Zhang Y, Du J, Bai S, Xie J, Zhang Z, Li Y, Wang X, Cheung O, Sharma M, Liu J, Hu B. Real-time automated diagnosis of precancerous lesions and early esophageal squamous cell carcinoma using a deep learning model (with videos). *Gastrointest Endosc* 2020; **91**: 41-51 [PMID: 31445040 DOI: 10.1016/j.gie.2019.08.018]

World Journal of Gastroenterology

Submit a Manuscript: https://www.f6publishing.com

World J Gastroenterol 2021 January 21; 27(3): 294-304

DOI: 10.3748/wjg.v27.i3.294

ISSN 1007-9327 (print) ISSN 2219-2840 (online)

CASE REPORT

Peritoneal dissemination of pancreatic cancer caused by endoscopic ultrasound-guided fine needle aspiration: A case report and literature review

Hideaki Kojima, Minoru Kitago, Eisuke Iwasaki, Yohei Masugi, Yohji Matsusaka, Hiroshi Yagi, Yuta Abe, Yasushi Hasegawa, Shutaro Hori, Masayuki Tanaka, Yutaka Nakano, Yusuke Takemura, Seiichiro Fukuhara, Yoshiyuki Ohara, Michiie Sakamoto, Shigeo Okuda, Yuko Kitagawa

ORCID number: Hideaki Kojima 0000-0003-2449-9726; Minoru Kitago 0000-0002-4909-1199; Eisuke Iwasaki 0000-0001-8010-5117; Yohei Masugi 0000-0002-6952-4043; Yohji Matsusaka 0000-0003-3471-2762; Hiroshi Yagi 0000-0002-9897-8108; Yuta Abe 0000-0003-4746-0584; Yasushi Hasegawa 0000-0002-4990-0419; Shutaro Hori 0000-0001-9213-0758; Masayuki Tanaka 0000-0003-0335-3912; Yutaka Nakano 0000-0003-3228-3474; Yusuke Takemura 0000-0003-3791-9902; Seiichiro Fukuhara 0000-0003-1675-5670; Yoshiyuki Ohara 0000-0002-0013-8726; Michiie Sakamoto 0000-0003-3507-7369; Shigeo Okuda 0000-0002-7874-9527; Yuko Kitagawa 0000-0001-6469-2155.

Author contributions: Kojima H interpreted the patient data based on the case notes and drafted the manuscript; Kitago M performed the surgery and supervised the manuscript; Masugi Y, Ohara Y, and Sakamoto M evaluated the pathological findings; all other members equally contributed to the medical treatment.

Informed consent statement: Written informed consent was obtained from the patient for the publication of this case report and

Hideaki Kojima, Minoru Kitago, Hiroshi Yagi, Yuta Abe, Yasushi Hasegawa, Shutaro Hori, Masayuki Tanaka, Yutaka Nakano, Yusuke Takemura, Yuko Kitagawa, Department of Surgery, Keio University School of Medicine, Tokyo 160-8582, Japan

Eisuke Iwasaki, Seiichiro Fukuhara, Division of Gastroenterology and Hepatology, Department of Internal Medicine, Keio University School of Medicine, Tokyo 160-8582, Japan

Yohei Masugi, Yoshiyuki Ohara, Michiie Sakamoto, Department of Pathology, Keio University School of Medicine, Tokyo 160-8582, Japan

Yohji Matsusaka, Shigeo Okuda, Department of Radiology, Keio University School of Medicine, Tokyo 160-8582, Japan

Corresponding author: Minoru Kitago, PhD, Reader (Associate Professor), Department of Surgery, Keio University School of Medicine, 35 Shinanomachi, Shinjuku-ku, Tokyo 160-8582, Japan. dragonpegasus@keio.jp

Abstract

BACKGROUND

Endoscopic ultrasound-guided fine needle aspiration (EUS-FNA) is a biopsy technique widely used to diagnose pancreatic tumors because of its high sensitivity and specificity. Although needle-tract seeding caused by EUS-FNA has been recently reported, dissemination of pancreatic cancer cells is generally considered to be a rare complication that does not affect patient prognosis. However, the frequency of dissemination and needle-tract seeding appears to have been underestimated. We present a case of peritoneal dissemination of pancreatic cancer due to preoperative EUS-FNA.

CASE SUMMARY

An 81-year-old man was referred to the Department of Surgery of our hospital in Japan owing to the detection of a pancreatic mass on computed tomography during medical screening. Trans-gastric EUS-FNA revealed that the mass was an adenocarcinoma; hence laparoscopic distal pancreatectomy with lympha-denectomy was performed. No intraoperative peritoneal dissemination and liver

metastasis were visually detected, and pelvic lavage cytology was negative for carcinoma cells. The postoperative surgical specimen was negative for carcinoma cells at the dissected margin and the cut end margin; however, pathological findings revealed adenocarcinoma cells on the peritoneal surface proximal to the needle puncture site, and the cells were suspected to be disseminated *via* EUS-FNA. Hence, the patient received adjuvant therapy with S-1 (tegafur, gimeracil, and oteracil potassium); however, computed tomography performed 5 mo after surgery revealed liver metastasis and cancerous peritonitis. The patient received palliative therapy and died 8 mo after the operation.

CONCLUSION
The indications of EUS-FNA should be carefully considered to avoid iatrogenic dissemination, especially for cancers in the pancreatic body or tail.

Key Words: Case report; Pancreatic carcinoma; Endoscopic ultrasound-guided fine needle aspiration; Peritoneal dissemination; Cancerous peritonitis; Biopsy

Core Tip: Along with the development of preoperative chemotherapy, there is an increasing need for tissue sample collection using endoscopic ultrasound-guided fine needle aspiration (EUS-FNA). Peritoneal dissemination and needle-tract seeding caused by EUS-FNA were previously considered rare events with minimal prognostic impact. However, we experienced a case of peritoneal dissemination of pancreatic cancer—secondary to EUS-FNA—that markedly affected postoperative survival. We provide suggestions for the use of EUS-FNA along with a review of literature.

Citation: Kojima H, Kitago M, Iwasaki E, Masugi Y, Matsusaka Y, Yagi H, Abe Y, Hasegawa Y, Hori S, Tanaka M, Nakano Y, Takemura Y, Fukuhara S, Ohara Y, Sakamoto M, Okuda S, Kitagawa Y. Peritoneal dissemination of pancreatic cancer caused by endoscopic ultrasound-guided fine needle aspiration: A case report and literature review. *World J Gastroenterol* 2021; 27(3): 294-304
URL: https://www.wjgnet.com/1007-9327/full/v27/i3/294.htm
DOI: https://dx.doi.org/10.3748/wjg.v27.i3.294

INTRODUCTION

Endoscopic ultrasound-guided fine needle aspiration (EUS-FNA) is a type of biopsy procedure to collect tissue from mass lesions or body fluid inside and outside the gastrointestinal tract wall. It was first clinically used for pancreatic cancer in 1992 by Vilmann *et al*[1] and has been widely used for the qualitative diagnosis of pancreatic tumors, as it has a high sensitivity of 85%-92% and a high specificity of 96%-98% for the diagnosis of pancreatic cancer[2,3]. The main indications of EUS-FNA are the differentiation of benign and malignant tumors, acquisition of histological evidence for introducing chemotherapy and selecting an appropriate drug regimen, and diagnosis of cancer progression. Considering recently developed therapies, such as neoadjuvant chemotherapy and chemoradiotherapy for pancreatic cancer, the need for collecting tissue samples *via* EUS-FNA will increase in the future[4-6]. EUS-FNA is a relatively safe method with few complications[7,8]. The incidence rate of complications is approximately 1%-2%, and complications mainly include abdominal pain, pancreatitis, hematoma, bleeding, fever, and abdominal discomfort. Although peritoneal dissemination and needle-tract seeding are rare events among the limited complications, they are an issue because they can influence patient prognosis. In this regard, previous studies concluded that EUS-FNA does not affect postoperative survival or peritoneal recurrence[9-11]. However, cases of dissemination or needle-tract seeding caused by EUS-FNA have been recently reported, with most cases being intra-gastric wall metastases due to needle tract seeding; peritoneal dissemination is rare[9,12-31]. Herein, we report a case of peritoneal dissemination of pancreatic cancer that was revealed to be caused by preoperative EUS-FNA based on pathological findings

the accompanying images.

Conflict-of-interest statement: The authors declare that they have no competing interests.

CARE Checklist (2016) statement: The guidelines of the "CARE Checklist-2016: Information for writing a case report" have been adopted by the authors.

Manuscript source: Unsolicited manuscript

Specialty type: Gastroenterology and hepatology

Country/Territory of origin: Japan

Peer-review report's scientific quality classification
Grade A (Excellent): A, A
Grade B (Very good): B, B
Grade C (Good): 0
Grade D (Fair): 0
Grade E (Poor): 0

Received: December 5, 2020
Peer-review started: December 5, 2020
First decision: December 17, 2020
Revised: December 28, 2020
Accepted: January 6, 2021
Article in press: January 6, 2021
Published online: January 21, 2021

P-Reviewer: Geramizadeh B, Krishna SG, Park WS
S-Editor: Zhang H
L-Editor: A
P-Editor: Ma YJ

and resulted in radical disease progression, along with a review of the literature.

CASE PRESENTATION

Chief complaints

An 81-year-old man was found to have a 16-mm hypodense mass lesion at the pancreatic tail region as well as dilation of the main pancreatic duct on undergoing computed tomography (CT) performed during the course of an annual medical check-up in Japan. The patient was then referred to the Department of Surgery for further examination and treatment.

History of present illness

The patient did not have any specific subjective or objective symptoms.

History of past illness

The patient had a history of diabetes.

Personal and family history

There was no family history of malignant tumors.

Physical examination

No jaundice or palpable masses were observed.

Laboratory examinations

A blood test revealed normal protein levels, including carbohydrate antigen 19-9 (15 U/mL; normal range, 0-37 U/mL), carcinoembryonic antigen (1.7 ng/mL; normal, < 5 ng/mL), s-pancreas-1 antigen (11 U/mL; normal, < 30 U/mL), duke pancreatic monoclonal antigen type 2 (< 25 U/mL; normal, < 150 U/mL), and elastase-1 (40 ng/dL; normal, < 300 ng/dL).

Imaging examinations

Contrast-enhanced CT of the chest, abdomen, and pelvis and magnetic resonance cholangiopancreatography revealed a pancreatic mass at the pancreatic tail region with a prolonged contrast effect, as well as dilation of the main pancreatic duct (Figure 1A and B). Positron emission tomography-CT (PET-CT) revealed abnormal accumulation of fluorodeoxyglucose in the same lesion (Figure 1C). These findings were strongly suspected to be pancreatic cancer and associated obstructive pancreatitis; however, there remained a possibility that the tumor was benign, such as mass-forming pancreatitis or autoimmune pancreatitis.

FURTHER DIAGNOSTIC WORK-UP

Hence, trans-gastric EUS-FNA was performed with a 22-gauge needle to obtain a qualitative diagnosis by an experienced gastroenterologist. During the procedure, the needle passed four times through the gastric wall. Tumor tissue was then successfully collected, with no early complications (Figure 1D). The pathological findings indicated a diagnosis of adenocarcinoma (Figure 2A). PET-CT and contrast-enhanced CT scans showed no evidence of distant metastasis, no infiltration into the anterior or posterior adipose tissue, and no involvement of the major arteries (celiac axis, superior mesenteric artery, common hepatic artery) or veins (superior mesenteric vein, portal vein) in the tumor. The preoperative diagnosis was pancreatic invasive ductal adenocarcinoma, cT1c, cN0, and cM0 cStage IA, per both the 7th edition of the Japanese Pancreas Society classification (JPS 7th ed) and the 8th edition of the Union for International Cancer Control (UICC 8th ed). After establishing the diagnosis, laparoscopic distal pancreatectomy with lymphadenectomy was performed. No intra-operative peritoneal dissemination and liver metastasis were visually observed, and pelvic lavage cytology was negative for carcinoma cells (P0, CY0). The pancreatic tumor did not invade the surrounding organs or adipose tissue, which was confirmed by intra-operative ultrasound examination of the pancreas. The operation was successfully performed as planned without exposing the tumor during surgery. The patient had an uneventful postoperative recovery and was discharged on

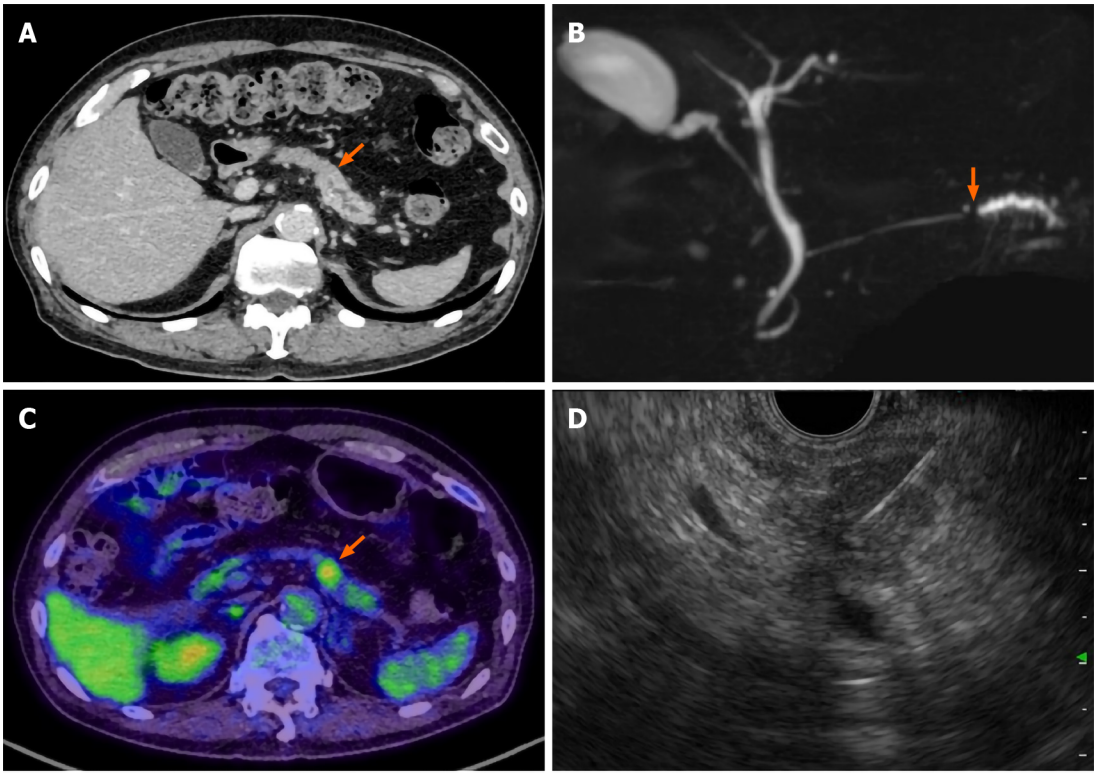

Figure 1 Pre-operative imaging findings. A: Contrast-enhanced computed tomography (CT) scan showing a hypodense mass lesion (arrow) in the pancreatic tail region as well as dilation of the main pancreatic duct; B: Magnetic resonance cholangiopancreatography showing obstruction (arrow) and dilation of the main pancreatic duct; C: Positron emission tomography-CT scan showing the high uptake (arrow) of fluorodeoxyglucose by the pancreatic tail mass; D: Endoscopic ultrasound-guided fine needle aspiration performed using a 22-gauge needle through the posterior gastric wall.

postoperative day 13. The final pathological findings revealed that the dissected and cut end margins were negative for carcinoma cells. The tumor was observed to be a poorly circumscribed whitish mass that was located within the pancreatic parenchyma, and direct infiltration into the anterior and posterior adipose tissues was not observed (Figure 2B). There were two areas of peritoneal thickening with reddish and whitish appearance at a distance from the main tumor site, where a trabecular fibrotic scar associated with peritoneal surface hemorrhage owing to needle puncture *via* EUS-FNA was observed under a high-power view (Figure 2B, E and F). In this area, small aggregates of tumor cells were observed that were similar to those of the main tumor, indicating that these tumor cells were disseminated *via* EUS-FNA from the main lesion (Figure 2D, G and H).

FINAL DIAGNOSIS

The final diagnosis was Pt, TS1 (13 × 12 × 10 mm), infiltrative, ductal adenocarcinoma, pT1c, int, INFc, ly1, v3, ne1, mpd0, pS0, pCHX, pDUX, pPVsp0, pAsp0, pPL0, pPCM0, pDPM0, N1a (1/36, #11p), M1 (P), pStage IV (JPS 7th ed) and pT1c, pN1, and pM1 pStage IV (UICC 8th ed).

TREATMENT

Accordingly, the patient underwent adjuvant therapy with S-1 (tegafur, gimeracil, and oteracil potassium). However, a CT scan of the chest, abdomen, and pelvis obtained 5 mo after the operation revealed liver metastasis and cancerous peritonitis (Figure 3). The patient was offered a more effective chemotherapy regimen for recurrent pancreatic cancer; however, he did not want further treatment.

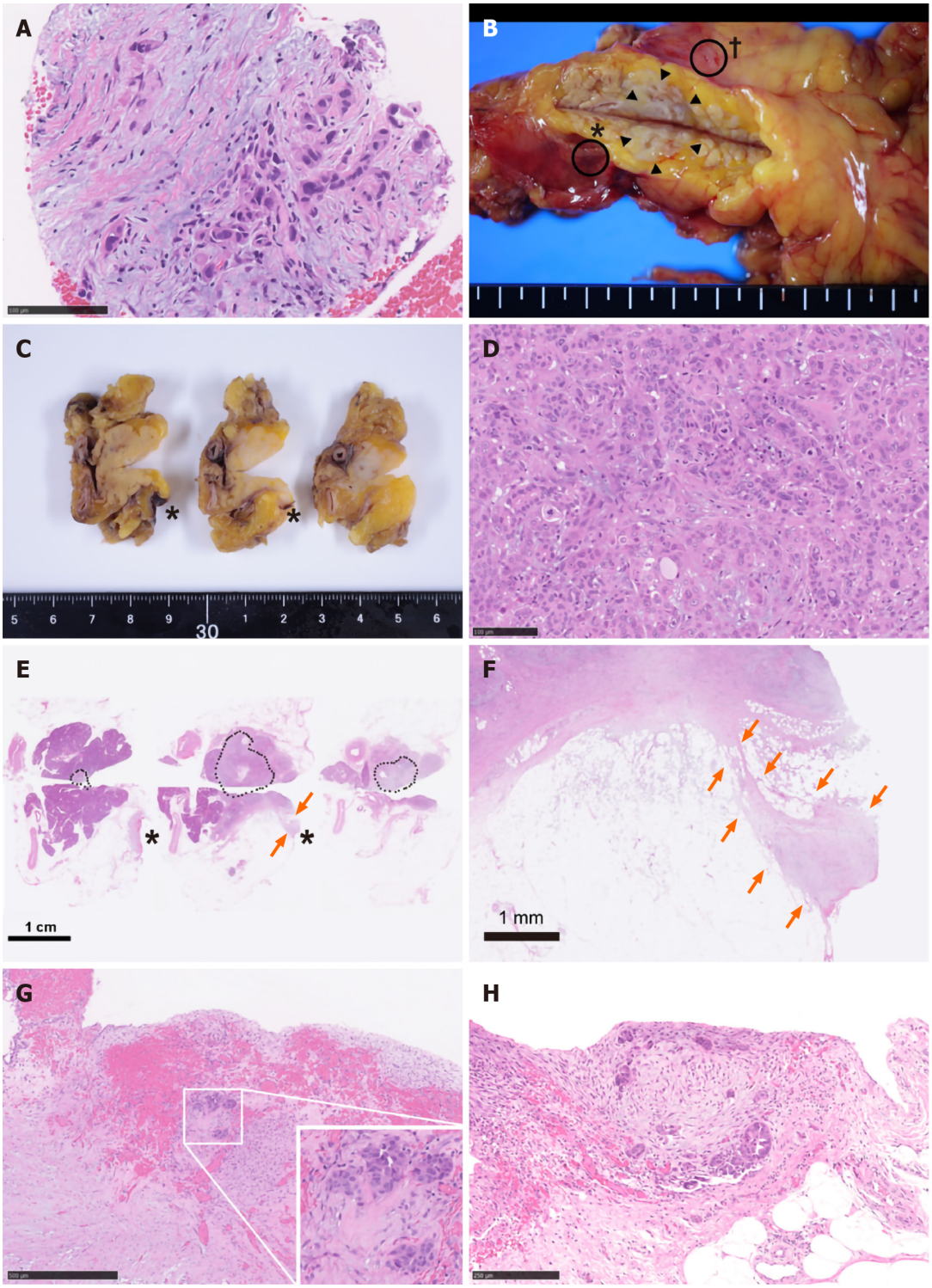

Figure 2 Pathological findings. A: Specimens obtained *via* endoscopic ultrasound-guided fine needle aspiration (EUS-FNA) biopsy. Atypical cells with enlarged and hyperchromatic nuclei infiltrating the fibrous stroma are visible; B: A fresh gross image of the resected pancreas: a poorly circumscribed whitish tumor mass (arrowheads) is observed within pancreas parenchyma at the cut surface. Two areas of peritoneal thickening with reddish (asterisk) and whitish (dagger) appearance are observed at a distance from the tumor site; C: The cut surface of the formalin-fixed specimen: the peritoneal side is on the right, and the retroperitoneal side on the left; D: Histological image of the main tumor: the tumor is predominantly composed of poorly differentiated carcinoma cells with ill-defined ductular structures; E: A loupe image correspondence to the macroscopic image observed in panel C: the area surrounded by black dots is the main tumor lesion. A trabecular fibrotic scar (arrows) associated with peritoneal surface hemorrhage (asterisks) is observed; F: A low-power view of the fibrotic scar (arrows in E) possibly due to the needle tract injected during EUS-FNA; G: A high-magnification image of hemorrhagic peritoneum (asterisks in B, C, and E) proximal to the fibrotic scar. In this area (considered to be the needle puncture site), small aggregates of tumor cells (inset) are embedded in the fibrotic stroma; H: A high-power microscopic view of the whitish thickened peritoneum (dagger in B). Disseminated tumor cells focally forming the ductular structures are seen on the surface of the serosa.

OUTCOME AND FOLLOW-UP

He received palliative therapy and died 8 mo after the operation.

DISCUSSION

Peritoneal dissemination or needle-tract seeding *via* EUS-FNA is an issue because it impairs patient survival. However, the frequency of dissemination is extremely low. Moreover, several studies have evaluated the long-term prognosis of patients with pancreatic cancer; the results showed that EUS-FNA was not associated with recurrence in the gastric or peritoneal wall or with overall survival of patients who underwent resection for pancreatic cancer[9-11]. Similar to the results of previous studies, Yane *et al*[32] reported that EUS-FNA does not affect recurrence-free survival and overall survival. However, the authors also mentioned non-negligible effects of needle-tract seeding after EUS-FNA as 6 of 176 (3.4%) patients had recurrences in the intra-gastric wall[32]. Furthermore, some researchers have indicated that EUS-FNA might promote distant metastasis by blood dissemination and puncture dissemination. Levy *et al*[33] analyzed cell-free DNA (cfDNA) before and after EUS-FNA of pancreatic adenocarcinoma to assess the risk of the distant metastasis due to EUS-FNA. cfDNA is the nuclear material from a tumor that disseminates into the bloodstream (tumoremia); it has been developed a useful biomarker for various tumors (including pancreatic cancer) to predict the therapeutic response and prognosis[34,35]. Levy *et al*[33] reported an insignificant increase in the plasma concentration of cfDNA and increased detection of *KRAS* mutations in cfDNA after EUS-FNA. Additionally, a significant number of new distant metastases were detected in patients with tumoremia. Although the study was a preliminary evaluation with only a small number of patients, the findings suggest that EUS-FNA might contribute to increased distant metastases. Accordingly, we are planning to evaluate cfDNA in preserved plasma from the case presented in this report.

Considering the findings of these studies, the frequency of dissemination and needle-tract seeding due to EUS-FNA appears to have been underestimated. There are several possible causes of underestimation, as clarified in the previously reported 24 cases including the present case (Table 1). First, upper endoscopy is not performed, and EUS-FNA puncture sites are not examined if patients have no symptoms. Second, the needle tract could be also resected with the main tumor lesion; hence, dissemination does not tend to be evaluated. Third, peritoneal dissemination may be unlikely in cases of pancreatic head tumors, because there is no space between the pancreatic head and the duodenum. Finally, it is difficult to distinguish between procedure-related dissemination and disease progression *via* imaging. These reasons may explain why most cases reported needle-tract seeding into the intra-gastric wall and not the peritoneal wall, and there was no case of the primary tumor being in the pancreatic head. From a prognostic point of view, additional gastrectomy seemed to be effective for cases of intra-gastric wall recurrence[17,29,30]; therefore, the puncture site should be regularly investigated postoperatively, and surgical intervention should be considered in cases of local recurrence. In contrast, some cases develop inoperative short-term recurrences[25], as observed in the current case. Therefore, the indications for a trans-gastric biopsy from the pancreatic body and tail should be carefully considered before being performed. Cumulative case reports and a large prospective cohort study are needed to clarify the frequency of procedure-related dissemination and its effect on long-term outcomes.

To the best of our knowledge, the current case is the first report in which peritoneal dissemination associated with EUS-FNA was pathologically proven by using a post-operative specimen. In the current case, some small peritoneal disseminations were observed that were discontinuous from the main lesion. Similar pathological findings and dismal prognoses have been observed in cases of intra-pancreatic metastasis or multi-centric carcinogenesis[36,37]. Therefore, if a small cancerous lesion is observed within the pancreatic parenchyma, it needs to be differentiated from needle tract seeding. Unlike previous reports that state that preoperative EUS-FNA does not affect the prognosis, the current patient showed aggressive disease progression. Although the liver metastasis might be explained by the high degree of pathological vascular invasion, it is clinically unusual to present with such acute cancerous peritonitis when the intra-operative cytology results were negative for carcinoma cells. In addition to the pathological findings, the unusual disease progression is also consistent with EUS-FNA-related dissemination.

Table 1 Clinical features of 24 previous cases of dissemination after endoscopic ultrasound-guided fine needle aspiration

No	Author [ref.], year	Primary lesion					EUS-FNA		Recurrence				
		Diagnosis	size, mm	Location	Initial therapy	Cystic lesion	Puncture site	Passes, *n*	Interval from EUS-FNA, mo	Location	size, mm	Treatment	Outcomes
1	Hirooka *et al*[12], 2003	IPMC	20	Pb	DP+LG	(+)	Trans-gastric		0	G/Wserosa	7		Died 25 mo after surgery
2	Paquin *et al*[13], 2005	IPMC	8	Pt	DP	(+)	Trans-gastric	5	21	G/W	30	Palliative Chemotherapy	Died 12 mo after diagnosis
3	Ahmed *et al*[14], 2011	PDAC		Pb	MPAdj gefinitiveRadiation	(+)	Trans-gastric	multiple	48	G/W	45	TG	Died of another malignancy
4	Chong *et al*[15], 2011	IDC	28	Pt	DP	(+)	Trans-gastric	2	26	G/W	40		
5	Katanuma *et al*[16], 2012	IDC	20	Pb	DP	(-)	Trans-gastric	4	22	G/W			
6	Ngamruengphong *et al*[9], 2013	IDC		Pb, Pt	Subtotal PancreatomyRadiation	(+)	Trans-gastric	3	27	G/W			
7	Ngamruengphong *et al*[9], 2013	IDC	40	Pt	DP+LGAdj Chemoradiation	(+)	Trans-gastric	3	26	G/W			
8	Sakurada *et al*[17], 2015	Adeno-squamous	25	Pb	DP	(-)	Trans-gastric		19	G/W	20	LG	No recurrence after 16 mo follow-up
9	Tomonari *et al*[18], 2015	IDC	20	Pb	DPAdj S-1	(-)	Trans-gastric	2	28	G/W	32	Subtotal Gastrectomy	
10	Minaga *et al*[19], 2015	IDC	20	Pt	DP	(-)	Trans-gastric	3	8	G/W	12	LG	
11	Hirohito *et al*[20], 2015	IDC	20	Pb	GEM⇒S-1	(-)	Trans-gastric	4	9	G/W	16	Palliative Chemotherapy	Died 11 mo after diagnosis
12	Yamauchi *et al*[21], 2016	IDC	25	Pb	DP	(-)	Trans-gastric	1	23	G/W	30	LG	
13	Iida *et al*[22], 2016	IDC			DP	(-)	Trans-gastric	3	6	G/W	18	DGAdj S-1	Recurrence after 21 mo follow-up
14	Kita *et al*[23], 2016	IDC		Pb, Pt	Radiation	(-)	Trans-gastric	2	7	G/W			
15	Minaga *et al*[24], 2016	IDC	10	Pb	DP	(-)	Trans-gastric		24	G/W	30		
16	Yamabe *et al*[25], 2016	IPMC	30	Pb	GEM	(+)	Trans-gastric		3	G/W	24	Palliative Chemotherapy	Died 26 months after diagnosis
17	Yasumoto *et al*[26], 2018	IDC	10	Pb	DPAdj S-1	(-)	Trans-gastric		22	G/W		LG	
19	Sakamoto *et al*[27], 2018	IDC	38	Pt	DPAdj S-1+Gem	(-)	Trans-gastric	2	24	G/W	20	LG	

18	Matsumoto *et al*[28], 2018	IDC	25	Pb	Chemotherapy	(-)	Trans-gastric	3	8	G/W		DP+LG	
20	Matsui *et al*[29], 2019	IDC	15	Pb	DPPartial Gx	(-)	Trans-gastric	4	0	G/Wserosa		Adj S-1	Recurrence 6 mo after surgery; Died 18 mo after surgery
21	Matsui *et al*[29], 2019	IDC	15	Pb	DP+LG	(-)	Trans-gastric	1	0	G/Wserosa		Adj S-1	No recurrence after 18 mo follow-up
22	Sato *et al*[30], 2020	IDC	25	Pb	DPAdj S-1	(-)	Trans-gastric	2	25	G/W	23	LG	No recurrence after 5 mo follow-up
23	Yamaguchi *et al*[31], 2020	SPN	60	Pb	DP	(+)	Trans-gastric	4	60	G/W	40	DG	
24	Current case	IDC	16	Pb	DP	(-)	Trans-gastric	4	0	Peritoneum			Cancerous peritonitis and liver metastasis 5 mo after surgeryDied 8 mo after surgery

EUS-FNA: Endoscopic ultrasound-guided fine needle aspiration; IDC: Invasive ductal carcinoma; IPMC: Intraductal papillary mucinous carcinoma; SPN: Solid-pseudopapillary neoplasm; Pb: Pancreatic body; Pt: Pancreatic tail; DP: Distal pancreatectomy; MP: Middle pancreatectomy; LG: Local gastrectomy; DG: Distal gastrectomy; TG: Total gastrectomy; Adj: Adjuvant; S-1: Tegafur, gineracil, oteracil potassium; GEM: Gemcitabine hydrochloride; G/W: Gastric wall.

EUS-FNA is widely used when it is difficult to distinguish between benign and malignant tumors *via* imaging, because it helps to avoid unnecessary surgery. In addition, EUS-FNA is recommended for both resectable cases and unresectable advanced cases because a histological diagnosis is needed to select an appropriate drug regimen for neoadjuvant chemotherapy or palliative chemotherapy. However, it is not always necessary to obtain a definitive preoperative pathological diagnosis when the tumor is strongly suspected to be pancreatic cancer and when up-front surgery has been already planned.

This case highlights the importance of recognizing the risk of disease dissemination associated with EUS-FNA. Thorough discussion should be conducted on individual cases prior to performing EUS-FNA.

CONCLUSION

The indications for EUS-FNA should be thoroughly discussed with radiologists and endoscopists to avoid iatrogenic dissemination, especially for cancers in the pancreatic body or tail. In addition, careful observation is required not only of the surgical site but also of the puncture site.

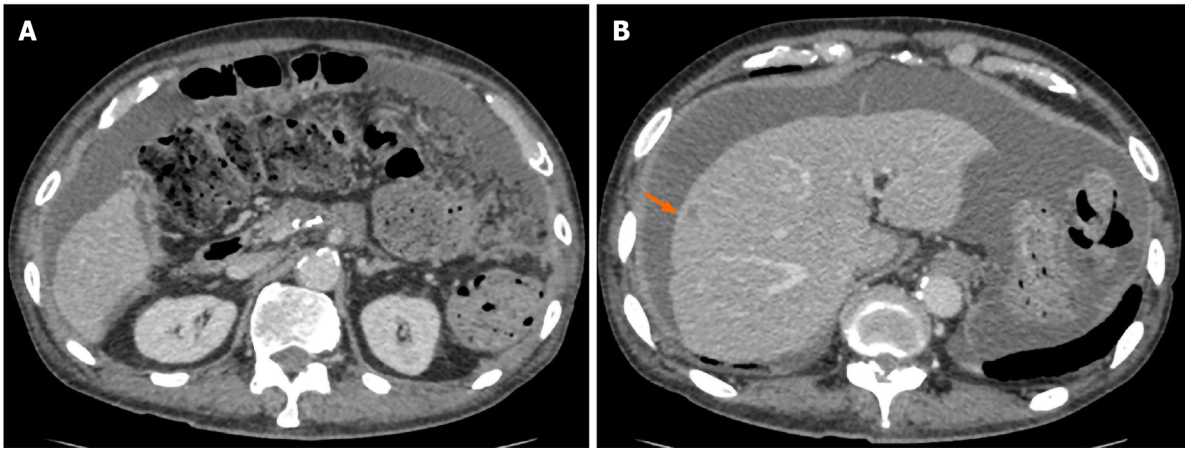

Figure 3 Computed tomography obtained 5 mo after surgery. An ascites associated with cancerous peritonitis and liver metastasis (arrow) was observed.

ACKNOWLEDGEMENTS

We would like to thank Kazumasa Fukuda, a staff member of the Department of Surgery at Keio University School of Medicine, for her help in preparing this manuscript.

REFERENCES

1 **Vilmann P**, Jacobsen GK, Henriksen FW, Hancke S. Endoscopic ultrasonography with guided fine needle aspiration biopsy in pancreatic disease. *Gastrointest Endosc* 1992; **38**: 172-173 [PMID: 1568614 DOI: 10.1016/s0016-5107(92)70385-x]

2 **Hewitt MJ**, McPhail MJ, Possamai L, Dhar A, Vlavianos P, Monahan KJ. EUS-guided FNA for diagnosis of solid pancreatic neoplasms: a meta-analysis. *Gastrointest Endosc* 2012; **75**: 319-331 [PMID: 22248600 DOI: 10.1016/j.gie.2011.08.049]

3 **Puli SR**, Bechtold ML, Buxbaum JL, Eloubeidi MA. How good is endoscopic ultrasound-guided fine-needle aspiration in diagnosing the correct etiology for a solid pancreatic mass? *Pancreas* 2013; **42**: 20-26 [PMID: 23254913 DOI: 10.1097/MPA.0b013e3182546e79]

4 **Motoi F**, Kosuge T, Ueno H, Yamaue H, Satoi S, Sho M, Honda G, Matsumoto I, Wada K, Furuse J, Matsuyama Y, Unno M; Study Group of Preoperative Therapy for Pancreatic Cancer (Prep) and Japanese Study Group of Adjuvant Therapy for Pancreatic cancer (JSAP). Randomized phase II/III trial of neoadjuvant chemotherapy with gemcitabine and S-1 versus upfront surgery for resectable pancreatic cancer (Prep-02/JSAP05). *Jpn J Clin Oncol* 2019; **49**: 190-194 [PMID: 30608598 DOI: 10.1093/jjco/hyy190]

5 **Endo Y**, Kitago M, Aiura K, Shinoda M, Yagi H, Abe Y, Oshima G, Hori S, Nakano Y, Itano O, Fukada J, Masugi Y, Kitagawa Y. Efficacy and safety of preoperative 5-fluorouracil, cisplatin, and mitomycin C in combination with radiotherapy in patients with resectable and borderline resectable pancreatic cancer: a long-term follow-up study. *World J Surg Oncol* 2019; **17**: 145 [PMID: 31420046 DOI: 10.1186/s12957-019-1687-4]

6 **Fujii-Nishimura Y**, Nishiyama R, Kitago M, Masugi Y, Ueno A, Aiura K, Kawachi S, Kawaida M, Abe Y, Shinoda M, Itano O, Tanimoto A, Sakamoto M, Kitagawa Y. Two Cases of Pathological Complete Response to Neoadjuvant Chemoradiation Therapy in Pancreatic Cancer. *Keio J Med* 2015; **64**: 26-31 [PMID: 26118369 DOI: 10.2302/kjm.2014-0014-CR]

7 **Yamao K**, Sawaki A, Mizuno N, Shimizu Y, Yatabe Y, Koshikawa T. Endoscopic ultrasound-guided fine-needle aspiration biopsy (EUS-FNAB): past, present, and future. *J Gastroenterol* 2005; **40**: 1013-1023 [PMID: 16322944 DOI: 10.1007/s00535-005-1717-6]

8 **Jenssen C**, Alvarez-Sánchez MV, Napoléon B, Faiss S. Diagnostic endoscopic ultrasonography: assessment of safety and prevention of complications. *World J Gastroenterol* 2012; **18**: 4659-4676 [PMID: 23002335 DOI: 10.3748/wjg.v18.i34.4659]

9 **Ngamruengphong S**, Xu C, Woodward TA, Raimondo M, Stauffer JA, Asbun HJ, Wallace MB. Risk of gastric or peritoneal recurrence, and long-term outcomes, following pancreatic cancer resection with preoperative endosonographically guided fine needle aspiration. *Endoscopy* 2013; **45**: 619-626 [PMID: 23881804 DOI: 10.1055/s-0033-1344216]

10 **Ngamruengphong S**, Swanson KM, Shah ND, Wallace MB. Preoperative endoscopic ultrasound-guided fine needle aspiration does not impair survival of patients with resected pancreatic cancer. *Gut* 2015; **64**: 1105-1110 [PMID: 25575893 DOI: 10.1136/gutjnl-2014-307475]

11 **Tsutsumi H**, Hara K, Mizuno N, Hijioka S, Imaoka H, Tajika M, Tanaka T, Ishihara M, Yoshimura

K, Shimizu Y, Niwa Y, Sasaki Y, Yamao K. Clinical impact of preoperative endoscopic ultrasound-guided fine-needle aspiration for pancreatic ductal adenocarcinoma. *Endosc Ultrasound* 2016; **5**: 94-100 [PMID: 27080607 DOI: 10.4103/2303-9027.180472]

12 **Hirooka Y**, Goto H, Itoh A, Hashimoto S, Niwa K, Ishikawa H, Okada N, Itoh T, Kawashima H. Case of intraductal papillary mucinous tumor in which endosonography-guided fine-needle aspiration biopsy caused dissemination. *J Gastroenterol Hepatol* 2003; **18**: 1323-1324 [PMID: 14535994 DOI: 10.1046/j.1440-1746.2003.03040.x]

13 **Paquin SC**, Gariépy G, Lepanto L, Bourdages R, Raymond G, Sahai AV. A first report of tumor seeding because of EUS-guided FNA of a pancreatic adenocarcinoma. *Gastrointest Endosc* 2005; **61**: 610-611 [PMID: 15812422 DOI: 10.1016/s0016-5107(05)00082-9]

14 **Ahmed K**, Sussman JJ, Wang J, Schmulewitz N. A case of EUS-guided FNA-related pancreatic cancer metastasis to the stomach. *Gastrointest Endosc* 2011; **74**: 231-233 [PMID: 21168837 DOI: 10.1016/j.gie.2010.10.008]

15 **Chong A**, Venugopal K, Segarajasingam D, Lisewski D. Tumor seeding after EUS-guided FNA of pancreatic tail neoplasia. *Gastrointest Endosc* 2011; **74**: 933-935 [PMID: 21951481 DOI: 10.1016/j.gie.2010.10.020]

16 **Katanuma A**, Maguchi H, Hashigo S, Kaneko M, Kin T, Yane K, Kato R, Kato S, Harada R, Osanai M, Takahashi K, Shinohara T, Itoi T. Tumor seeding after endoscopic ultrasound-guided fine-needle aspiration of cancer in the body of the pancreas. *Endoscopy* 2012; **44** Suppl 2 UCTN: E160-E161 [PMID: 22622721 DOI: 10.1055/s-0031-1291716]

17 **Sakurada A**, Hayashi T, Ono M, Ishiwatari H, Ogino J, Kimura Y, Kato J. A case of curatively resected gastric wall implantation of pancreatic cancer caused by endoscopic ultrasound-guided fine-needle aspiration. *Endoscopy* 2015; **47** Suppl 1 UCTN: E198-E199 [PMID: 26062146 DOI: 10.1055/s-0034-1377592]

18 **Tomonari A**, Katanuma A, Matsumori T, Yamazaki H, Sano I, Minami R, Sen-yo M, Ikarashi S, Kin T, Yane K, Takahashi K, Shinohara T, Maguchi H. Resected tumor seeding in stomach wall due to endoscopic ultrasonography-guided fine needle aspiration of pancreatic adenocarcinoma. *World J Gastroenterol* 2015; **21**: 8458-8461 [PMID: 26217099 DOI: 10.3748/wjg.v21.i27.8458]

19 **Minaga K**, Kitano M, Yamashita Y. Surgically resected needle tract seeding following endoscopic ultrasound-guided fine-needle aspiration in pancreatic cancer. *J Hepatobiliary Pancreat Sci* 2015; **22**: 708-709 [PMID: 26084566 DOI: 10.1002/jhbp.269]

20 **Naruse H**, Yamato H, Yamamoto Y, Hatanaka K, Yamamoto K, Horimoto M, Matsuda K, Yamanashi K, Kudou K, Shimoyama N. An autopsy-confirmed case of needle tract seeding of pancreatic cancer following EUS-guided FNA. *Gastroenterol Endosc* 2015; **57**: 1616-1622 [DOI: 10.11280/gee.57.1616]

21 **Yamauchi J**, Kobayashi S, Miyazaki K, Ajiki T, Tsuchihara K, Ishiyama S. A case of curative resection of needle tract seeding after EUS-guided fine needle aspiration for pancreatic body cancer. *J Jpn Surg Assoc* 2016; **77**: 2994-2999 [DOI: 10.3919/jjsa.77.2994]

22 **Iida T**, Adachi T, Ohe Y, Nakagaki S, Yabana T, Kondo Y, Nakase H. Re-recurrence after distal gastrectomy for recurrence caused by needle tract seeding during endoscopic ultrasound-guided fine-needle aspiration of a pancreatic adenocarcinoma. *Endoscopy* 2016; **48**: E304-E305 [PMID: 27669534 DOI: 10.1055/s-0042-116431]

23 **Kita E**, Yamaguchi T, Sudo K. A case of needle tract seeding after EUS-guided FNA in pancreatic cancer, detected by serial positron emission tomography/CT. *Gastrointest Endosc* 2016; **84**: 869-870 [PMID: 26853299 DOI: 10.1016/j.gie.2016.01.060]

24 **Minaga K**, Kitano M, Enoki E, Kashida H, Kudo M. Needle-Tract Seeding on the Proximal Gastric Wall After EUS-Guided Fine-Needle Aspiration of a Pancreatic Mass. *Am J Gastroenterol* 2016; **111**: 1515 [PMID: 27808133 DOI: 10.1038/ajg.2016.307]

25 **Yamabe A**, Irisawa A, Shibukawa G, Hoshi K, Fujisawa M, Igarashi R, Sato A, Maki T, Hojo H. Rare condition of needle tract seeding after EUS-guided FNA for intraductal papillary mucinous carcinoma. *Endosc Int Open* 2016; **4**: E756-E758 [PMID: 27556091 DOI: 10.1055/s-0042-107072]

26 **Yasumoto M**, Okabe Y, Ishikawa H, Kisaki J, Akiba J, Naito Y, Ishida Y, Ushijima T, Tsuruta O, Torimura T. A case of gastric wall implantation caused by EUS-FNA 22 months after pancreatic cancer resection. *Endosc Ultrasound* 2018; **7**: 64-66 [PMID: 29451172 DOI: 10.4103/eus.eus_58_17]

27 **Sakamoto U**, Fukuba N, Ishihara S, Sumi S, Okada M, Sonoyama H, Ohshima N, Moriyama I, Kawashima K, Kinoshita Y. Postoperative recurrence from tract seeding after use of EUS-FNA for preoperative diagnosis of cancer in pancreatic tail. *Clin J Gastroenterol* 2018; **11**: 200-205 [PMID: 29392646 DOI: 10.1007/s12328-018-0822-z]

28 **Matsumoto K**, Kato H, Tanaka N, Okada H. Preoperative Detection of Tumor Seeding after Endoscopic Ultrasonography-guided Fine Needle Aspiration for Pancreatic Cancer. *Intern Med* 2018; **57**: 1797-1798 [PMID: 29434140 DOI: 10.2169/internalmedicine.0321-17]

29 **Matsui T**, Nishikawa K, Yukimoto H, Katsuta K, Nakamura Y, Tanaka S, Oiwa M, Nakahashi H, Shomi Y, Haruki Y, Taniguchi K, Shimomura M, Isaji S. Needle tract seeding following endoscopic ultrasound-guided fine-needle aspiration for pancreatic cancer: a report of two cases. *World J Surg Oncol* 2019; **17**: 134 [PMID: 31382964 DOI: 10.1186/s12957-019-1681-x]

30 **Sato N**, Takano S, Yoshitomi H, Furukawa K, Takayashiki T, Kuboki S, Suzuki D, Sakai N, Kagawa S, Mishima T, Nakadai E, Mikata R, Kato N, Ohtsuka M. Needle tract seeding recurrence of pancreatic cancer in the gastric wall with paragastric lymph node metastasis after endoscopic ultrasound-guided fine needle aspiration followed by pancreatectomy: a case report and literature

review. *BMC Gastroenterol* 2020; **20**: 13 [PMID: 31941458 DOI: 10.1186/s12876-020-1159-x]

31 **Yamaguchi H**, Morisaka H, Sano K, Nagata K, Ryozawa S, Okamoto K, Ichikawa T. Seeding of a Tumor in the Gastric Wall after Endoscopic Ultrasound-guided Fine-needle Aspiration of Solid Pseudopapillary Neoplasm of the Pancreas. *Intern Med* 2020; **59**: 779-782 [PMID: 31787691 DOI: 10.2169/internalmedicine.3244-19]

32 **Yane K**, Kuwatani M, Yoshida M, Goto T, Matsumoto R, Ihara H, Okuda T, Taya Y, Ehira N, Kudo T, Adachi T, Eto K, Onodera M, Sano I, Nojima M, Katanuma A. Non-negligible rate of needle tract seeding after endoscopic ultrasound-guided fine-needle aspiration for patients undergoing distal pancreatectomy for pancreatic cancer. *Dig Endosc* 2020; **32**: 801-811 [PMID: 31876309 DOI: 10.1111/den.13615]

33 **Levy MJ**, Kipp BR, Milosevic D, Schneider AR, Voss JS, Avula R, Kerr SE, Henry MR, Highsmith E Jr, Liu MC, Gleeson FC. Analysis of Cell-Free DNA to Assess Risk of Tumoremia Following Endoscopic Ultrasound Fine-Needle Aspiration of Pancreatic Adenocarcinomas. *Clin Gastroenterol Hepatol* 2018; **16**: 1632-1640. e1 [PMID: 29526691 DOI: 10.1016/j.cgh.2018.02.048]

34 **Shinozaki M**, O'Day SJ, Kitago M, Amersi F, Kuo C, Kim J, Wang HJ, Hoon DS. Utility of circulating B-RAF DNA mutation in serum for monitoring melanoma patients receiving biochemotherapy. *Clin Cancer Res* 2007; **13**: 2068-2074 [PMID: 17404088 DOI: 10.1158/1078-0432.CCR-06-2120]

35 **Nakano Y**, Kitago M, Matsuda S, Nakamura Y, Fujita Y, Imai S, Shinoda M, Yagi H, Abe Y, Hibi T, Fujii-Nishimura Y, Takeuchi A, Endo Y, Itano O, Kitagawa Y. KRAS mutations in cell-free DNA from preoperative and postoperative sera as a pancreatic cancer marker: a retrospective study. *Br J Cancer* 2018; **118**: 662-669 [PMID: 29360815 DOI: 10.1038/bjc.2017.479]

36 **Fujita Y**, Kitago M, Masugi Y, Itano O, Shinoda M, Abe Y, Hibi T, Yagi H, Fujii-Nishimura Y, Sakamoto M, Kitagawa Y. Two cases of pancreatic ductal adenocarcinoma with intrapancreatic metastasis. *World J Gastroenterol* 2016; **22**: 9222-9228 [PMID: 27895409 DOI: 10.3748/wjg.v22.i41.9222]

37 **Fujita Y**, Matsuda S, Sasaki Y, Masugi Y, Kitago M, Yagi H, Abe Y, Shinoda M, Tokino T, Sakamoto M, Kitagawa Y. Pathogenesis of multiple pancreatic cancers involves multicentric carcinogenesis and intrapancreatic metastasis. *Cancer Sci* 2020; **111**: 739-748 [PMID: 31799787 DOI: 10.1111/cas.14268]

Published by **Baishideng Publishing Group Inc**
7041 Koll Center Parkway, Suite 160, Pleasanton, CA 94566, USA
Telephone: +1-925-3991568
E-mail: bpgoffice@wjgnet.com
Help Desk: https://www.f6publishing.com/helpdesk
https://www.wjgnet.com